

Boosting t-SNE Efficiency for Sequencing Data: Insights from Kernel Selection

Avais Jan¹, Prakash Chourasia¹, Sarwan Ali^{2*}, Murray Patterson^{1*}

¹Department of Computer Science, Georgia State University, Atlanta, GA, USA.

²Department of Neurology, Columbia University Irving Medical Center, New York, NY, USA.

*Corresponding author(s). E-mail(s): sa4559@cumc.columbia.edu;

mpatterson30@gsu.edu;

Contributing authors: ajan3@student.gsu.edu;

pchourasia1@student.gsu.edu;

Abstract

Dimensionality reduction techniques are essential for visualizing and analyzing high-dimensional biological sequencing data. t-distributed Stochastic Neighbor Embedding (t-SNE) is widely used for this purpose, traditionally employing the Gaussian kernel to compute pairwise similarities. However, the Gaussian kernel's lack of data-dependence and computational overhead limit its scalability and effectiveness for categorical biological sequences. Recent work proposed the isolation kernel as an alternative, yet it may not optimally capture sequence similarities. In this study, we comprehensively evaluate nine different kernel functions for t-SNE applied to molecular sequences, using three embedding methods: One-Hot Encoding, Spike2Vec, and minimizers. Through both subjective visualization and objective metrics (including neighborhood preservation scores), we demonstrate that the cosine similarity kernel in general outperforms other kernels, including Gaussian and isolation kernels, achieving superior runtime efficiency and better preservation of pairwise distances in low-dimensional space. We further validate our findings through extensive classification and clustering experiments across six diverse biological datasets (Spike7k, Host, ShortRead, Rabies, Genome, and Breast Cancer), employing multiple machine learning algorithms and evaluation metrics. Our results show that kernel selection significantly impacts not only visualization quality but also downstream analytical tasks, with the cosine similarity kernel providing the most robust performance across different data

types and embedding strategies, making it particularly suitable for large-scale biological sequence analysis.

Keywords: Kernel Methods, t-SNE, k -mer, Minimizer, Classification, Clustering, SARS-CoV-2 Spike Sequences

1 Introduction

The advent of high-throughput sequencing technologies has revolutionized biological research, generating unprecedented volumes of genomic data that require sophisticated computational methods for analysis and interpretation. The COVID-19 pandemic, caused by SARS-CoV-2, has particularly accelerated the generation of viral sequence data, with millions of genome sequences deposited in public databases [1, 2]. This surge in sequencing data has pushed viral genomics into the “Big Data” realm, presenting significant challenges for traditional analytical approaches [3]. Understanding the evolutionary dynamics and structural variations in viral proteins, especially the spike protein, which mediates viral entry into host cells, is crucial for tracking viral evolution, identifying variants of concern, and developing effective therapeutic strategies [4, 5].

Machine learning (ML) techniques have emerged as powerful tools for analyzing biological sequence data, offering capabilities for classification, clustering, and pattern recognition [6, 7]. However, the high dimensionality of genomic data poses a fundamental challenge: biological sequences cannot be directly used as input to most ML models and must first be transformed into fixed-length numerical representations. This dimensionality challenge is further compounded when attempting to visualize and interpret the relationships between sequences. While various embedding methods such as k -mer based approaches [8], word2vec-inspired techniques [9, 10], and more recent deep learning methods [11] have been proposed to convert sequences into numerical vectors, these representations often remain high-dimensional, necessitating further dimensionality reduction for effective visualization and analysis.

The t -distributed Stochastic Neighbor Embedding (t-SNE) [12] has become one of the most popular techniques for dimensionality reduction and visualization in computational biology. The method works by preserving pairwise similarities between data points when projecting from high-dimensional space to low-dimensional (typically 2D or 3D) representations. At its core, t-SNE relies on a kernel function to compute similarity matrices between pairs of sequences. The choice of kernel function is crucial as it determines how distances and relationships are measured in the original high-dimensional space. Traditionally, the Gaussian kernel (also known as the Radial Basis Function kernel) has been the default choice for t-SNE [12]. However, the Gaussian kernel is not data-dependent and uses Euclidean distance as its basis, which may not be optimal for categorical data such as biological sequences where edit distance or other sequence-specific metrics might be more appropriate [11].

Recent work by Zhu and Ting [13] proposed using the isolation kernel as an alternative to the Gaussian kernel for t-SNE, demonstrating improved computational

efficiency and better preservation of local data structure. The isolation kernel is data-dependent and adapts to local density distributions, requiring only a single parameter for tuning. While this approach showed promise on standard benchmark datasets, its effectiveness for biological sequence data, which has unique characteristics such as a categorical nature and evolutionary relationships, remains understudied. Moreover, the isolation kernel may still not be optimal for capturing the specific types of similarities that are meaningful in biological contexts. The fundamental question remains: what is the most appropriate kernel function for t-SNE when working with biological sequence data?

The choice of kernel function is not merely a technical detail but can fundamentally impact the quality of dimensionality reduction and subsequent downstream analyses. Different kernels encode different notions of similarity, and the “No Free Lunch” theorem [14] reminds us that no single kernel systematically outperforms others across all domains and tasks. For biological sequences, the Euclidean distance underlying the Gaussian kernel may not capture the discrete, combinatorial nature of sequence dissimilarity [11]. For instance, two sequences of different lengths might have large Euclidean distance despite small edit distance, potentially misrepresenting their biological similarity. This observation motivates a systematic investigation of alternative kernel functions that might better capture sequence relationships.

Beyond visualization, the choice of embedding method and kernel function can significantly impact downstream analytical tasks such as classification and clustering. Previous studies have shown that different embedding techniques yield varying performance in variant identification [8] and clustering of SARS-CoV-2 sequences [15, 16]. However, the interplay between embedding methods, kernel functions, and the performance of t-SNE for both visualization and subsequent machine learning tasks has not been comprehensively studied. Understanding these relationships is essential for developing robust analytical pipelines for biological sequence analysis.

In this paper, we present a comprehensive evaluation of nine different kernel functions for t-SNE applied to biological sequence data, with a focus on SARS-CoV-2 spike protein sequences and other genomic datasets. We evaluate these kernels using three different sequence embedding methods: One-Hot Encoding (OHE), Spike2Vec [10], and minimizers. Our evaluation encompasses both subjective assessment through visual inspection of 2D scatter plots and objective quantification using neighborhood preservation metrics. Furthermore, we extend our analysis to assess how kernel choice impacts downstream classification and clustering tasks across six diverse biological datasets, providing insights into the practical implications of kernel selection for comprehensive sequence analysis pipelines.

The contributions of this work are as follows:

- We conduct the first comprehensive evaluation of nine different kernel functions (cosine similarity, linear, polynomial, Gaussian, isolation, Laplacian, sigmoid, chi-squared, and additive-chi-squared) for t-SNE applied to biological sequence data, demonstrating that the cosine similarity kernel in general outperforms others, including the widely-used Gaussian kernel and the recently proposed isolation kernel.

- We evaluate t-SNE performance using both subjective criteria (visual quality of 2D plots) and objective metrics (neighborhood preservation scores computed via k-ary neighborhood agreement), providing a rigorous assessment framework for dimensionality reduction quality.
- We demonstrate that the cosine similarity kernel achieves superior computational efficiency compared to Gaussian and isolation kernels, with runtime analysis showing linear scaling behavior that makes it particularly suitable for large-scale biological sequence datasets.
- We extend the evaluation beyond visualization to assess the impact of kernel choice on downstream analytical tasks, performing extensive classification experiments with seven ML algorithms (SVM, Naive Bayes, MLP, KNN, Random Forest, Logistic Regression, and Decision Tree) and clustering analysis with multiple evaluation metrics across six diverse biological datasets (Spike7k, Host, ShortRead, Rabies, Genome, and Breast Cancer).
- We investigate the interaction between embedding methods and kernel functions, showing that while the cosine similarity kernel performs best across different embeddings, the choice of embedding method also significantly impacts overall performance, providing practical guidance for method selection in biological sequence analysis.

This work represents an extension of our preliminary conference paper [17], which initially explored kernel selection for t-SNE on SARS-CoV-2 spike sequences. The conference version is available online at https://link.springer.com/chapter/10.1007/978-981-99-7074-2_35. The current manuscript extends that work by: (1) evaluating performance on five additional diverse biological datasets beyond the original Spike7k dataset, (2) conducting comprehensive classification and clustering experiments that were not included in the conference version, (3) providing detailed runtime analysis and scalability assessment, (4) including extensive experimental results with multiple machine learning algorithms and evaluation metrics, and (5) offering deeper insights into the interplay between embedding methods, kernel functions, and downstream analytical performance.

2 Related Work

Dimensionality reduction has been a fundamental challenge in machine learning and data analysis for decades. Principal Component Analysis (PCA) [18], one of the earliest and most widely used techniques, performs linear dimensionality reduction by identifying orthogonal directions of maximum variance in the data. While computationally efficient and providing global structure preservation, PCA often fails to capture complex nonlinear relationships present in biological data [19]. To address these limitations, various nonlinear dimensionality reduction techniques have been developed, including Isomap [20], Locally Linear Embedding (LLE) [21], and Laplacian Eigenmaps [22]. These manifold learning methods attempt to preserve local neighborhood structure but often struggle with complex, high-dimensional biological datasets.

The t-distributed Stochastic Neighbor Embedding (t-SNE) [12] emerged as a significant advancement in dimensionality reduction, particularly for visualization purposes. Unlike its predecessor Stochastic Neighbor Embedding (SNE) [23], t-SNE employs a Student t-distribution in the low-dimensional space to alleviate the crowding problem, resulting in more separated and interpretable clusters. The method has gained widespread adoption in computational biology, particularly for single-cell RNA sequencing analysis [24], flow cytometry data visualization [25], and genomic data exploration [26]. However, t-SNE’s computational complexity of $O(n^2)$ and sensitivity to hyperparameters have motivated various improvements and extensions.

Several variants of t-SNE have been proposed to address its limitations. Barnes-Hut t-SNE [27] reduces computational complexity to $O(n \log n)$ using spatial trees for approximating repulsive forces, enabling application to larger datasets. Parametric t-SNE [28] learns an explicit mapping function using neural networks, allowing for out-of-sample extension. Heavy-tailed Symmetric Stochastic Neighbor Embedding [29] explores different probability distributions in the embedding space. More recently, UMAP (Uniform Manifold Approximation and Projection) [30] has emerged as a competitive alternative to t-SNE, offering faster runtime and better preservation of global structure while maintaining local neighborhood relationships. Despite these advances, the fundamental question of optimal kernel selection for similarity computation in t-SNE remains relatively unexplored, particularly for domain-specific applications such as biological sequence analysis.

Kernel methods constitute a cornerstone of modern machine learning, providing a principled way to handle nonlinear relationships by implicitly mapping data into high-dimensional feature spaces [31, 32]. The kernel trick allows algorithms to operate in these high-dimensional spaces without explicitly computing the coordinates of the data in that space, requiring only the computation of inner products. Support Vector Machines (SVMs) [33] popularized kernel methods, demonstrating their effectiveness for classification tasks. Various kernel functions have been proposed for different data types and applications, including polynomial kernels for capturing interactions between features [31], Gaussian (RBF) kernels for smooth decision boundaries [31], and string kernels specifically designed for sequence data [34].

The choice of kernel function significantly impacts algorithm performance, yet this choice is often guided by empirical evaluation rather than theoretical guarantees. Kernel selection and optimization have been studied extensively in the context of SVMs [35] and Gaussian processes [36]. Multiple Kernel Learning (MKL) [37] approaches attempt to automatically learn optimal kernel combinations from data. More recently, data-dependent kernels that adapt to local data characteristics have gained attention. The isolation kernel [13, 38] represents a significant development in this direction, defining similarity based on the expected height at which two points are isolated in random partitioning trees, thereby adapting to local density distributions without requiring distance metric assumptions.

For biological sequence data, specialized kernels have been developed to capture domain-specific similarities. String kernels [34] measure similarity based on common subsequences, while spectrum kernels [39] have been specifically designed for protein and DNA sequences. Profile kernels [40] incorporate biological knowledge through

position-specific scoring matrices. However, these specialized kernels have primarily been applied in supervised learning contexts (particularly for classification) and their effectiveness for unsupervised tasks like dimensionality reduction with t-SNE remains understudied.

The COVID-19 pandemic has generated an unprecedented volume of viral sequence data, with over 15 million SARS-CoV-2 genomes deposited in GISAID as of 2024 [41]. This data deluge has motivated extensive computational analysis efforts. Phylogenetic analysis has been the traditional approach for understanding viral evolution [42], but the scale of available data has necessitated development of more scalable computational methods. Machine learning approaches have been increasingly applied to various aspects of SARS-CoV-2 analysis, including variant classification [8], and host prediction [43].

Clustering and classification of SARS-CoV-2 sequences have received particular attention. Multiple studies have explored different approaches to variant identification and lineage assignment [16, 44]. The Pangolin lineage assignment system [45] provides a standardized nomenclature, while computational methods attempt to identify emerging variants and characterize their properties. Dimensionality reduction techniques, particularly t-SNE, have been employed to visualize the landscape of viral sequence diversity [8], revealing patterns of viral evolution and geographic distribution of variants. However, these studies typically employ default t-SNE parameters and kernel functions without systematic evaluation of alternatives.

The spike protein of SARS-CoV-2 has been the focus of intense research due to its critical role in viral entry and its status as the primary target for vaccines and therapeutic antibodies [46]. Mutations in the spike protein, particularly in the receptor-binding domain (RBD), can affect transmissibility, immune evasion, and disease severity [47]. Understanding the relationships between spike protein sequences from different variants is crucial for pandemic surveillance and response. This motivates the need for effective visualization and analysis methods that can accurately represent sequence similarities and differences.

Converting biological sequences into numerical representations suitable for machine learning is a fundamental preprocessing step. Traditional approaches include one-hot encoding [43], which creates binary vectors where each position corresponds to a specific residue, and physicochemical property encoding [48], which represents amino acids by their biochemical properties. While simple and interpretable, these methods often produce high-dimensional sparse representations that may not capture sequence context.

K-mer based methods [39] have gained popularity for representing sequences through the frequencies of contiguous subsequences of length k . These methods have been successfully applied to various sequence analysis tasks [8] and form the basis for alignment-free sequence comparison [49]. Minimizers [50, 51], originally developed for efficient sequence indexing, select a representative subset of k -mers based on lexicographic ordering, providing a more compact representation while maintaining sequence similarity relationships [52].

Deep learning-based representations have emerged as powerful alternatives. Word2vec-inspired approaches [9] treat biological sequences as sentences and k -mers as

words, learning distributed representations that capture semantic relationships. Protein language models such as ESM [53], ProtBERT [54], and more recent foundation models [55] learn contextualized embeddings from large sequence databases, capturing evolutionary and functional information. For SARS-CoV-2 specifically, Spike2Vec [10] adapts the word2vec paradigm to learn embeddings from spike protein sequences. However, these sophisticated embedding methods still benefit from dimensionality reduction for visualization and exploratory analysis.

Assessing the quality of dimensionality reduction is challenging due to the inherent information loss when projecting from high to low dimensions. Evaluation approaches can be broadly categorized into subjective (visual) and objective (quantitative) methods. Visual assessment [12] examines the interpretability and separation of clusters in low-dimensional plots but is inherently subjective and can be influenced by perceptual biases. Quantitative metrics attempt to measure specific aspects of embedding quality.

Local structure preservation metrics focus on whether neighborhoods are maintained during dimensionality reduction. The k-ary neighborhood agreement [56] measures the overlap between k-nearest neighbors in high and low dimensions. The trustworthiness and continuity metrics [57] quantify false neighbors (points that are neighbors in low dimension but not in high dimension) and missing neighbors (vice versa), respectively. The co-ranking matrix [58] provides a comprehensive framework for evaluating both local and global structure preservation.

Global structure preservation can be assessed through metrics such as the preservation of pairwise distances or rank correlations between distance matrices [59]. The normalized stress [60] measures the difference between distances in the original and embedded spaces. The Area Under the RNX curve (AUC_{RNX}) [61] aggregates neighborhood preservation across multiple scales, providing a single comprehensive score. These objective metrics enable rigorous comparison of different dimensionality reduction methods and parameter settings.

While extensive research has been conducted on dimensionality reduction techniques, kernel methods, and biological sequence analysis, several important gaps remain. First, despite the widespread use of t-SNE in computational biology, the impact of kernel function selection on t-SNE performance for biological sequences has not been systematically investigated. Most studies employ the default Gaussian kernel without exploring alternatives that might be more appropriate for categorical sequence data. Second, while the isolation kernel has been proposed as an improvement over the Gaussian kernel for general datasets [13], its effectiveness for biological sequences with their unique properties (discrete alphabet, evolutionary relationships, varying lengths) remains unexplored. Third, the interplay between sequence embedding methods and kernel functions has not been comprehensively studied, leaving practitioners without clear guidance on method selection. Finally, most prior work focuses solely on visualization quality without examining how kernel choice affects downstream analytical tasks such as classification and clustering, which are often the ultimate goals of sequence analysis pipelines. This paper addresses these gaps through systematic evaluation of nine kernel functions across multiple embedding methods and datasets, with assessment spanning visualization quality, computational efficiency, and downstream task performance.

3 Kernel Matrix Computation

In this section, we describe different methods to compute the kernel matrix.

3.1 Cosine similarity

Cosine similarity works on any two given row vectors by computing the L2-normalized dot product between them,

$$k(x, y) = \frac{\|x\| \|y\| \times \cos(\theta)}{\|x\| \|y\|} = \frac{x \cdot y}{\|x\| \|y\|} \quad (1)$$

It is the cosine of the angles (a.k.a angle of separation) between the two points derived from the euclidean normalization of vectors. It uses the cosine value of the angle between two row vectors. The values range between 1 and 0. Where 1 denotes two row vectors are similar while 0 represents opposite. The kernel matrix $n \times n$ is computed using the cosine similarity-based method for n sequences.

3.2 Linear Kernel

The linear kernel is a specific case of the polynomial kernel with a degree 1. Given two column vectors, it takes the inner product of these vectors and adds an optional constant c ,

$$k(x, y) = x^T y + c \quad (2)$$

It can be applied to linearly separable data.

3.3 Polynomial Kernel

Given two row vectors x and y , it gives the relationship between them across dimensions. Can be defined by,

$$k(x, y) = (x^T y + r)^d \quad (3)$$

where r is polynomial's coefficient and d represents the degree of the polynomial. And these parameters are determined using cross-validation. The polynomial kernel is used to compute the relationship between observations in higher dimensions when data is non-linearly separable in lower dimensions.

3.4 Gaussian Kernel

For any N points, the N -dimensional Gaussian kernel is computed by calculating the kernel coordinates of each point in the data space. For a point, the coordinates are determined by calculating its distance to the chosen points and taking the Gaussian function of these distances. In short, this kernel translates the dot product in N -dimensional space into the Gaussian function of the distance between points in the data space. The Gaussian kernel in 2D is defined as,

$$\mathcal{K}(x, y) = \exp\left(\frac{-\|x - y\|^2}{2\sigma^2}\right) \quad (4)$$

here σ defines the width of the kernel. We use Squared Euclidean distance to compute the difference with perplexity value 250 and we are tuning σ .

3.5 Isolation Kernel

It is a data-dependent kernel that is efficient to compute due to only one parameter being used. Unlike the Gaussian kernel, it adapts to local density distribution. The formal definition of isolated kernel given by authors of [13] is as follows:

For points $x, y \in \mathbb{R}^d$, the Isolation kernel of x and y wrt D is defined to be the expectation taken over the probability distribution on all partitioning $H \in \mathbb{H}_\psi(D)$ that both x and y fall into the same isolating partition $\theta[z] \in H, z \in D$:

$$K_\psi(x, y | D) = \mathbb{E}_{\mathbb{H}_\psi(D)}[\mathcal{K}(x, y \in \theta[z] | \theta[z] \in H)] \quad (5)$$

3.6 Laplacian

The laplacian kernel is a variant of RBF where the Manhattan distance between input feature vectors is used instead of Euclidean distance. Can be denoted by,

$$k(x, y) = \exp\left(-\frac{1}{2\sigma^2}\|x - y\|_1\right) \quad (6)$$

where x and y are the input vectors and $\|x - y\|_1$ is the Manhattan distance between the input vectors.

3.7 Sigmoid Kernel

Computes the sigmoid kernel between two input feature vectors x and y . The sigmoid kernel is also known as a hyperbolic tangent or multilayer perceptron. It is defined as,

$$k(x, y) = \tanh(\gamma x^\top y + c_0) \quad (7)$$

where x, y are the input vectors, γ is slope, and c_0 is intercept.

3.8 Chi-squared Kernel

The input feature vector is assumed to be non-negative and is often normalized to have an L1-norm of one. The normalization is rationalized with the connection to the chi-squared distance, which is the distance between discrete probability distributions. The chi-squared kernel is given by:

$$k(x, y) = \exp\left(-\gamma \sum_i \frac{(x_i - y_i)^2}{x_i + y_i}\right) \quad (8)$$

3.9 Additive-chi-squared (Additive-chi2) Kernel

It is a Fourier approximation to chi-squared kernel. Given feature vectors x and y , it computes the additive-chi2 kernel. Its idea is to consider x and y to be non-negative. The additive-chi2 kernel is given by:

$$k(x, y) = \sum_i \frac{2x_i y_i}{x_i + y_i} \quad (9)$$

4 Applying t-SNE with Kernel Matrices

The t-SNE algorithm accepts an $n \times n$ kernel matrix as its input, with n representing the count of sequences (embedding vectors). It generates a lower-dimensional representation with dimensionality d , where $d = \{1, 2, \dots, n-1\}$. In essence, t-SNE aims to transform high-dimensional (HD) data into a low-dimensional (LD) space while maintaining the pairwise distances among embedding vectors. The objective is to ensure that inter-point distances in the LD space Y mirror those in the HD space X as faithfully as possible. The methodology proceeds through the following stages:

4.1 Computing Pairwise Affinities

Initially, t-SNE computes the Euclidean distance from each data point to every other point in the high-dimensional space. Various kernel functions can be employed for this purpose. These distances are subsequently transformed into conditional probabilities, referred to as pairwise affinities or similarity measures.

4.2 Probability Distribution in High Dimensions

The conditional probabilities are aggregated to form a joint distribution over point pairs, organized into a symmetric matrix. The joint probability is expressed as shown in Equation 10 (following [62]):

$$p_{j|i} = \frac{\exp\left(-\|x_i - x_j\|^2 / 2\sigma_i^2\right)}{\sum_{k \neq i} \exp\left(-\|x_i - x_k\|^2 / 2\sigma_i^2\right)} \quad (10)$$

4.3 Initialization of Low-Dimensional Solution

The low-dimensional representation Y is initialized with randomly generated values. These initial values undergo iterative optimization to achieve the optimal lower-dimensional mapping of the data.

4.4 Probability Distribution in Low Dimensions

Analogous to the high-dimensional case, conditional probabilities are computed for the low-dimensional space and aggregated into a joint probability distribution, defined as (per [63]):

$$Q_{ij} = \begin{cases} 0 & j = i \\ \frac{(1 + \|\mathbf{y}_i - \mathbf{y}_j\|^2)^{-1}}{\sum_{k \neq l} (1 + \|\mathbf{y}_k - \mathbf{y}_l\|^2)^{-1}} & j \neq i \end{cases} \quad (11)$$

4.5 KL Divergence Calculation and Gradient Computation

To quantify the discrepancy between the HD distribution P and LD distribution Q , the Kullback-Leibler (KL) divergence is utilized. This metric captures the distributional differences in pairwise distances. The KL divergence is formulated as:

$$J = \min KL(P\|Q) = \sum_i \sum_j p_{ij} \log \frac{p_{ij}}{q_{ij}} \quad (12)$$

where J denotes the objective function to be minimized, P and Q represent the HD and LD distributions respectively, and y_i, y_j are coordinates in the LD space Q .

The gradient of the cost function is derived using Equation 13 (as presented in [62]) to identify the minimum of J :

$$\nabla = \frac{\delta J}{\delta y_i} = 4 \sum_j (p_{ij} - q_{ij}) (y_i - y_j) \left(1 + \|y_i - y_j\|^2\right)^{-1} \quad (13)$$

The LD coordinates Y are iteratively refined to minimize J according to Equation 14. The application of the t-distribution in this Stochastic Neighborhood Embedding (SNE) framework, specifically applied to the LD distribution Q , produces heavier tails that enhance visualization quality.

$$y^{(t)} = y^{(t-1)} + \eta \nabla + \alpha(t) \left(y^{(t-1)} - y^{(t-2)}\right) \quad (14)$$

where $t \in T$ denotes the iteration number.

Figure 1 illustrates the t-SNE workflow. The procedure begins with computing pairwise affinities through kernel functions to construct a similarity matrix. Probability values are then derived from the distances for points X (where $X \in R^n$, representing the high-dimensional space). Subsequently, the solution Y is initialized randomly. The joint probabilities in both HD (P_{ij}) and LD (Q_{ij}) are computed. KL divergence measures the distributional discrepancy, and through gradient descent of this objective function, the optimal Y emerges after multiple iterations. This optimized Y constitutes the LD representation of the HD data points X .

The initial step of deriving probabilities from distances is fundamental. The calculated distances significantly influence how data distributes on the t-distribution for visualization and affects dimensionality reduction effectiveness. Kernel functions are crucial in determining inter-point distances in the original data space. Algorithm 1 presents the detailed workflow for t-SNE computation using a kernel matrix as input.

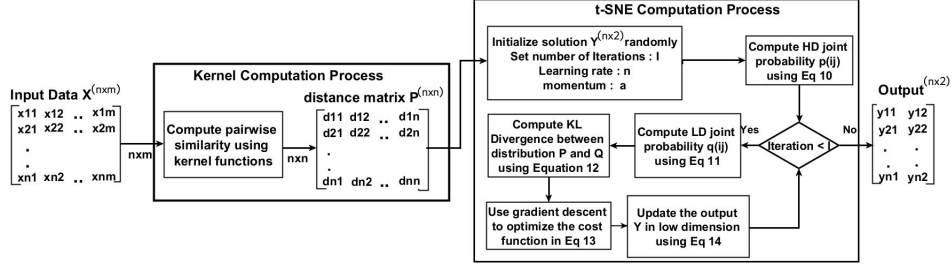


Fig. 1: Overall architecture of the proposed approach. Starting from the input data, we compute a kernel matrix through various kernel functions, followed by the t-SNE algorithm to obtain the low-dimensional embedding.

Algorithm 1 t-SNE Algorithm Workflow.

```

1: Input:  $(KM, dim)$ 
    $KM = x[i][j], x_{ij} \in R^n$ 
   dim: target dimensionality
   ▷ KM represents the Kernel Matrix
   ▷ desired output dimension

2: Output:  $Y = [y_1, y_2, y_3, \dots, y_N], y_i \in R^{dim}$ 
3: Function: tSNE( $KM, dim$ )
4:  $Y = matrix(n, dim)$ 
   ▷ initialize output with random values
5: //Initialize hyperparameters for optimization
6:  $I = 1000$ 
   ▷ Maximum iterations
7:  $\eta = 500$ 
   ▷ Step size parameter
8:  $\alpha = 0.5$ 
   ▷ momentum coefficient
9:  $P = matrix(n \times n)$ 
   ▷ HD probability distribution
10: for  $i \leftarrow 1$  to  $n$  do
11:   for  $j \leftarrow 1$  to  $n$  do
12:      $P_{ij} = COMPUTEPROBABILITY(KM_{i,j})$ 
   ▷ via Eq 10
13:  $Q = matrix(n \times 2)$ 
   ▷ LD probability distribution
14: for  $k \leftarrow 1$  to  $I$  do
   ▷ Main optimization loop
15:   for  $i \leftarrow 1$  to  $n$  do
16:     for  $j \leftarrow 1$  to  $n$  do
17:        $Q_{ij} = COMPUTEPROBABILITY(Y_{i,j})$ 
   ▷ via Eq. 11
18:    $J = COMPUTEKLDIVERGENCE(P, Q)$ 
   ▷ Calculate KL Divergence using Eq 12
19:
20:    $\nabla = COMPUTEGRADIENT(J)$ 
   ▷ via Eq 13
21:    $Y = UPDATEOUTPUT(Y, \alpha, \eta, \nabla)$ 
   ▷ via Eq 14
22:   if  $(k == 250)$  then  $\alpha = 0.8$ 
   ▷ adjust momentum at iteration 250
23: return  $Y$ 

```

5 Generation of Feature Embeddings

This section presents three distinct embedding techniques employed to transform biological sequences into fixed-dimensional numerical vectors.

1. One Hot Encoding (OHE) - We employ OHE [8, 43] to encode amino acids into their numerical counterparts.

2. Spike2Vec [10] - This approach produces fixed-dimensional numerical vectors by leveraging the k -mer (n-gram) methodology. The technique utilizes a sliding window mechanism to extract substrings (termed mers) of length k (corresponding to the window size) as demonstrated in Figure 2.

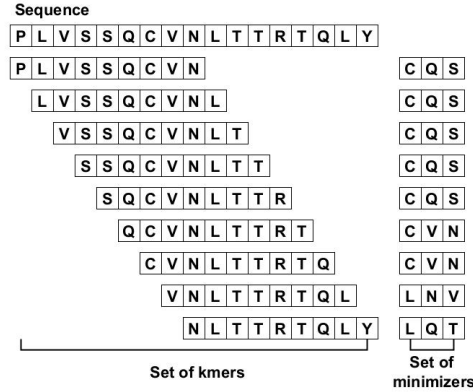


Fig. 2: Illustration of k mers and minimizers for the amino acid sequence “PLVSSQCVNLTTRTQLP”.

3. Minimizers - From each k mer, a minimizer is extracted as a substring (mer) with length m (satisfying $m < k$) that represents the lexicographically smallest element when comparing both forward and reverse orientations of the k -mer. The minimizer computation process is depicted in Figure 3 and detailed in Algorithm 2.
4. Spaced k-mers [64] - This method generates a non-contiguous variant of k-mers by initially constructing g -mers, where $g \leq k$. Subsequently, the k -mer is derived from the g -mer by selecting the first k amino acids/nucleotides when arranged in lexicographic order considering both forward and reverse orientations. The final embedding is constructed based on the frequency of these non-contiguous k-mers.

Algorithm 2 Algorithm for Minimizer Extraction

```

1: Input: Sequence  $seq$ , parameters  $klen$  and  $mle$ n
2: Output: Set of Minimizers
3:  $minis = \emptyset$ 
4:  $q = []$  ▷ queue for m-mers
5:  $ind = 0$  ▷ index tracking current minimizer
6:
7: for  $i \leftarrow 1$  to  $|seq| - klen + 1$  do
8:    $kmer = seq[i : i + klen]$ 
9:   if  $ind > 1$  then
10:     $q.dequeue$ 
11:     $mmer = seq[i + klen - mle : i + k]$  ▷ extract new m-mer
12:     $ind \leftarrow ind - 1$  ▷ adjust minimizer index
13:     $mmer = \min(mmer, backward(mmer))$  ▷ select lexicographic minimum
14:     $q.enqueue(mmer)$ 
15:    if  $mmer < q[ind]$  then  $ind = klen - mle$  ▷ refresh minimizer position
16:  else
17:     $q = []$  ▷ reinitialize queue
18:     $ind = 0$ 
19:    for  $j \leftarrow 1$  to  $klen - mle + 1$  do ▷ generate m-mer
20:       $mmer = kmer[j : j + mle]$ 
21:       $mmer = \min(mmer, reverse(mmer))$ 
22:       $q.enqueue(mmer)$ 
23:      if  $mmer < q[ind]$  then
24:         $ind = j$  ▷ track minimizer position
25:     $minis \leftarrow minis \cup q[ind]$  ▷ store identified minimizer
26: return ( $minis$ )
  
```

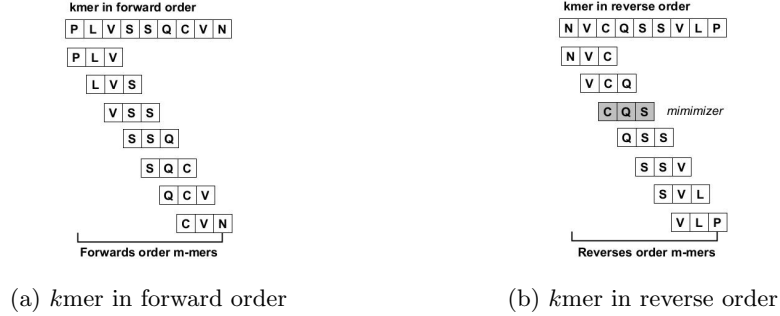


Fig. 3: Computation of minimizer from $kmer$.

6 Experimental Setup

In this section, we first discuss the dataset statistics followed by the goodness metrics used to evaluate the performance of t-SNE, classification, and clustering methods. All experiments are performed on Intel (R) Core i5 system with a 2.40 GHz processor and 32 GB memory. Also, we use the 5 fold cross-validation.

6.1 Datasets

We use the following datasets in this study.

6.1.1 Spike7k

The dataset we use is Spike7k [8] consists of sequences of the SARS-CoV-2 virus. It has 22 unique lineages as the label with the following distribution: B.1.1.7 (3369), B.1.617.2 (875), AY.4 (593), B.1.2 (333), B.1 (292), B.1.177 (243), P.1 (194), B.1.1 (163), B.1.429 (107), B.1.526 (104), AY.12 (101), B.1.160 (92), B.1.351 (81), B.1.427 (65), B.1.1.214 (64), B.1.1.519 (56), D.2 (55), B.1.221 (52), B.1.177.21 (47), B.1.258 (46), B.1.243 (36), R.1 (32).

6.1.2 Host

The NIAD Virus Pathogen Database and Analysis Resource (ViPR) [65] and GISAID [1] are used to retrieve Spike molecular sequences of CoVs for all hosts. The dataset comprises of 5558 complete unaligned spike protein sequences with the 21 host types with the following counts of sequences: Humans(1813), Rats(26), Cats(123), Environment(1034), Pangolins(21), Bovines(88), Weasel(994), Hedgehog(15), Dogs(40), Swine(558), Dolphin(7), Python(2), Birds(374), Equine(5), Monkey(2), Camels(297), Fish(2), Cattle(1), Bats(153), Unknown(2), Turtle(1).

6.1.3 ShortRead

This dataset is generated by taking 10181 SARS-CoV-2 nucleotide sequences and simulating short reads from each sequence using inSilicoSeq¹ with the miseq model (all other settings were default settings). The lineages/class labels (count/distribution) in this dataset is as follows: B.1.1.7 (2587), B.1.617.2 (1198), AY.4 (1167), AY.43 (412), AY.25 (275), B.1.2 (253), AY.44 (249), B.1 (200), B.1.177 (184), AY.3 (166), P.1 (137), B.1.1 (128), B.1.526 (112), AY.9 (108), AY.5 (96), AY.29 (86), AY.39 (85), B.1.429 (81), B.1.160 (79), Others (2578). There are 496 unique lineages for 10181 sequences.

6.1.4 Rabies

We used the labeled Nucleotide genome sequences for rabies virus hosts dataset from RABV-GLUE², where the label is the name of the host for which we are classifying the sequences. The statistics of the rabies dataset are given in Table 1.

¹<https://github.com/HadrienG/InSilicoSeq>

²<http://rabv-glue.cvr.gla.ac.uk/#/home>

Name	Type	Source	Sequence Count	Classes	Sequence Length			
					Min	Max	Avg	Mode
Rabies Virus Data	Nucleotide sequences for rabies virus hosts	RABV-GLUE [66]	20051	12	90	11930	1948.4	1353

Table 1: Data Statistics.

6.1.5 Genome

Using the well-known and widely used database of SARS-CoV-2, GISAID [1], we retrieve the full-length nucleotide sequences of the coronavirus. We include the COVID-19 variant information and 8220 nucleotide sequences in our dataset. In our sample, there are 41 different versions altogether. The dataset statistics for the pre-processed genome data are provided in Table 2. The length of the Spike2Vec-based feature vector is $5^3 = 125$ (5 is a unique character in the sequence “ACGT-”).

Lineages	Sequence count	Lineages	Sequence count	Lineages	Sequence count	Lineages	Sequence count
AY.103	2271	AY.121	40	AY.4	100	AY.114	15
AY.44	1416	AY.75	37	AY.117	94	AY.34	14
AY.100	717	AY.3.1	30	AY.113	94	AY.125	14
AY.3	710	AY.3.3	28	AY.118	86	AY.46.1	14
AY.25	585	AY.107	27	AY.43	85	AY.92	13
AY.25.1	382	AY.34.1	25	AY.122	84	AY.127	12
AY.39	248	AY.46.6	21	BA.1	79	AY.46.4	12
AY.119	242	AY.98.1	20	AY.119.2	74	AY.98	12
B.1.617.2	175	AY.13	19	AY.47	73	AY.111	10
AY.20	130	AY.116.1	18	AY.39.1	70		
AY.26	107	AY.126	17				
						Total	8220

Table 2: Dataset Statistics for full length **Genome (nucleotide) data** (8000 sequences) comprised of 41 lineages (class labels).

6.1.6 Breast Cancer

The dataset on Membranolytic anticancer peptides (ACPs) [67] provides details regarding peptide sequences and their corresponding anticancer effectiveness against breast and lung cancer cell lines. The target labels are classified into four groups: “very active,” “moderately active,” “experimental inactive,” and “virtual inactive.” In total, the dataset comprises 949 peptide sequences for breast cancer. Table 3 shows the distribution.

6.2 Clustering Algorithms Evaluation

For clustering-based analysis of different embedding methods, we use standard k -means and k -modes algorithms. To get the optimal number of clusters, we use the elbow method [68]. For this purpose, we measure the trade-off between clustering

ACPs Category	Count	Min.	Max.	Average
Inactive-Virtual	750	8	30	16.64
Moderate Active	98	10	38	18.44
Inactive-Experimental	83	5	38	15.02
Very Active	18	13	28	19.33
Total				949

Table 3: Dataset statistics for the Breast cancer data. Columns represent the min., max., and average lengths of the sequence.

runtime and the sum of squared distances from each point to its center (also called distortion) for the different number of clusters (ranging from 2 to 14). The optimal number of clusters selected is 5 from the elbow method. To measure the goodness of clustering approaches, the first metric we use is silhouette coefficient [69], which uses cohesion (within the cluster) and separation (between different clusters) combined to compute a goodness score for a given clustering. Its value is between -1 to 1 with a higher value being better. The second metric that we are using is the Calinski–Harabasz index [70], which measures the ratio of inter-cluster dispersion for all clusters and the sum of intra-clusters dispersion (higher value is better). The third metric that we are using is Davies–Bouldin score [71], which measures the similarity of each cluster with its most similar cluster, repeats this process for all clusters and reports the average (a lower value is better). We also use clustering computation runtime as the fourth evaluation metric.

6.3 Classification Algorithms Evaluation

For classification, we use Support Vector Machine (SVM), Naive Bayes (NB), Multi-Layer Perceptron (MLP), K-Nearest Neighbour (KNN) (with $K = 5$, which decided using standard validation set approach [72]), Random Forest (RF), Logistic Regression (LR), and Decision Tree (DT) classifiers. We use average accuracy, precision, recall, weighted, and ROC area under the curve (AUC) as evaluation metrics for measuring the goodness of classification algorithms.

6.4 Evaluating t-SNE

For objectively evaluation of the t-SNE model, we use a method called k -ary neighborhood agreement (k -ANA) method [13]. The k -ANA method (for different k nearest neighbors) checks the neighborhood agreement (Q) between HD and LD and takes the intersection on the numbers of neighbors. More formally:

$$Q(k) = \sum_{i=1}^n \frac{1}{nk} |kNN(x_i) \cap kNN(x'_i)| \quad (15)$$

where $kNN(x)$ is set of k nearest neighbours of x in high-dimensional and $kNN(x')$ is set of k nearest neighbours of x in corresponding low-dimensional.

We use a quality assessment tool that quantifies the neighborhood preservation and is denoted by $R(k)$, which uses Equation 15 to evaluate on scalar metric whether neighbors are preserved[56] in low dimensions. More formally:

$$R(k) = \frac{(n-1)Q(k) - k}{n-1-k} \quad (16)$$

$R(k)$ represents the measurement for k -ary neighborhood agreement. Its value lies between 0 and 1, the higher score represents better preservation of the neighborhood in LD space. In our experiment we computed $R(k)$ for $k \in 1, 2, 3, \dots, 99$ then considered the area under the curve (AUC) formed by k and $R(k)$. Finally, to aggregate the performance for different k-ANN, we calculate the area under the $R(k)$ curve in the log plot (AUC_{RNX}) [61]. More formally:

$$AUC_{RNX} = \frac{\sum_k \frac{R(k)}{k}}{\sum_k \frac{1}{k}} \quad (17)$$

where AUC_{RNX} denotes the average quality weight for k nearest neighbors.

7 Subjective and Objective Evaluation of t-SNE

The subjective evaluation for different embedding methods is shown below.

7.1 OHE [43]

The t-SNE plots for one-hot embedding are given in Figure 4 for different kernel methods. For the Alpha variant (B.1.1.7), we can see that Gaussian, Isolation, Linear, and Cosine kernel are able to generate a clear grouping. However, for the other variants having small representation in the dataset (e.g. B.1.617.2 and AY.4), we can observe that the Cosine and linear kernels are better than the Gaussian and Isolation kernel. This could mean that the Gaussian and Isolation kernels tend to show biased behavior towards the more representative class (alpha variant).

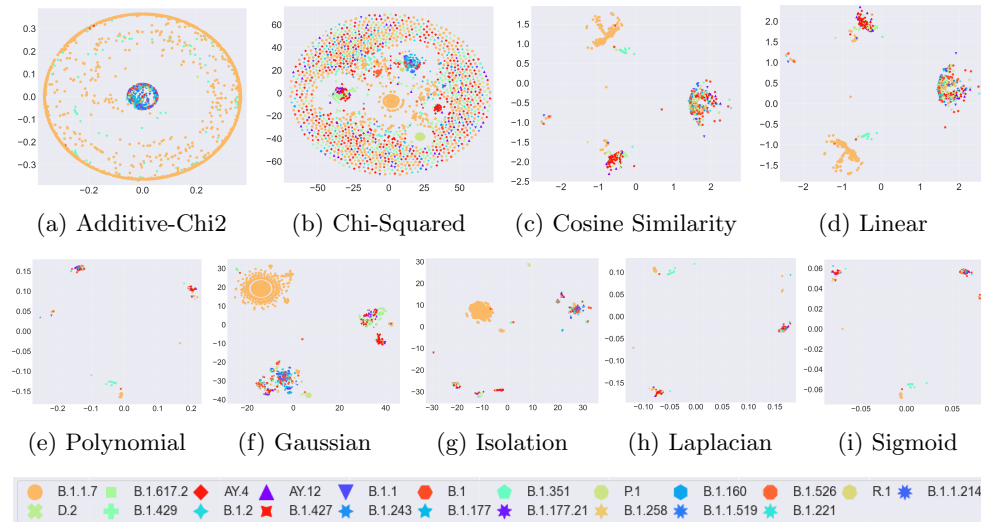


Fig. 4: t-SNE plots for different kernel methods using One-Hot Embedding. This figure is best seen in color.

7.2 Spike2Vec [10]

The t-SNE plots for Spike2vec-based embeddings are given in Figure 5 using different kernel methods. It is similar behavior to OHE, where the Gaussian and isolation kernels group the alpha (B.1.1.7) variant almost perfectly, however, all other variants are scattered around in the plot.

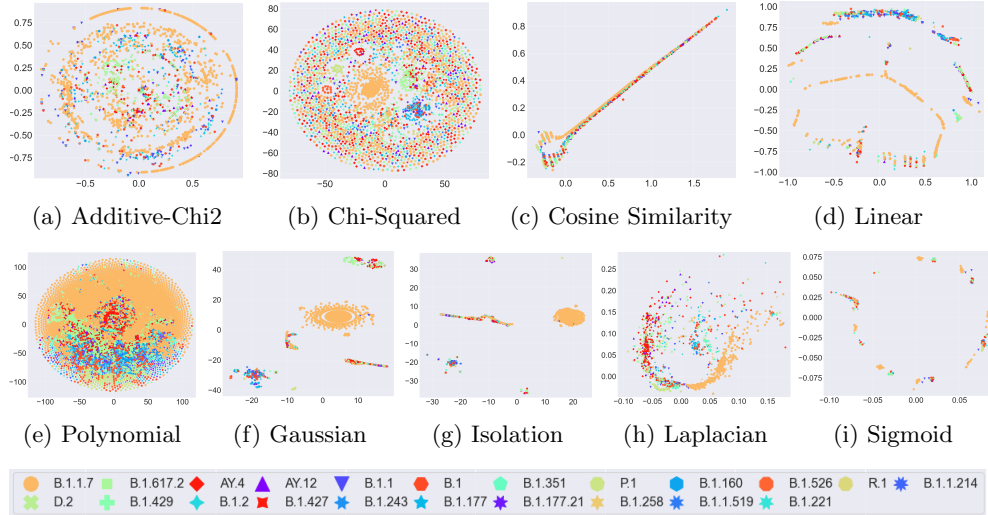


Fig. 5: t-SNE plots for different kernel methods using Spike2Vec-based Embedding. This figure is best seen in color.

7.3 Minimizer

The t-SNE plots for one-hot embedding are given in Figure 6 for different kernel methods. For the Gaussian and isolation kernel, we can observe similar behavior for the alpha (B.1.1.7) variant. Note that similar behavior is observed for the Spaced k-mers embedding. Moreover, Figure 7 shows the top 3 performing kernels in terms of AUC_{RNX} score for the respective embedding.

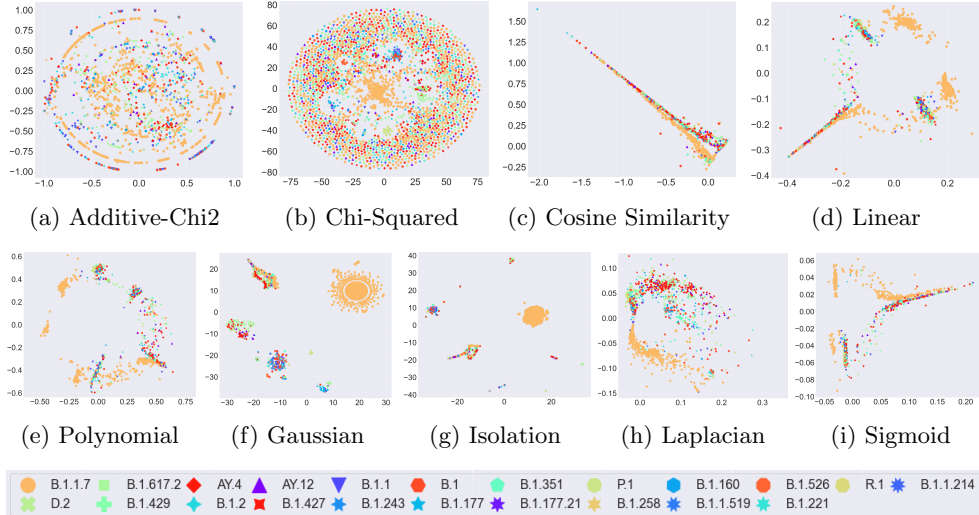


Fig. 6: t-SNE plots for different kernel methods using minimizers-based Embedding.

We also show the 3D plots for t-SNE using the Cosine similarity kernel in Figure 8 (for Spike2Vec and Minimizers-based embedding using Spike7k dataset). We can see for Spike2Vec, the Alpha variant shows clear grouping. Similarly, the delta and epsilon variant also contains a few small groups.

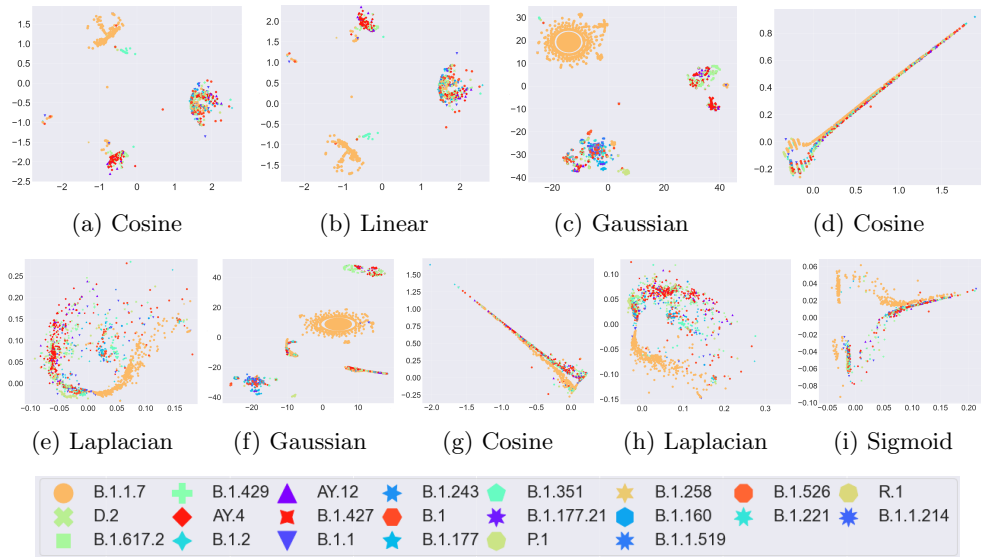


Fig. 7: t-SNE plots for top performing kernel methods for different embedding. This figure is best seen in color. (a), (b) and (c) are from OHE. (d), (e), and (f) are from Spike2Vec. (g), (h) and (i) are from Minimizer encoding

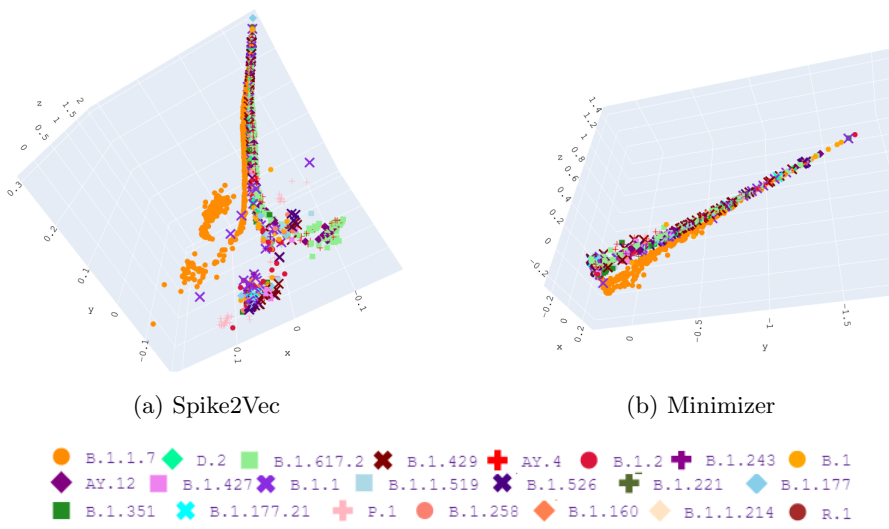


Fig. 8: t-SNE 3d plots using Cosine similarity kernel.

8 Objective evaluation of t-SNE

For objective evaluation of different kernel methods and embeddings on different datasets, we use the formulation mentioned in Equation 17. Table 4 demonstrates that cosine similarity achieves superior performance on the Spike7k dataset, particularly when combined with Spike2Vec encoding ($AUC_{RNX} = 0.331$). The computational efficiency of cosine similarity is notable, with kernel computation times substantially lower than chi-squared or Laplacian kernels. Spaced-Kmer encoding shows near-zero AUC_{RNX} values across all kernels, suggesting poor neighborhood preservation for this representation on spike protein sequences.

Kernel	OHE		Spike2Vec		Minimizer		Spaced-Kmer	
	Kernel Comput. Time	AUC_{RNX}	Kernel Comput. Time	AUC_{RNX}	Kernel Comput. Time	AUC_{RNX}	Kernel Comput. Time	AUC_{RNX}
Cosine similarity	37.351	0.262	15.865	0.331	17.912	0.278	92.516	0.00009
Linear	51.827	0.260	30.978	0.197	27.503	0.165	66.546	0.00006
Gaussian	94.784	0.199	54.192	0.235	65.096	0.206	560469.5	0.00009
Sigmoid	57.298	0.190	30.037	0.168	27.813	0.229	74.722	0.00002
Laplacian	2250.30	0.184	721.834	0.260	983.26	0.242	59670.6	0.00021
Polynomial	57.526	0.177	28.427	0.059	28.666	0.166	79.763	0.00010
Isolation	39.329	0.161	24.162	0.189	27.266	0.172	106.152	0.00005
Chi-squared	1644.86	0.131	495.264	0.104	921.63	0.095	139165.3	0.00003
Additive-chi2	1882.45	0.110	495.221	0.121	576.92	0.125	128310.4	0.00007

Table 4: AUC_{RNX} values for t-SNE using different kernel and encoding methods on **Spike7k datasets**. The best values are shown in bold.

For the Host dataset (Table 5), chi-squared and sigmoid kernels with Spike2Vec encoding yield the highest AUC_{RNX} values (0.144 using Chi-squared and 0.143 using Sigmoid, respectively), though at considerable computational cost in case of Chi-squared kernel.

Kernel	OHE		Spike2Vec		Minimizer		Spaced-Kmer	
	Kernel Comput. Time	AUC_{RNX}						
Cosine similarity	11.203	0.0205	5.072	0.126	2.781	0.094	174.508	0.129
Linear	7.936	0.0087	4.127	0.043	4.527	0.106	100.539	0.037
Gaussian	7636.44	0.0180	197498.2	0.139	12847.7	0.122	44046.5	0.135
Sigmoid	9.55	0.0206	6.16	0.143	4.477	0.0006	147.634	0.031
Laplacian	5811.897	0.0214	1019.6	0.135	1252.822	0.131	24516.9	0.135
Polynomial	9.366	0.0011	8.506	0.005	8.523	0.106	140.172	0.099
Isolation	49.641	0.00004	66.745	0.0007	47.847	0.0001	66.431	0.011
Chi-squared	19447.176	0.0201	3482.3	0.144	3581.766	0.105	57711.9	0.136
Additive-chi2	3241.723	0.0136	3547.94	0.048	3227.774	0.069	57408.6	0.041

Table 5: AUC_{RNX} values for t-SNE using different kernel and encoding methods on **Host datasets**. The best values are shown in bold.

Table 6 reports AUC_{RNX} values for different kernels and embeddings on short read dataset. The near-zero values across most kernel-encoding combinations indicate poor neighbourhood preservation quality for short read sequences.

Kernel	OHE		Spike2Vec		Minimizer		Spaced-Kmer	
	Kernel Comput. Time	AUC_{RNX}						
Cosine similarity	28.702	0.00009	1.271	0.0001	1.338	0.406	0.969	0.0625
Linear	20.649	0.00001	1.342	0.0007	1.296	0.00013	0.945	0.0001
Gaussian	170685.3	0.00002	2494.6	0.0002	2545.1	2.681	3278.294	0.0007
Sigmoid	22.484	0.00001	2.847	0.0004	2.574	0.0012	2.397	0.0002
Laplacian	32735.7	0.00004	21.449	0.0001	21.176	0.0007	117.818	0.0005
Polynomial	25.675	0.00008	16.387	0.0006	16.557	0.0001	16.645	0.0251
Isolation	144.783	0.00006	139.55	0.0001	138.88	0.0005	138.307	0.0004
Chi-squared	175684.8	0.00002	60.684	0.0009	50.787	0.0275	490.043	0.0009
Additive-chi2	176235.1	0.00011	57.273	0.0003	45.024	0.0942	371.799	0.0944

Table 6: AUC_{RNX} values for t-SNE using different kernel and encoding methods on **Short Read dataset**. The best values are shown in bold.

On the Rabies dataset (Table 7), Minimizer and Spaced-Kmer encodings demonstrate strong neighborhood preservation ($AUC_{RNX} \approx 0.13 - 0.15$) when paired with cosine similarity, Gaussian, or Laplacian kernels. These results are achieved with moderate computational overhead (other than gaussian kernel), establishing an effective balance between accuracy and efficiency for viral genome analysis.

Kernel	OHE		Spike2Vec		Minimizer		Spaced-Kmer	
	Kernel Comput. Time	AUC_{RNX}						
Cosine similarity	57.115	0.033630	32.92	0.029732	5.446	0.15034	7.833	0.134273
Linear	49.279	0.028748	25.18	0.005480	13.017	0.018272	11.082	0.014808
Gaussian	284038.726	0.023793	102629.365	0.024123	4938.652	0.147844	6018.947	0.133738
Sigmoid	59.17	0.004990	60.5	0.029248	21.495	0.000685	18.433	0.133057
Laplacian	66975.297	0.031071	16292.126	0.031966	234.528	0.147133	549.362	0.133938
Polynomial	74.54	0.023586	95.51	0.000480	131.311	0.001318	36.505	0.001871
Isolation	1997.925	0.000023	1843.375	0.000071	1774.019	0.000054	2443.647	0.000071
Chi-squared	80852.645	0.034822	20574.939	0.036115	375.659	0.147215	580.142	0.133544
Additive-chi2	125464.199	0.004369	18511.205	0.009503	332.14	0.028714	580.384	0.052454

Table 7: AUC_{RNX} values for t-SNE using different kernel and encoding methods on **Rabies datasets**. The best values are shown in bold.

Table 8 shows modest AUC_{RNX} values across all configurations, with Laplacian and Gaussian kernels paired with Minimizer or Spaced-Kmer encodings achieving the best performance ($AUC_{RNX} \approx 0.034 - 0.038$). The substantially longer computation times for certain kernels suggest that genome-scale data requires careful consideration of the accuracy-efficiency tradeoff.

For the Breast Cancer dataset (Table 9), chi-squared kernel with Minimizer encoding achieves the highest AUC_{RNX} (0.0458), though polynomial kernel with Spaced-Kmer also performs well (0.09228). The relatively low computation times

Kernel	OHE		Spike2Vec		Minimizer		Spaced-Kmer	
	Kernel Comput. Time	AUC_{RNX}						
Cosine similarity	512.508	0.000363	2.584	0.002	2.131	0.003	3.015	0.012
Linear	376.152	0.000216	1.666	0.0301	1.795	0.0336	2.828	0.032
Gaussian	959921.408	0.000196	4267.259	0.034	4004.788	0.0387	4305.981	0.034
Sigmoid	466.266	0.000240	4.082	0.0001	2.803	0.0211	3.871	0.0003
Laplacian	181529.777	0.000428	34.778	0.0336	28.244	0.0389	127.441	0.0351
Polynomial	497.364	0.000424	26.636	0.0323	19.756	0.034	15.552	0.0341
Isolation	191.014	0.000050	190.145	0.0225	231.071	0.0250	152.033	0.0001
Chi-squared	455003.79	0.000560	91.718	0.0341	90.251	0.0379	422.979	0.034
Additive-chi2	449293.663	0.000364	74.021	0.004	62.237	0.0159	404.173	0.0047

Table 8: AUC_{RNX} values for t-SNE using different kernel and encoding methods on **Genome datasets**. The best values are shown in bold.

across most configurations indicate this smaller dataset enables exploration of more computationally intensive kernel methods without prohibitive runtime penalties.

Kernel	OHE		Spike2Vec		Minimizer		Spaced-Kmer	
	Kernel Comput. Time	AUC_{RNX}						
Cosine similarity	0.184	0.001059	1.841	0.0018	1.86	0.037	39.556	0.0226
Linear	0.168	0.000826	1.767	0.0015	1.599	0.0281	33.601	0.0136
Gaussian	73.039	0.000581	139.648	0.0006	155.362	0.00955	3822.062	0.00521
Sigmoid	0.37	0.001120	1.992	0.0009	2.985	0.0289	32.741	0.0002
Laplacian	2.764	0.001558	31.888	0.0005	35.299	0.04002	1070.505	0.0136
Polynomial	0.523	0.000187	1.686	0.0006	1.926	0.0398	31.912	0.09228
Isolation	0.975	0.000812	0.807	0.0003	0.847	0.00057	5.048	0.00012
Chi-squared	8.122	0.002648	57.782	0.0004	55.306	0.0458	1589.326	0.0193
Additive-chi2	8.623	0.000286	55.848	0.0001	57.097	0.0132	1779.769	0.00361

Table 9: AUC_{RNX} values for t-SNE using different kernel and encoding methods on **Breast Cancer datasets**. The best values are shown in bold.

9 Clustering Results

We assess the quality of various embedding approaches by applying clustering algorithms with different kernel methods to the embeddings. Table 10 presents the clustering performance (for both k -means and k -modes) measured through multiple internal validation metrics. The results reveal that for k -means clustering, the sigmoid kernel demonstrates superior performance according to Silhouette Coefficient and Calinski-Harabasz metrics, whereas the Gaussian kernel excels based on the Davies-Bouldin metric. For k -modes clustering, the chi-squared kernel achieves the best results across all three evaluation criteria. Table 10 also reports clustering performance for Spike2Vec embeddings. When applying k -means, the polynomial kernel yields optimal Silhouette Coefficient and Calinski-Harabasz values, while the Gaussian kernel produces the best Davies-Bouldin score. For k -modes clustering, the chi-squared kernel again dominates across all metrics, mirroring the pattern observed with OHE. Clustering results for minimizer-based embeddings are presented in Table 10. The k -means algorithm exhibits the same kernel preference as Spike2Vec embeddings: polynomial kernel leads for Silhouette Coefficient and Calinski-Harabasz metrics, while Gaussian kernel performs best for Davies-Bouldin score. However, for k -modes clustering, the Gaussian kernel achieves superior Silhouette Coefficient and Calinski-Harabasz scores, whereas the additive-chi2 kernel provides the best Davies-Bouldin performance.

Algo.	Kernel	OHE				Spike2vec				Minimizer				Spaced k-mer			
		Silhouette Coeff- cient	Calinski Harabasz Score	Davies- Bouldin Score	Clustering Run- time (Sec.)	Silhouette Coeff- cient	Calinski Harabasz Score	Davies- Bouldin Score	Clustering Run- time (Sec.)	Silhouette Coeff- cient	Calinski Harabasz Score	Davies- Bouldin Score	Clustering Run- time (Sec.)	Silhouette Coeff- cient	Calinski Harabasz Score	Davies- Bouldin Score	Clustering Run- time (Sec.)
k -means	Additive-chi2	0.841	31248.241	0.502	0.182	0.580	2880.192	1.273	0.164	0.527	2641.231	1.279	0.132	0.549	1130.892	1.810	4.850
	Chi-squared	0.485	2367.888	1.156	0.115	0.702	2926.907	0.342	0.091	0.677	2850.682	0.416	0.110	0.527	1930.648	0.578	3.623
	Cosine	0.841	31248.241	0.502	0.116	0.565	30861.077	0.755	0.178	0.549	12474.205	0.949	0.187	0.576	18573.876	0.984	3.072
	Gaussian	0.086	217.357	1.174	0.125	0.079	219.713	1.885	0.144	0.068	212.031	1.172	0.140	0.503	1943.049	0.629	3.946
	Isolation	0.166	310.932	1.426	0.127	0.149	273.187	1.345	0.156	0.165	282.180	1.347	0.221	0.847	281.357	0.628	6.754
	Laplacian	0.840	30573.981	0.501	0.166	0.528	2526.604	1.255	0.144	0.533	0.530	1392.3	1.553	20.909	18092.820	0.724	6.863
	Linear	0.841	31248.241	0.502	0.167	0.843	27829.114	0.496	0.150	0.740	13683.298	0.655	0.163	0.825	26567.483	0.385	11.527
Polynomial	0.840	30592.941	0.501	0.107	0.919	0.899	12497.3	0.286	4.888	98941.860	0.409	0.171	0.928	14345.965	0.244	8.427	
Sigmoid	0.841	31719.471	0.502	0.189	0.557	26013.129	0.773	0.129	0.538	11183.672	0.910	0.187	0.828	27887.420	0.392	2.298	
k -modes	Additive-chi2	-0.248	93.070	1.131	24.906	-0.383	27.507	1.854	17.810	-0.374	18.366	1.521	18.478	-0.647	19.314	1.327	8405.023
	Chi-squared	0.019	250.247	0.751	23.813	0.058	191.749	0.714	17.869	-0.351	10.807	2.136	22.274	-0.023	23.120	0.825	2216.556
	Cosine	-0.303	21.589	1.180	13.550	-0.522	4.697	1.678	14.733	-0.485	7.071	1.600	14.924	-0.712	1.558	1.673	3404.789
	Gaussian	-0.479	0.302	2.897	8.718	-0.468	0.293	2.855	8.646	-0.473	0.310	2.987	8.667	-0.093	62.989	17.431	3755.273
	Isolation	-0.489	0.212	3.272	8.528	-0.501	0.215	3.449	8.646	-0.490	0.270	3.418	9.065	-0.551	7.279	5.154	12523.985
	Laplacian	-0.308	13.880	1.187	15.750	-0.406	1.112	1.570	8.598	-0.386	0.908	1.563	9.593	-0.674	1.740	1.175	3167.464
	Linear	-0.255	94.817	1.130	23.265	-0.651	10.568	1.649	18.532	-0.500	27.030	1.595	18.902	-0.642	15.241	1.582	2580.823
Polynomial	-0.286	38.201	1.169	8.923	-0.817	0.037	1.842	11.054	-0.688	0.544	1.865	13.802	-0.703	0.750	1.654	842.016	
Sigmoid	-0.312	2.223	1.194	10.256	-0.385	0.745	1.781	8.578	-0.636	0.746	1.609	9.597	-0.715	5.497	1.297	1320.494	

Table 10: Internal clustering quality metrics for different kernels and embeddings on Spike7k dataset.

For the Host dataset (Table 11), the polynomial kernel demonstrates exceptional performance with k -means clustering, achieving remarkably high Silhouette Coefficient (0.975) and Calinski-Harabasz scores (13378.873) for both OHE and Spike2Vec embeddings, along with favorable Davies-Bouldin scores (0.516). The isolation kernel also exhibits strong clustering quality across all embeddings, though with relatively longer computation times. In contrast, k -modes clustering shows predominantly negative Silhouette Coefficients across all kernel-embedding combinations, indicating poor cluster separation. The Minimizer embedding with chi-squared kernel achieves the best k -modes performance (Calinski-Harabasz: 146.595), though computational overhead remains substantial.

Algo.	Kernel	OHE				Spike2vec				Minimizer				Spaced k-mer				
		Silhouette Coeff.	Calinski Harabasz Score	Davies-Bouldin	Clustering Runtime (Sec.)	Silhouette Coeff.	Calinski Harabasz Score	Davies-Bouldin	Clustering Runtime (Sec.)	Silhouette Coeff.	Calinski Harabasz Score	Davies-Bouldin	Clustering Runtime (Sec.)	Silhouette Coeff.	Calinski Harabasz Score	Davies-Bouldin	Clustering Runtime (Sec.)	
<i>k</i> -means	Additive-chi2	0.548	2160.474	1.279	2.012	0.552	2221.759	1.368	2.113	0.603	1962.352	1.389	2.489	0.647	2059.385	1.481	9.244	1.881
	Chi-squared	0.337	563.682	0.596	2.171	0.339	575.577	0.595	2.474	0.410	698.690	0.789	5.490	0.346	570.304	0.587	4.504	1.504
	Cosine	-0.630	9.605	1.261	4699.372	0.667	2697.411	1.425	11.714	0.595	2516.870	1.215	11.896	0.413	1964.520	1.251	15.052	1.502
	Gaussian	0.367	611.175	0.601	4.265	0.348	518.095	0.609	3.591	0.419	819.697	0.654	4.225	0.327	423.378	0.618	4.763	1.618
	Isolation	0.853	108.170	0.333	2.140	0.778	120.465	0.580	3.653	0.769	124.567	0.660	3.638	0.736	111.291	0.819	2.002	1.002
	Laplacian	0.324	2011.987	1.320	9.128	0.626	2095.452	1.432	6.957	0.634	1875.474	1.468	5.106	0.543	2073.552	1.539	8.310	1.539
	Linear	0.866	14136.462	0.484	6.483	0.806	14136.462	0.484	6.882	0.633	3986.076	0.532	5.015	0.864	13973.043	0.488	4.474	1.474
	Polynomial	0.975	13378.873	0.516	3.966	0.975	13378.873	0.516	3.734	0.715	12237.580	0.381	1.797	0.897	9566.441	0.547	3.320	1.897
Sigmoid	0.628	3555.245	1.226	4.695	0.694	3555.692	1.278	4.130	0.609	7.240	22.297	1.961	0.712	13184.251	0.526	1.897	0.526	
<i>k</i> -modes	Additive-chi2	-0.504	12.170	1.156	2322.139	-0.491	16.369	1.837	3079.973	-0.460	12.037	1.861	4362.988	-0.393	20.463	1.725	2636.756	1.725
	Chi-squared	-0.409	5.339	5.736	2190.884	-0.408	5.427	5.735	2754.262	-0.347	146.595	2.551	3430.494	-0.393	6.930	5.989	1844.897	5.989
	Cosine	-0.630	9.605	1.261	4699.372	-0.508	18.408	1.317	6415.113	-0.683	2.432	1.620	4327.268	-0.551	17.584	1.319	6613.378	1.319
	Gaussian	-0.154	16.150	21.112	2670.864	-0.153	14.777	20.500	4486.247	-0.151	29.165	21.684	4333.309	-0.152	14.544	19.867	3168.317	19.867
	Isolation	-0.368	10.444	6.477	9829.114	-0.655	2.859	6.959	17960.518	-0.410	3.236	6.799	17561.721	-0.438	4.867	7.691	9865.705	7.691
	Laplacian	-0.458	8.255	1.350	1600.797	-0.476	3.668	1.446	1599.906	-0.529	3.074	1.382	2317.782	-0.438	2.529	1.167	1456.450	1.167
	Linear	-0.517	14.229	1.752	847.966	-0.487	18.161	1.744	591.437	-0.334	26.566	2.432	1815.314	-0.536	7.276	1.758	976.420	1.758
	Polynomial	-0.793	1.638	1.866	648.035	-0.826	1.871	2.284	648.198	-0.563	31.853	2.093	1337.207	-0.638	0.859	1.863	703.717	1.863
Sigmoid	-0.578	4.035	1.392	5175.608	-0.626	4.447	1.467	6982.080	-0.100	0.674	1.209	615.030	-0.390	0.950	1.537	639.617	1.537	

Table 11: Internal clustering quality metrics for different kernels and embeddings on **Host** dataset.

The ShortRead dataset results (Table 12) reveal that the isolation kernel delivers superior clustering quality for *k*-means across all embeddings, with Silhouette Coefficients exceeding 0.90 and maintaining reasonable computation times. The Linear and Polynomial kernels paired with Spike2Vec, Minimizer, and Spaced k-mer embeddings also demonstrate strong performance, achieving notably high Calinski-Harabasz scores. For *k*-modes clustering, the Sigmoid kernel with Spike2Vec encoding yields the best results (Silhouette: 0.178, Davies-Bouldin: 0.669), though most configurations produce negative Silhouette values. The additive-chi2 kernel with Minimizer embedding presents an anomalous case where identical values appear in both *k*-means and *k*-modes results, suggesting potential data overlap or processing artifacts.

Algo.	Kernel	OHE				Spike2vec				Minimizer				Spaced k-mer				
		Silhouette Coeff.	Calinski Harabasz Score	Davies-Bouldin	Clustering Runtime (Sec.)	Silhouette Coeff.	Calinski Harabasz Score	Davies-Bouldin	Clustering Runtime (Sec.)	Silhouette Coeff.	Calinski Harabasz Score	Davies-Bouldin	Clustering Runtime (Sec.)	Silhouette Coeff.	Calinski Harabasz Score	Davies-Bouldin	Clustering Runtime (Sec.)	
<i>k</i> -means	Additive-chi2	0.465	5445.396	0.619	3.840	0.684	2245.383	0.727	2.206	0.653	19297.977	0.757	26.296	0.614	16581.801	0.875	2.817	1.875
	Chi-squared	0.673	37.330	0.769	10.221	0.447	14.721	0.937	24.267	0.137	13.138	3.602	37.869	0.568	14.211	0.504	3.983	3.983
	Cosine	0.465	5445.396	0.619	3.388	0.745	93896.412	0.529	23.620	0.729	49085.719	0.524	33.267	0.663	114154.429	0.614	11.227	11.227
	Gaussian	-0.025	76.595	15.802	10.812	0.560	14.124	2.110	34.046	0.467	11.952	2.640	15.376	0.469	13.877	0.739	19.827	19.827
	Isolation	0.917	229.720	0.982	7.165	0.905	100.900	0.856	7.853	0.908	97.650	0.786	5.642	0.914	138.229	0.812	12.221	12.221
	Laplacian	0.465	5365.724	0.620	10.796	0.388	13.676	3.469	26.740	0.001	6.925	15.816	4.828	0.480	13.847	0.998	16.371	16.371
	Linear	0.465	5445.396	0.619	7.775	0.780	61422.728	0.472	9.831	0.730	48513.324	0.927	12.310	0.775	66533.842	0.472	6.449	6.449
	Polynomial	0.465	5380.650	0.620	8.783	0.779	59049.256	0.476	2.683	0.730	4810.028	0.534	2.831	0.775	52560.712	0.464	3.371	3.371
Sigmoid	0.465	5515.529	0.618	6.184	0.684	2245.943	0.727	24.429	-0.001	10.290	22.430	2.487	-0.002	10.827	20.230	2.487	20.230	
<i>k</i> -modes	Additive-chi2	-0.417	0.690	1.181	2927.511	-0.541	0.468	1.367	1283.833	0.653	19297.977	0.757	26.296	-0.063	0.712	1.692	1652.229	1.692
	Chi-squared	-0.679	0.045	9.109	5811.840	-0.415	0.622	2.556	7327.263	-0.430	1.301	2.110	5887.333	-0.459	0.753	2.882	5782.701	2.882
	Cosine	-0.185	0.400	1.212	3297.832	-0.863	1.511	3.111	4616.545	-0.054	0.330	1.853	1783.293	-0.834	0.409	2.012	3943.872	3.943
	Gaussian	-0.078	1.401	56.106	5515.107	-0.397	0.855	1.665	7077.646	-0.434	0.343	2.055	5302.751	-0.422	0.450	2.254	5388.310	5.388
	Isolation	-0.563	11.948	6.255	8625.942	-0.363	3.337	9.337	8424.060	-0.395	3.563	9.617	7149.288	-0.253	2.693	8.415	30170.856	30.170
	Laplacian	-0.395	0.378	1.028	2823.894	-0.440	1.871	2.335	6947.622	-0.036	1.017	0.997	3075.104	-0.451	0.584	2.168	4978.428	4.978
	Linear	-0.351	0.741	1.021	2920.750	-0.703	3.002	1.383	3188.894	-0.578	0.312	1.320	1527.236	-0.702	1.577	1.697	1363.664	1.697
	Polynomial	-0.469	0.507	1.150	2557.172	-0.808	0.360	1.922	3272.108	-0.739	0.228	1.899	1538.851	-0.786	0.218	1.724	1347.649	1.724
Sigmoid	-0.420	0.514	1.106	2598.769	0.178	2.155	0.609	2133.886	-0.146	0.532	1.344	880.223	-0.145	0.566	1.333	850.938	1.333	

Table 12: Internal clustering quality metrics for different kernels and embeddings on **ShortRead** dataset.

Table 13 demonstrates that the Polynomial kernel excels with *k*-means clustering across Spike2Vec, Minimizer, and Spaced k-mer embeddings, achieving exceptionally high Silhouette Coefficients (0.985-0.996) and Calinski-Harabasz scores reaching beyond 600,000 for Minimizer encoding. The isolation kernel shows good performance across different embeddings with efficient computation times. For *k*-modes clustering, performance varies significantly across configurations, with chi-squared kernel and Minimizer encoding achieving the highest Calinski-Harabasz score (91.468) and a positive Silhouette Coefficient (0.301). The Sigmoid kernel with Spaced k-mer encoding produces an exceptionally high Calinski-Harabasz score (2926.083) for *k*-modes, suggesting potentially well-separated clusters, though this requires careful interpretation given the unusual magnitude.

Algo.	Kernel	OHE				Spike2vec				Minimizer				Spaced k-mer			
		Silhouette Coeff.	Calinski Harabasz Score	Davies-Bouldin Score	Clustering Runtime (Sec.)	Silhouette Coeff.	Calinski Harabasz Score	Davies-Bouldin Score	Clustering Runtime (Sec.)	Silhouette Coeff.	Calinski Harabasz Score	Davies-Bouldin Score	Clustering Runtime (Sec.)	Silhouette Coeff.	Calinski Harabasz Score	Davies-Bouldin Score	Clustering Runtime (Sec.)
k -means	Additivechi2	0.187	402.000	1.200	31.988	0.177	112867.481	0.439	49.925	0.533	89547.624	0.512	15.309	0.346	4661.675	1.070	90.265
	Chi-squared	0.531	216.896	1.249	4.319	0.044	210.251	1.662	62.677	0.209	222.433	1.281	121.588	0.492	410.654	0.382	11.122
	Cosine	0.170	2565.670	2.204	21.132	0.235	2711.211	1.586	291.112	0.227	3507.135	1.474	292.261	0.205	2112.364	1.691	186.789
	Gaussian	0.646	459.827	0.241	8.027	0.646	464.056	0.241	38.197	0.603	492.833	0.274	67.811	0.644	494.341	0.243	75.072
	Isolation	0.989	275.123	0.568	10.977	0.957	249.999	0.507	7.279	0.955	259.133	0.520	6.612	0.944	288.276	0.515	12.152
	Laplacian	0.258	3430.153	1.537	27.947	0.457	31070.489	0.693	109.818	0.487	1250.415	3.408	179.241	0.205	3378.445	1.897	165.092
	Linear	0.345	3528.133	1.145	24.403	0.633	316957.694	0.841	37.924	0.639	432955.835	0.410	56.297	0.911	124886.361	0.344	85.801
	Polynomial	0.656	5447.339	1.207	4.110	0.986	325677.263	0.382	40.584	0.985	624187.091	0.122	50.107	0.996	193683.606	0.197	33.559
	Sigmoid	0.318	3786.543	1.097	13.041	0.333	13727.034	1.459	50.469	0.999	27151.997	0.278	50.842	-0.474	12.827	1.598	8012.191
	k -modes	Additivechi2	-0.401	18.868	1.228	13098.226	-0.400	18.621	1.226	6222.203	-0.538	1.883	1.909	6769.886	-0.361	8.132	1.151
Chi-squared		-0.635	0.685	15.698	9785.699	-0.076	28.279	0.910	5776.951	0.301	91.468	0.534	11234.866	-0.608	0.203	16.393	3556.649
Cosine		0.024	92.713	0.931	6019.710	-0.348	16.788	1.783	12691.892	-0.302	6.576	1.151	8389.929	-0.182	64.033	0.889	13641.548
Gaussian		-0.550	3.748	16.298	11464.403	-0.516	5.515	16.536	12986.981	-0.536	3.192	16.392	16892.643	-0.373	6.566	15.808	20405.049
Isolation		-0.443	4.339	9.533	35971.307	-0.530	2.534	9.768	13883.651	-0.454	3.813	9.747	7021.328	-0.719	1.412	9.601	48983.839
Laplacian		-0.397	5.838	1.298	12115.963	-0.404	2.864	1.284	6018.343	-0.033	62.789	0.982	6654.140	-0.062	18.401	1.032	10257.329
Linear		-0.379	4.000	1.434	10764.303	-0.726	2.249	1.962	6138.794	-0.750	7.149	1.213	5767.488	-0.565	18.341	1.430	4496.649
Polynomial		-0.232	5.180	1.361	2447.411	-0.886	0.589	1.851	6659.856	-0.971	7.111	1.258	6167.346	-0.891	0.040	2.079	3939.441
Sigmoid		-0.380	4.953	1.219	6420.327	-0.141	34.853	0.895	4379.701	-0.758	0.036	6.288	6123.163	0.892	2926.083	1.892	1088.023

Table 13: Internal clustering quality metrics for different kernels and embeddings on Rabies dataset.

For the Genome dataset (Table 14), the isolation kernel outperforms other methods in k -means clustering, achieving Silhouette Coefficients above 0.89 across all embeddings with minimal computational cost. The Cosine and Sigmoid kernels with Spaced k -mer encoding also demonstrate strong clustering quality (Silhouette: 0.886 and Davies-Bouldin: 0.333). The k -modes results show mixed performance, with most configurations yielding negative Silhouette Coefficients. Notably, the Laplacian kernel with Spike2Vec encoding achieves a positive Silhouette (0.137) and competitive Davies-Bouldin score (0.722), while chi-squared kernel with Spaced k -mer produces the highest Silhouette (0.056) among k -modes configurations. The additive-chi2 kernel again shows identical values between k -means and k -modes for Minimizer embedding.

Algo.	Kernel	OHE				Spike2vec				Minimizer				Spaced k-mer			
		Silhouette Coeff.	Calinski Harabasz Score	Davies-Bouldin Score	Clustering Runtime (Sec.)	Silhouette Coeff.	Calinski Harabasz Score	Davies-Bouldin Score	Clustering Runtime (Sec.)	Silhouette Coeff.	Calinski Harabasz Score	Davies-Bouldin Score	Clustering Runtime (Sec.)	Silhouette Coeff.	Calinski Harabasz Score	Davies-Bouldin Score	Clustering Runtime (Sec.)
k -means	Additivechi2	0.701	1581.100	1.306	1.824	0.667	20226.302	0.751	51.845	0.594	13108.837	0.863	107.852	0.824	65181.226	0.446	3.798
	Chi-squared	0.430	952.541	1.280	1.969	0.423	4474.053	1.104	41.280	0.360	3518.464	1.238	72.189	0.780	53485.827	0.304	3.029
	Cosine	0.754	1741.799	1.620	3.593	0.617	48396.107	0.783	51.435	0.540	29457.328	1.034	94.370	0.886	196623.437	0.333	3.559
	Gaussian	0.719	35.729	3.050	5.708	0.699	33.868	0.202	99.454	0.680	34.868	0.208	55.513	0.788	96.620	0.128	4.522
	Isolation	0.902	98.655	0.565	2.112	0.915	95.627	0.635	1.919	0.903	94.709	0.531	4.025	0.894	118.551	0.672	2.219
	Laplacian	0.757	1775.133	1.475	5.406	0.136	1157.928	2.443	74.059	0.117	955.283	2.690	121.627	0.581	31109.936	0.676	6.853
	Linear	0.684	1913.539	1.510	4.853	0.751	48302.567	0.566	70.012	0.572	21631.400	0.801	83.521	0.645	23308.094	0.532	6.783
	Polynomial	0.757	1772.842	1.321	3.014	0.733	40629.911	0.596	67.203	0.406	15132.253	1.246	113.842	0.645	23442.238	0.530	5.150
	Sigmoid	0.758	1757.739	1.274	2.685	0.901	10.775	22.667	5.668	0.901	10.778	22.784	5.813	0.001	10.724	22.771	7.820
	k -modes	Additivechi2	-0.585	1.224	1.085	3681.682	-0.469	0.003	1.541	2881.500	0.594	13108.837	0.863	107.852	-0.658	0.829	1.111
Chi-squared		-0.455	1.767	3.230	3366.333	-0.045	1.084	0.953	2918.957	-0.235	3.929	0.969	484.650	0.056	6.830	0.739	1313.927
Cosine		-0.532	1.398	0.996	5662.487	-0.683	1.754	1.275	6654.192	-0.375	0.399	1.287	5611.547	-0.733	0.773	1.075	2734.444
Gaussian		-0.278	0.818	26.718	15240.669	-0.281	1.065	25.428	36843.879	-0.184	1.107	36.419	9657.544	-0.417	44.183	1.712	5243.214
Isolation		-0.271	4.017	9.406	3988.195	-0.457	3.005	9.419	9011.211	-0.349	2.357	9.342	24640.874	-0.287	5.380	8.711	9811.822
Laplacian		-0.608	1.019	1.070	5052.798	0.137	6.494	0.722	10365.885	-0.062	1.305	1.064	3796.223	-0.477	2.187	2.074	1199.087
Linear		-0.439	1.203	1.086	3653.515	-0.362	0.272	1.489	10292.275	-0.436	0.796	1.417	3095.170	-0.547	1.368	1.467	1878.157
Polynomial		-0.628	1.155	1.003	5334.133	-0.661	2.377	1.087	8678.394	-0.569	1.783	1.944	3501.511	-0.591	4.795	1.122	1945.527
Sigmoid		-0.597	1.096	1.028	3936.777	-0.039	1.037	1.022	1130.992	-0.026	0.941	1.028	987.253	-0.629	0.942	1.035	1010.187

Table 14: Internal clustering quality metrics for different kernels and embeddings on Genome dataset.

The Breast Cancer dataset (Table 15) exhibits moderate clustering performance overall, with the isolation kernel providing the best k -means results across all embeddings (Silhouette Coefficients: 0.325-0.659), despite relatively modest Calinski-Harabasz scores. The Sigmoid kernel with Minimizer encoding achieves the highest Silhouette Coefficient (0.267) among other kernels, combined with favorable Davies-Bouldin scores. For k -modes clustering, the Cosine kernel with Spaced k -mer encoding yields the best Silhouette Coefficient (0.027) and highest Davies-Bouldin score (11.379), though values remain low overall. The Polynomial kernel with Spike2Vec shows slight improvement (Silhouette: 0.011), while most other configurations produce negative Silhouette values, indicating challenging cluster structure in this dataset regardless of the chosen embedding method.

Algo.	Kernel	OHE				SpitzVec				Minimizer				Spaced k-mer			
		Silhouette Coefficient	Calinski Harabasz Score	Davies-Bouldin Score	Clustering Runtime (Sec.)	Silhouette Coefficient	Calinski Harabasz Score	Davies-Bouldin Score	Clustering Runtime (Sec.)	Silhouette Coefficient	Calinski Harabasz Score	Davies-Bouldin Score	Clustering Runtime (Sec.)	Silhouette Coefficient	Calinski Harabasz Score	Davies-Bouldin Score	Clustering Runtime (Sec.)
k-means	Additive-chi2	0.019	17.447	5.123	0.487	0.013	23.777	2.207	0.144	0.050	29.455	1.915	0.165	0.066	15.256	1.547	0.112
	Chi-squared	-0.055	2.450	3.136	0.458	-0.056	2.347	5.818	0.945	0.023	12.428	2.765	0.274	0.128	7.764	1.224	0.081
	Cosine	0.015	18.778	5.641	0.824	0.047	30.859	2.209	0.229	0.052	34.895	2.442	0.182	0.079	20.133	2.688	0.181
	Gaussian	0.065	1.462	0.816	0.323	-0.005	1.571	0.962	0.559	0.028	3.028	0.870	0.137	0.113	4.578	0.744	0.545
	Isolation	0.581	28.520	0.927	0.350	0.659	36.862	1.170	0.116	0.438	23.250	0.818	0.125	0.325	75.083	0.998	0.414
	Laplacian	0.012	16.594	6.836	1.046	0.025	24.121	2.432	0.139	0.059	26.529	2.213	0.119	0.146	14.099	1.819	0.124
	Linear	0.014	17.142	6.123	0.558	0.110	38.117	2.255	0.534	0.119	29.624	2.340	0.520	0.074	26.299	1.653	0.121
	Polynomial	0.019	19.665	7.158	0.748	0.179	40.066	1.823	0.165	0.059	40.198	1.527	0.121	0.242	19.632	1.652	0.121
	Sigmoid	-0.056	13.129	7.465	0.561	0.149	41.463	1.755	0.609	0.267	49.654	1.182	0.391	0.085	26.031	1.440	0.403
	k-medes	Additive-chi2	-0.077	1.226	0.987	150.826	-0.156	0.910	1.256	106.128	-0.318	1.201	6.193	106.282	-0.271	0.176	14.237
Chi-squared		-0.090	1.109	0.982	608.331	-0.127	0.984	1.047	655.013	-0.286	0.710	2.573	159.327	-0.352	0.851	4.461	210.192
Cosine		-0.044	0.985	1.017	163.095	0.001	1.082	0.966	130.729	-0.019	1.034	5.575	117.911	0.027	1.464	11.379	239.816
Gaussian		-0.194	0.976	1.111	493.225	-0.230	1.052	1.125	464.578	-0.003	1.262	21.973	257.913	-0.139	1.077	10.865	848.657
Isolation		-0.344	2.059	5.046	471.227	-0.389	2.912	3.988	264.000	-0.384	1.396	5.388	982.025	-0.464	2.410	2.892	1182.255
Laplacian		-0.106	0.781	1.159	157.846	-0.147	1.649	1.141	132.096	-0.214	0.511	1.557	127.406	-0.439	1.611	9.283	112.490
Linear		-0.014	1.109	0.960	151.999	-0.171	0.966	1.276	127.811	-0.351	0.381	4.815	216.572	-0.347	0.561	12.109	144.863
Polynomial		-0.033	1.004	1.017	104.546	0.011	1.162	0.931	117.900	-0.273	0.298	2.111	112.545	-0.437	0.547	9.811	131.135
Sigmoid		-0.163	0.657	1.353	104.484	-0.113	0.731	1.184	114.074	-0.153	0.727	1.208	103.679	-0.397	0.765	3.647	100.370

Table 15: Internal clustering quality metrics for different kernels and embeddings on Breast Cancer dataset.

10 Classification Results

In this section, we report the classification results for different kernels, embeddings, classifiers, and datasets.

10.1 Results for Spike7k Data

Table 16 presents the classification performance on the Spike7k dataset using OHE encoding across various classifiers and evaluation metrics. The classification objective involves categorizing SARS-CoV-2 viral sequences into 22 distinct lineages (class distribution detailed in Section 6.1). Results indicate that the linear kernel combined with random forest achieves superior performance across nearly all metrics, with the exception of ROC-AUC, where the polynomial kernel paired with KNN demonstrates the best results. The classification outcomes for k -mers-based representations are detailed in Table 17, while minimizer-based embedding results appear in Table 18. These results reveal that linear and cosine kernels, when combined with either logistic regression or random forest classifiers, yield the strongest predictive capabilities compared to alternative kernel-classifier combinations. For spaced k -mers embeddings, Table 19 shows that the Additive-chi2 kernel with logistic regression attains the peak accuracy of 85.7%.

Kernels	ML Algo.	Acc.	Prec.	Recall	F1 weigh.	ROC-AUC	Train. run-time (sec.)	Kernels	ML Algo.	Acc.	Prec.	Recall	F1 weigh.	ROC-AUC	Train. run-time (sec.)	
Additive-chi2	SVM	0.786	0.773	0.786	0.763	0.735	0.280	Laplacian	SVM	0.614	0.536	0.614	0.554	0.555	0.312	
	NB	0.700	0.763	0.700	0.717	0.755	0.408		NB	0.637	0.698	0.637	0.640	0.743	0.322	
	MLP	0.764	0.761	0.764	0.757	0.753	2.568		MLP	0.767	0.746	0.767	0.749	0.762	2.077	
	KNN	0.790	0.792	0.790	0.781	0.771	0.410		KNN	0.792	0.780	0.792	0.778	0.761	0.403	
	RF	0.799	0.799	0.799	0.792	0.790	0.509		RF	0.803	0.776	0.803	0.778	0.786	0.504	
	LR	0.772	0.757	0.772	0.750	0.701	0.356		LR	0.579	0.350	0.579	0.436	0.526	0.261	
	DT	0.767	0.773	0.767	0.763	0.766	0.219		DT	0.776	0.753	0.776	0.758	0.769	0.254	
Chi-squared	SVM	0.676	0.631	0.676	0.610	0.656	0.294	Linear	SVM	0.800	0.767	0.800	0.772	0.748	0.290	
	NB	0.532	0.758	0.532	0.604	0.731	0.325		NB	0.692	0.780	0.692	0.717	0.776	0.333	
	MLP	0.720	0.685	0.720	0.677	0.718	1.826		MLP	0.771	0.772	0.771	0.767	0.756	2.251	
	KNN	0.705	0.708	0.705	0.699	0.714	0.387		KNN	0.802	0.807	0.802	0.800	0.780	0.386	
	RF	0.723	0.698	0.723	0.692	0.724	0.477		RF	0.817	0.809	0.817	0.808	0.795	0.461	
	LR	0.658	0.577	0.658	0.577	0.605	0.233		LR	0.791	0.765	0.791	0.764	0.725	0.306	
DT	0.716	0.689	0.716	0.689	0.726	0.230	DT	0.789	0.787	0.789	0.781	0.783	0.215			
Cosine	SVM	0.653	0.630	0.653	0.625	0.586	0.301	Polynomial	SVM	0.612	0.537	0.612	0.554	0.555	0.308	
	NB	0.697	0.728	0.697	0.700	0.751	0.378		NB	0.707	0.769	0.707	0.726	0.765	0.396	
	MLP	0.775	0.760	0.775	0.760	0.762	2.149		MLP	0.776	0.760	0.776	0.759	0.764	2.272	
	KNN	0.787	0.778	0.787	0.774	0.753	0.386		KNN	0.801	0.799	0.801	0.788	0.796	0.407	
	RF	0.803	0.802	0.803	0.795	0.787	0.468		RF	0.806	0.794	0.806	0.785	0.788	0.510	
	LR	0.638	0.610	0.638	0.610	0.563	0.238		LR	0.611	0.520	0.611	0.546	0.554	0.231	
DT	0.770	0.778	0.770	0.767	0.774	0.214	DT	0.770	0.762	0.770	0.761	0.770	0.228			
Isolation	SVM	0.483	0.233	0.483	0.314	0.500	0.328	Sigmoid	SVM	0.582	0.354	0.582	0.440	0.526	0.314	
	NB	0.747	0.770	0.747	0.749	0.768	0.303		NB	0.701	0.757	0.701	0.712	0.731	0.278	
	MLP	0.786	0.764	0.786	0.764	0.750	2.232		MLP	0.788	0.764	0.788	0.769	0.773	1.685	
	KNN	0.795	0.773	0.795	0.776	0.760	0.388		KNN	0.791	0.766	0.791	0.774	0.736	0.384	
	RF	0.797	0.791	0.797	0.784	0.766	0.530		RF	0.805	0.783	0.805	0.781	0.780	0.497	
	LR	0.483	0.233	0.483	0.314	0.500	0.212		LR	0.481	0.232	0.481	0.313	0.500	0.227	
DT	0.770	0.772	0.770	0.767	0.759	0.217	DT	0.784	0.772	0.784	0.771	0.767	0.248			
Gaussian	SVM	0.479	0.229	0.479	0.310	0.500	0.381									
	NB	0.528	0.718	0.528	0.577	0.764	0.495									
	MLP	0.780	0.788	0.780	0.778	0.762	3.272									
	KNN	0.773	0.781	0.773	0.773	0.736	0.580									
	RF	0.777	0.778	0.777	0.774	0.755	0.632									
	LR	0.479	0.229	0.479	0.310	0.500	0.239									
DT	0.743	0.749	0.743	0.743	0.720	0.249										

Table 16: Classification comparing for different kernel methods and classifiers on OHE-based embeddings for Spike7k dataset. The best values are shown in bold.

Kernels	ML Algo.	Acc.	Prec.	Recall	F1 weigh.	ROC-AUC	Train. run-time (sec.)	Kernels	ML Algo.	Acc.	Prec.	Recall	F1 weigh.	ROC-AUC	Train. run-time (sec.)
Additive-chi2	SVM	0.835	0.811	0.835	0.817	0.802	0.289	Laplacian	SVM	0.606	0.425	0.606	0.467	0.530	0.355
	NB	0.719	0.788	0.719	0.744	0.776	0.336		NB	0.680	0.735	0.680	0.696	0.726	0.338
	MLP	0.786	0.797	0.786	0.780	0.781	1.859		MLP	0.780	0.770	0.780	0.771	0.765	1.958
	KNN	0.800	0.798	0.800	0.793	0.757	0.407		KNN	0.793	0.780	0.793	0.782	0.724	0.305
	RF	0.820	0.813	0.820	0.806	0.794	0.483		RF	0.811	0.792	0.811	0.794	0.781	0.475
	LR	0.838	0.810	0.838	0.816	0.799	0.308		LR	0.485	0.235	0.485	0.317	0.500	0.220
DT	0.790	0.794	0.790	0.785	0.776	0.216	DT	0.784	0.778	0.784	0.777	0.762	0.217		
Chi-squared	SVM	0.653	0.610	0.653	0.583	0.639	0.325	Linear	SVM	0.835	0.818	0.835	0.819	0.812	0.340
	NB	0.480	0.735	0.480	0.558	0.684	0.340		NB	0.730	0.810	0.730	0.761	0.793	0.420
	MLP	0.718	0.682	0.718	0.672	0.695	1.785		MLP	0.769	0.761	0.769	0.759	0.780	1.986
	KNN	0.715	0.715	0.715	0.707	0.710	0.419		KNN	0.768	0.767	0.768	0.765	0.766	0.518
	RF	0.735	0.707	0.735	0.706	0.718	0.591		RF	0.811	0.802	0.811	0.800	0.793	0.555
	LR	0.636	0.568	0.636	0.556	0.599	0.293		LR	0.838	0.815	0.838	0.817	0.804	0.322
DT	0.722	0.693	0.722	0.698	0.718	0.243	DT	0.776	0.784	0.776	0.773	0.776	0.221		
Cosine	SVM	0.619	0.509	0.619	0.545	0.544	0.329	Polynomial	SVM	0.636	0.492	0.636	0.522	0.542	0.343
	NB	0.694	0.778	0.694	0.725	0.749	0.341		NB	0.687	0.725	0.687	0.685	0.705	0.355
	MLP	0.740	0.746	0.740	0.736	0.749	1.879		MLP	0.805	0.776	0.805	0.781	0.779	2.389
	KNN	0.787	0.804	0.787	0.780	0.747	0.399		KNN	0.762	0.757	0.762	0.752	0.755	0.411
	RF	0.819	0.815	0.819	0.802	0.787	0.536		RF	0.818	0.795	0.818	0.793	0.780	0.485
	LR	0.631	0.436	0.631	0.514	0.540	0.235		LR	0.523	0.314	0.523	0.378	0.515	0.249
DT	0.783	0.775	0.783	0.774	0.769	0.235	DT	0.781	0.768	0.781	0.770	0.756	0.215		
Isolation	SVM	0.481	0.232	0.481	0.313	0.500	0.330	Sigmoid	SVM	0.481	0.231	0.481	0.312	0.500	0.320
	NB	0.614	0.718	0.614	0.639	0.702	0.432		NB	0.703	0.779	0.703	0.727	0.766	0.331
	MLP	0.764	0.739	0.764	0.747	0.730	2.628		MLP	0.772	0.767	0.772	0.762	0.762	1.987
	KNN	0.753	0.721	0.753	0.735	0.709	0.421		KNN	0.773	0.772	0.773	0.769	0.735	0.391
	RF	0.758	0.737	0.758	0.745	0.722	0.525		RF	0.813	0.788	0.813	0.792	0.775	0.486
	LR	0.481	0.232	0.481	0.313	0.500	0.214		LR	0.481	0.231	0.481	0.312	0.500	0.218
DT	0.732	0.723	0.732	0.725	0.700	0.224	DT	0.770	0.773	0.770	0.766	0.751	0.210		
Gaussian	SVM	0.481	0.231	0.481	0.312	0.500	0.376	Gaussian	SVM	0.481	0.231	0.481	0.312	0.500	0.376
	NB	0.500	0.697	0.500	0.553	0.732	0.403		NB	0.500	0.697	0.500	0.553	0.732	0.403
	MLP	0.732	0.718	0.732	0.719	0.742	2.594		MLP	0.732	0.718	0.732	0.719	0.742	2.594
	KNN	0.747	0.734	0.747	0.733	0.749	0.454		KNN	0.747	0.734	0.747	0.733	0.749	0.454
	RF	0.747	0.733	0.747	0.737	0.747	0.636		RF	0.747	0.733	0.747	0.737	0.747	0.636
	LR	0.481	0.231	0.481	0.312	0.500	0.253		LR	0.481	0.231	0.481	0.312	0.500	0.253
DT	0.715	0.725	0.715	0.717	0.734	0.263	DT	0.715	0.725	0.715	0.717	0.734	0.263		

Table 17: Classification comparison for different kernel methods and classifiers on k -mer-based embeddings for Spike7k dataset. The best values are shown in bold.

Kernels	ML Algo.	Acc.	Prec.	Recall	F1 weigh.	ROC-AUC	Train. run-time (sec.)	Kernels	ML Algo.	Acc.	Prec.	Recall	F1 weigh.	ROC-AUC	Train. run-time (sec.)
Additive-chi2	SVM	0.816	0.806	0.816	0.798	0.786	0.351	Laplacian	SVM	0.523	0.307	0.523	0.374	0.513	0.365
	NB	0.746	0.784	0.746	0.752	0.768	0.424		NB	0.715	0.788	0.715	0.737	0.768	0.398
	MLP	0.767	0.748	0.767	0.750	0.755	1.859		MLP	0.775	0.769	0.775	0.767	0.764	2.074
	KNN	0.800	0.783	0.800	0.785	0.763	0.437		KNN	0.806	0.808	0.806	0.801	0.777	0.409
	RF	0.815	0.784	0.815	0.792	0.773	0.536		RF	0.811	0.787	0.811	0.794	0.779	0.490
	LR	0.821	0.804	0.821	0.803	0.782	0.314		LR	0.484	0.234	0.484	0.315	0.500	0.221
DT	0.780	0.768	0.780	0.765	0.752	0.229	DT	0.781	0.774	0.781	0.771	0.763	0.259		
Chi-squared	SVM	0.665	0.633	0.665	0.600	0.643	0.290	Linear	SVM	0.817	0.800	0.817	0.798	0.788	0.346
	NB	0.487	0.732	0.487	0.553	0.685	0.352		NB	0.720	0.790	0.720	0.747	0.766	0.658
	MLP	0.693	0.658	0.693	0.643	0.690	1.750		MLP	0.764	0.750	0.764	0.750	0.749	2.521
	KNN	0.681	0.692	0.681	0.669	0.687	0.386		KNN	0.784	0.762	0.784	0.759	0.732	0.500
	RF	0.707	0.664	0.707	0.674	0.695	0.465		RF	0.817	0.805	0.817	0.800	0.775	0.622
	LR	0.645	0.560	0.645	0.564	0.577	0.230		LR	0.822	0.799	0.822	0.801	0.781	0.468
DT	0.700	0.669	0.700	0.671	0.695	0.208	DT	0.793	0.776	0.793	0.778	0.752	0.270		
Cosine	SVM	0.639	0.543	0.639	0.571	0.545	0.390	Polynomial	SVM	0.701	0.681	0.701	0.652	0.613	0.312
	NB	0.697	0.770	0.697	0.720	0.760	0.328		NB	0.702	0.753	0.702	0.712	0.713	0.439
	MLP	0.752	0.754	0.752	0.747	0.760	1.796		MLP	0.780	0.766	0.780	0.764	0.731	2.500
	KNN	0.778	0.793	0.778	0.778	0.756	0.458		KNN	0.770	0.772	0.770	0.765	0.763	0.428
	RF	0.816	0.810	0.816	0.803	0.800	0.514		RF	0.811	0.802	0.811	0.793	0.786	0.526
	LR	0.540	0.419	0.540	0.405	0.518	0.237		LR	0.671	0.572	0.671	0.571	0.568	0.284
DT	0.797	0.792	0.797	0.788	0.784	0.223	DT	0.775	0.771	0.775	0.766	0.763	0.214		
Isolation	SVM	0.483	0.233	0.483	0.314	0.500	0.311	Sigmoid	SVM	0.503	0.282	0.503	0.361	0.513	0.344
	NB	0.682	0.732	0.682	0.694	0.742	0.443		NB	0.677	0.752	0.677	0.690	0.732	0.335
	MLP	0.762	0.768	0.762	0.757	0.754	2.310		MLP	0.762	0.747	0.762	0.746	0.744	1.725
	KNN	0.770	0.762	0.770	0.760	0.748	0.379		KNN	0.779	0.764	0.779	0.766	0.725	0.400
	RF	0.769	0.769	0.769	0.764	0.750	0.516		RF	0.811	0.798	0.811	0.786	0.769	0.484
	LR	0.483	0.233	0.483	0.314	0.500	0.214		LR	0.485	0.259	0.485	0.330	0.503	0.224
DT	0.733	0.745	0.733	0.735	0.731	0.212	DT	0.774	0.767	0.774	0.762	0.743	0.217		
Gaussian	SVM	0.479	0.229	0.479	0.310	0.500	0.386	Gaussian	SVM	0.479	0.229	0.479	0.310	0.500	0.386
	NB	0.369	0.722	0.369	0.404	0.714	0.443		NB	0.369	0.722	0.369	0.404	0.714	0.443
	MLP	0.762	0.742	0.762	0.748	0.745	2.815		MLP	0.762	0.742	0.762	0.748	0.745	2.815
	KNN	0.748	0.726	0.748	0.731	0.718	0.459		KNN	0.748	0.726	0.748	0.731	0.718	0.459
	RF	0.763	0.746	0.763	0.751	0.742	0.617		RF	0.763	0.746	0.763	0.751	0.742	0.617
	LR	0.479	0.229	0.479	0.310	0.500	0.259		LR	0.479	0.229	0.479	0.310	0.500	0.259
DT	0.725	0.726	0.725	0.723	0.719	0.254	DT	0.725	0.726	0.725	0.723	0.719	0.254		

Table 18: Classification comparison for different kernel methods and classifiers on minimizer-based embeddings for Spike7k dataset. The best values are shown in bold.

Kernels	ML Algo.	Acc.	Prec.	Recall	F1 weigh.	F1 Macro	ROC-AUC	Train. run-time (sec.)	Kernels	ML Algo.	Acc.	Prec.	Recall	F1 weigh.	F1 Macro	ROC-AUC	Train. run-time (sec.)	
Additive-chi2	SVM	0.832	0.832	0.832	0.823	0.652	0.824	7.199	Laplacian	SVM	0.838	0.838	0.838	0.827	0.657	0.828	10.245	
	NB	0.741	0.569	0.247	0.311	0.396	0.694	0.160		NB	0.320	0.557	0.320	0.371	0.398	0.690	0.170	
	MLP	0.701	0.763	0.701	0.755	0.542	0.771	6.173		MLP	0.774	0.773	0.774	0.767	0.564	0.778	12.480	
	KNN	0.835	0.835	0.835	0.832	0.656	0.823	0.362		KNN	0.833	0.833	0.833	0.829	0.645	0.813	0.485	
	RF	0.827	0.814	0.827	0.805	0.626	0.801	4.712		RF	0.826	0.811	0.826	0.804	0.623	0.798	7.497	
	LR	0.857	0.851	0.857	0.845	0.683	0.840	27.998		LR	0.485	0.236	0.485	0.317	0.030	0.500	3.611	
DT	0.820	0.823	0.820	0.814	0.612	0.803	1.386	DT	0.820	0.822	0.820	0.813	0.608	0.803	1.672			
Chi-squared	SVM	0.667	0.682	0.667	0.609	0.421	0.668	0.906	Linear	SVM	0.834	0.837	0.834	0.825	0.660	0.826	7.202	
	NB	0.438	0.759	0.438	0.518	0.342	0.688	0.017		NB	0.414	0.730	0.414	0.487	0.453	0.720	0.115	
	MLP	0.719	0.710	0.719	0.686	0.485	0.710	7.803		MLP	0.758	0.749	0.758	0.748	0.538	0.767	7.199	
	KNN	0.733	0.735	0.733	0.730	0.540	0.749	0.330		KNN	0.813	0.813	0.813	0.810	0.621	0.798	0.373	
	RF	0.767	0.742	0.767	0.741	0.560	0.758	1.253		RF	0.828	0.816	0.828	0.810	0.636	0.802	4.697	
	LR	0.662	0.659	0.662	0.660	0.397	0.654	0.512		LR	0.856	0.851	0.856	0.844	0.689	0.841	25.972	
DT	0.763	0.739	0.763	0.737	0.553	0.756	0.112	DT	0.817	0.818	0.817	0.812	0.620	0.808	1.497			
Cosine	SVM	0.800	0.810	0.800	0.798	0.640	0.814	9.207	Polynomial	SVM	0.828	0.821	0.828	0.815	0.657	0.826	9.965	
	NB	0.375	0.730	0.375	0.419	0.421	0.722	0.176		NB	0.423	0.684	0.423	0.485	0.456	0.727	0.155	
	MLP	0.741	0.744	0.741	0.737	0.511	0.750	9.884		MLP	0.748	0.747	0.748	0.741	0.547	0.772	6.908	
	KNN	0.818	0.824	0.818	0.818	0.630	0.804	0.499		KNN	0.806	0.803	0.806	0.801	0.619	0.799	0.375	
	RF	0.829	0.820	0.829	0.812	0.634	0.799	6.377		RF	0.826	0.813	0.826	0.805	0.614	0.807	4.908	
	LR	0.743	0.652	0.743	0.689	0.234	0.621	7.500		LR	0.498	0.277	0.498	0.347	0.046	0.508	5.298	
DT	0.821	0.820	0.821	0.815	0.614	0.806	1.477	DT	0.810	0.808	0.810	0.803	0.607	0.807	1.765			
Isolation	SVM	0.509	0.522	0.509	0.365	0.088	0.517	6.128	Sigmoid	SVM	0.826	0.833	0.826	0.818	0.668	0.829	7.377	
	NB	0.059	0.712	0.059	0.093	0.048	0.512	0.104		NB	0.490	0.734	0.490	0.544	0.475	0.740	0.127	
	MLP	0.506	0.479	0.506	0.364	0.081	0.515	6.765		MLP	0.743	0.740	0.743	0.735	0.527	0.761	5.998	
	KNN	0.407	0.339	0.407	0.342	0.078	0.513	0.407		KNN	0.805	0.806	0.805	0.801	0.669	0.791	0.369	
	RF	0.509	0.489	0.509	0.367	0.075	0.513	1.167		RF	0.827	0.819	0.827	0.809	0.636	0.804	5.457	
	LR	0.490	0.240	0.490	0.322	0.030	0.500	0.490		LR	0.477	0.248	0.477	0.318	0.033	0.501	3.709	
DT	0.506	0.467	0.506	0.362	0.078	0.515	0.054	DT	0.818	0.822	0.818	0.812	0.631	0.812	1.671			
Gaussian	SVM	0.637	0.643	0.637	0.630	0.415	0.696	96.411										
	NB	0.073	0.618	0.073	0.070	0.129	0.599	0.167										
	MLP	0.634	0.619	0.634	0.619	0.384	0.679	12.632										
	KNN	0.640	0.637	0.640	0.621	0.432	0.676	0.396										
	RF	0.659	0.712	0.659	0.653	0.487	0.694	8.469										
	LR	0.672	0.663	0.672	0.614	0.403	0.657	7.994										
DT	0.637	0.634	0.637	0.628	0.417	0.698	4.440											

Table 19: Classification comparison for different kernel methods and classifiers on spaced-kmer-based embeddings for Spike7k dataset.

10.2 Results for Host Data

Table 20 presents classification results for the Host dataset using OHE encoding. The findings indicate that additive-chi2 and linear kernels paired with logistic regression achieve the highest accuracy (0.844 and 0.842, respectively) along with superior ROC-AUC scores (0.848 and 0.855). Random forest delivers good performance across multiple kernels, particularly with laplacian (accuracy: 0.847) and additive-chi2 (accuracy: 0.841). The isolation kernel exhibits notably poor performance across all classifiers, with accuracy values below 0.41, suggesting this kernel is unsuitable for OHE-encoded host sequence classification. KNN with laplacian kernel demonstrates competitive results (accuracy: 0.821), while Gaussian kernel shows moderate performance with substantially longer training times.

Kernels	ML Algo.	Acc.	Prec.	Recall	F1 weigh.	F1 Macro	ROC-AUC	Train. run-time (sec.)	Kernels	ML Algo.	Acc.	Prec.	Recall	F1 weigh.	F1 Macro	ROC-AUC	Train. run-time (sec.)	
Additive-chi2	SVM	0.792	0.805	0.792	0.793	0.625	0.799	4.121	Laplacian	SVM	0.802	0.815	0.802	0.803	0.645	0.812	6.498	
	NB	0.576	0.642	0.576	0.565	0.507	0.758	0.069		NB	0.578	0.635	0.578	0.562	0.509	0.766	0.101	
	MLP	0.762	0.760	0.762	0.755	0.450	0.723	4.833		MLP	0.762	0.765	0.762	0.756	0.476	0.729	8.809	
	KNN	0.812	0.812	0.812	0.810	0.651	0.831	0.263		KNN	0.821	0.818	0.821	0.818	0.651	0.828	0.286	
	RF	0.841	0.840	0.841	0.832	0.687	0.827	4.510		RF	0.847	0.848	0.847	0.839	0.692	0.831	4.746	
	LR	0.844	0.846	0.844	0.838	0.718	0.848	20.099		LR	0.862	0.850	0.862	0.845	0.686	0.835	3.297	
DT	0.795	0.794	0.795	0.791	0.661	0.831	1.478	DT	0.799	0.802	0.799	0.796	0.586	0.832	1.553			
Chi-squared	SVM	0.531	0.696	0.531	0.471	0.223	0.579	1.367	Linear	SVM	0.793	0.809	0.793	0.796	0.587	0.788	5.364	
	NB	0.258	0.653	0.258	0.346	0.151	0.606	0.020		NB	0.562	0.620	0.562	0.552	0.491	0.739	0.098	
	MLP	0.593	0.675	0.593	0.572	0.299	0.596	5.715		MLP	0.758	0.766	0.758	0.755	0.474	0.730	9.499	
	KNN	0.589	0.600	0.589	0.590	0.282	0.626	0.228		KNN	0.801	0.800	0.801	0.799	0.576	0.794	0.295	
	RF	0.629	0.649	0.629	0.618	0.318	0.635	1.630		RF	0.845	0.840	0.845	0.838	0.644	0.815	6.203	
	LR	0.510	0.721	0.510	0.440	0.179	0.561	0.553		LR	0.842	0.845	0.842	0.837	0.729	0.855	22.973	
DT	0.620	0.640	0.620	0.612	0.317	0.637	0.223	DT	0.795	0.796	0.795	0.792	0.591	0.805	1.497			
Cosine	SVM	0.792	0.806	0.792	0.794	0.617	0.797	4.371	Polynomial	SVM	0.791	0.810	0.791	0.792	0.650	0.824	4.368	
	NB	0.572	0.648	0.572	0.564	0.450	0.748	0.070		NB	0.520	0.645	0.520	0.510	0.497	0.762	0.098	
	MLP	0.759	0.764	0.759	0.756	0.495	0.747	6.738		MLP	0.766	0.764	0.766	0.757	0.489	0.745	6.535	
	KNN	0.809	0.805	0.809	0.805	0.673	0.835	0.301		KNN	0.788	0.791	0.788	0.786	0.616	0.815	0.279	
	RF	0.841	0.844	0.841	0.833	0.682	0.826	5.850		RF	0.839	0.846	0.839	0.832	0.705	0.843	1.550	
	LR	0.742	0.761	0.742	0.727	0.521	0.741	4.310		LR	0.726	0.757	0.726	0.701	0.374	0.674	9.189	
DT	0.799	0.801	0.799	0.796	0.614	0.821	1.494	DT	0.791	0.796	0.791	0.789	0.581	0.828	1.674			
Isolation	SVM	0.395	0.479	0.395	0.278	0.089	0.522	4.045	Sigmoid	SVM	0.791	0.804	0.791	0.793	0.611	0.787	5.651	
	NB	0.382	0.464	0.382	0.259	0.078	0.521	0.067		NB	0.566	0.649	0.566	0.559	0.456	0.739	0.077	
	MLP	0.401	0.459	0.401	0.286	0.090	0.523	2.909		MLP	0.749	0.754	0.749	0.745	0.493	0.731	6.698	
	KNN	0.256	0.252	0.256	0.236	0.081	0.514	0.232		KNN	0.794	0.791	0.794	0.791	0.640	0.817	0.293	
	RF	0.401	0.499	0.404	0.287	0.086	0.521	0.738		RF	0.837	0.839	0.837	0.829	0.678	0.823	5.300	
	LR	0.334	0.355	0.334	0.178	0.035	0.502	0.474		LR	0.571	0.442	0.571	0.486	0.231	0.667	3.533	
DT	0.401	0.464	0.401	0.286	0.089	0.522	0.064	DT	0.799	0.798	0.799	0.795	0.643	0.819	1.438			
Gaussian	SVM	0.629	0.632	0.629	0.626	0.340	0.654	36.019										
	NB	0.126	0.626	0.126	0.152	0.130	0.571	0.084										
	MLP	0.624	0.607	0.624	0.611	0.269	0.621	12.929										
	KNN	0.478	0.565	0.478	0.480	0.259	0.597	0.396										
	RF	0.655	0.689	0.655	0.627	0.380	0.647	8.422										
	LR	0.536	0.701	0.536	0.483	0.185	0.563	4.177										
DT	0.602	0.601	0.602	0.597	0.299	0.648	1.327											

Table 20: Classification comparison for different kernel methods and classifiers on OHE for Host Data.

For k-mer embeddings on the Host dataset (Table 21), additive-chi2 and linear kernels with logistic regression continue to dominate, achieving accuracies of 0.844 and 0.842, respectively, with ROC-AUC scores exceeding 0.85. Random forest maintains robust performance across various kernels, with linear kernel yielding 0.843 accuracy. The polynomial kernel paired with random forest achieves notable success (accuracy: 0.840, ROC-AUC: 0.863). Chi-squared kernel performance remains weak across most classifiers, though it shows improvement over OHE results. Isolation kernel again demonstrates inadequate classification capability with accuracy below 0.41 for all classifiers. Computational efficiency varies significantly, with logistic regression requiring substantially longer training times compared to other algorithms.

Table 22 reveals that cosine kernel with random forest attains the highest accuracy (0.824) on minimizer-encoded Host data, accompanied by strong ROC-AUC performance (0.833). Linear kernel with logistic regression achieves comparable accuracy (0.813) with exceptional ROC-AUC (0.862), though at considerably higher computational cost (41.384 seconds). Additive-chi2 kernel demonstrates competitive results

Kernels	ML Algo.							Kernels	ML Algo.								
	Algo.	Acc.	Prec.	Recall	F1 weigh.	F1 Macro	ROC-AUC		Train. run-time (sec.)	Algo.	Acc.	Prec.	Recall	F1 weigh.	F1 Macro	ROC-AUC	Train. run-time (sec.)
Additive-chi2	SVM	0.796	0.810	0.796	0.798	0.626	0.799	4.800	Laplacian	SVM	0.793	0.810	0.793	0.796	0.677	0.829	5.315
	NB	0.574	0.633	0.574	0.565	0.487	0.755	0.085		NB	0.574	0.638	0.574	0.558	0.496	0.752	0.111
	MLP	0.751	0.759	0.751	0.749	0.599	0.757	5.947		MLP	0.762	0.762	0.762	0.755	0.596	0.741	8.600
	KNN	0.808	0.811	0.808	0.807	0.636	0.817	0.304		KNN	0.815	0.814	0.815	0.812	0.632	0.820	0.337
	RF	0.841	0.844	0.841	0.835	0.679	0.825	4.864		RF	0.841	0.841	0.841	0.833	0.681	0.825	5.736
	LR	0.844	0.849	0.844	0.839	0.731	0.854	28.557		LR	0.842	0.848	0.842	0.835	0.694	0.841	4.335
DT	0.802	0.805	0.802	0.800	0.604	0.818	2.055	DT	0.793	0.797	0.793	0.791	0.589	0.827	2.141		
Chi-squared	SVM	0.429	0.328	0.429	0.320	0.099	0.530	0.690	Linear	SVM	0.802	0.812	0.802	0.803	0.626	0.791	4.843
	NB	0.223	0.526	0.223	0.273	0.101	0.582	0.007		NB	0.559	0.619	0.559	0.547	0.485	0.754	0.153
	MLP	0.478	0.445	0.476	0.488	0.138	0.553	6.303		MLP	0.757	0.762	0.757	0.752	0.478	0.726	10.660
	KNN	0.660	0.663	0.660	0.658	0.313	0.649	0.056		KNN	0.794	0.792	0.794	0.790	0.590	0.804	0.350
	RF	0.592	0.607	0.592	0.580	0.285	0.619	0.587		RF	0.843	0.845	0.843	0.835	0.667	0.821	5.645
	LR	0.416	0.328	0.416	0.305	0.088	0.525	0.094		LR	0.842	0.848	0.842	0.835	0.694	0.841	24.576
DT	0.587	0.603	0.587	0.577	0.284	0.619	0.020	DT	0.792	0.792	0.792	0.788	0.591	0.810	1.486		
Cosine	SVM	0.791	0.806	0.791	0.793	0.593	0.784	5.689	Polynomial	SVM	0.779	0.804	0.779	0.785	0.691	0.841	4.559
	NB	0.519	0.686	0.519	0.534	0.499	0.732	0.087		NB	0.519	0.686	0.519	0.534	0.499	0.732	0.087
	MLP	0.756	0.756	0.756	0.751	0.491	0.732	7.063		MLP	0.767	0.766	0.767	0.761	0.511	0.753	6.969
	KNN	0.813	0.807	0.813	0.809	0.653	0.822	0.282		KNN	0.797	0.796	0.797	0.794	0.657	0.829	0.302
	RF	0.836	0.837	0.836	0.828	0.669	0.820	5.072		RF	0.840	0.841	0.840	0.833	0.741	0.863	5.612
	LR	0.745	0.756	0.745	0.731	0.482	0.722	5.341		LR	0.731	0.748	0.731	0.706	0.385	0.679	10.179
DT	0.800	0.802	0.800	0.797	0.620	0.823	1.751	DT	0.792	0.792	0.792	0.788	0.643	0.840	1.557		
Isolation	SVM	0.391	0.493	0.391	0.274	0.077	0.518	4.217	Sigmoid	SVM	0.787	0.798	0.787	0.788	0.577	0.779	5.830
	NB	0.370	0.460	0.370	0.247	0.061	0.514	0.067		NB	0.569	0.645	0.569	0.562	0.449	0.730	0.080
	MLP	0.397	0.445	0.397	0.283	0.077	0.549	4.030		MLP	0.754	0.791	0.754	0.749	0.439	0.714	6.917
	KNN	0.133	0.106	0.133	0.105	0.040	0.493	0.275		KNN	0.796	0.794	0.796	0.793	0.606	0.801	0.300
	RF	0.463	0.505	0.463	0.289	0.079	0.519	0.767		RF	0.834	0.832	0.834	0.825	0.623	0.800	5.038
	LR	0.327	0.361	0.327	0.168	0.032	0.501	0.454		LR	0.584	0.459	0.584	0.502	0.239	0.611	3.341
DT	0.399	0.485	0.399	0.284	0.077	0.519	0.083	DT	0.792	0.791	0.792	0.789	0.547	0.793	1.501		
Gaussian	SVM	0.604	0.613	0.604	0.601	0.330	0.655	47.541									
	NB	0.133	0.646	0.133	0.165	0.139	0.608	0.087									
	MLP	0.643	0.629	0.643	0.631	0.284	0.631	14.832									
	KNN	0.472	0.507	0.472	0.476	0.255	0.597	0.320									
	RF	0.661	0.666	0.661	0.663	0.289	0.658	4.476									
	LR	0.538	0.699	0.538	0.484	0.186	0.564	4.076									
DT	0.609	0.611	0.609	0.605	0.300	0.659	1.554										

Table 21: Classification comparison for different kernel methods and classifiers on kmer for Host data.

when paired with logistic regression (accuracy: 0.821, ROC-AUC: 0.859). The sigmoid kernel exhibits catastrophic failure across all classifiers, with accuracy fixed at 0.330, indicating complete classification collapse. Isolation kernel shows poor performance, while Gaussian kernel shows marginal improvement over OHE and k-mer configurations. Overall, minimizer embeddings demonstrate slightly reduced performance compared to OHE and k-mer approaches.

Kernels	ML Algo.							Kernels	ML Algo.								
	Algo.	Acc.	Prec.	Recall	F1 weigh.	F1 Macro	ROC-AUC		Train. run-time (sec.)	Algo.	Acc.	Prec.	Recall	F1 weigh.	F1 Macro	ROC-AUC	Train. run-time (sec.)
Additive-chi2	SVM	0.781	0.794	0.781	0.778	0.666	0.786	6.099	Laplacian	SVM	0.775	0.788	0.775	0.772	0.612	0.785	6.205
	NB	0.489	0.579	0.489	0.466	0.408	0.722	0.080		NB	0.521	0.597	0.521	0.502	0.456	0.732	0.083
	MLP	0.733	0.738	0.733	0.727	0.470	0.727	7.216		MLP	0.736	0.741	0.736	0.726	0.457	0.718	6.878
	KNN	0.824	0.820	0.824	0.819	0.641	0.814	0.293		KNN	0.782	0.776	0.782	0.777	0.621	0.812	0.339
	RF	0.818	0.826	0.818	0.810	0.675	0.815	5.789		RF	0.816	0.823	0.816	0.805	0.645	0.806	5.740
	LR	0.821	0.834	0.821	0.814	0.723	0.859	23.856		LR	0.822	0.829	0.822	0.816	0.566	0.822	5.241
DT	0.785	0.787	0.785	0.779	0.627	0.818	1.475	DT	0.781	0.782	0.781	0.772	0.589	0.810	1.610		
Chi-squared	SVM	0.696	0.664	0.696	0.695	0.331	0.634	2.567	Linear	SVM	0.771	0.789	0.771	0.770	0.666	0.800	4.634
	NB	0.286	0.698	0.286	0.355	0.203	0.658	0.037		NB	0.427	0.494	0.427	0.392	0.405	0.713	0.087
	MLP	0.649	0.696	0.649	0.641	0.354	0.647	5.295		MLP	0.729	0.736	0.729	0.722	0.466	0.720	6.652
	KNN	0.663	0.675	0.663	0.662	0.382	0.668	0.246		KNN	0.753	0.752	0.753	0.750	0.671	0.821	0.311
	RF	0.692	0.693	0.692	0.682	0.387	0.671	2.293		RF	0.812	0.817	0.812	0.803	0.674	0.816	4.419
	LR	0.615	0.731	0.615	0.696	0.273	0.696	1.164		LR	0.813	0.826	0.813	0.804	0.746	0.862	41.384
DT	0.674	0.677	0.674	0.667	0.384	0.670	0.549	DT	0.767	0.773	0.767	0.761	0.604	0.817	1.454		
Cosine	SVM	0.801	0.812	0.801	0.796	0.651	0.835	1.867	Polynomial	SVM	0.779	0.792	0.779	0.777	0.580	0.788	5.001
	NB	0.613	0.639	0.613	0.603	0.454	0.755	0.036		NB	0.436	0.484	0.436	0.403	0.371	0.692	0.250
	MLP	0.782	0.786	0.782	0.775	0.547	0.778	5.568		MLP	0.735	0.735	0.735	0.727	0.445	0.709	7.250
	KNN	0.767	0.761	0.767	0.763	0.631	0.817	0.297		KNN	0.777	0.774	0.777	0.773	0.636	0.807	0.269
	RF	0.824	0.831	0.824	0.816	0.696	0.833	2.540		RF	0.841	0.841	0.841	0.832	0.658	0.811	4.684
	LR	0.336	0.274	0.336	0.185	0.036	0.503	0.735		LR	0.784	0.832	0.784	0.797	0.666	0.850	196.075
DT	0.784	0.788	0.784	0.778	0.596	0.796	0.438	DT	0.806	0.806	0.806	0.803	0.571	0.796	1.429		
Isolation	SVM	0.395	0.468	0.395	0.277	0.081	0.520	4.146	Sigmoid	SVM	0.330	0.109	0.330	0.164	0.028	0.500	4.833
	NB	0.383	0.457	0.383	0.258	0.071	0.518	0.068		NB	0.027	0.001	0.027	0.001	0.003	0.500	0.086
	MLP	0.400	0.443	0.400	0.282	0.081	0.520	3.429		MLP	0.330	0.109	0.330	0.164	0.028	0.500	2.123
	KNN	0.349	0.401	0.349	0.293	0.090	0.519	0.261		KNN	0.156	0.035	0.156	0.056	0.014	0.500	0.236
	RF	0.404	0.488	0.404	0.288	0.086	0.522	0.733		RF	0.330	0.109	0.330	0.164	0.028	0.500	0.788
	LR	0.332	0.278	0.332	0.173	0.033	0.502	0.440		LR	0.330	0.109	0.330	0.164	0.028	0.500	0.063
DT	0.461	0.461	0.461	0.284	0.085	0.521	0.078	DT	0.330	0.109	0.330	0.164	0.028	0.500	0.025		
Gaussian	SVM	0.491	0.517	0.491	0.481	0.315	0.639	70.511									
	NB	0.102	0.282	0.102	0.124	0.096	0.560	0.117									
	MLP	0.571	0.557	0.571	0.557	0.255	0.613	13.353									
	KNN	0.474	0.527	0.474	0.471	0.273	0.608	0.402									
	RF	0.633	0.665	0.633	0.618	0.397	0.659	8.697									
	LR	0.583	0.690	0.583	0.549	0.232	0.585	4.401									
DT	0.609	0.611	0.609	0.602	0.323	0.661	1.355										

Table 22: Classification comparison for different kernel methods and classifiers on minimizer for Host.

Classification results for spaced k-mer embeddings on Host data (Table 23) show that linear kernel with random forest achieves peak accuracy (0.850) alongside strong F1 and ROC-AUC scores. Additive-chi2 and polynomial kernels with random forest

also deliver excellent performance (accuracies: 0.841 and 0.842, respectively). Logistic regression paired with linear kernel produces competitive results (accuracy: 0.845, ROC-AUC: 0.848). Laplacian kernel with random forest demonstrates robust classification quality (accuracy: 0.838, ROC-AUC: 0.881). The isolation kernel continues its pattern of poor performance, while Gaussian kernel shows moderate effectiveness. Training times for spaced k-mer configurations are generally higher than other encoding methods, particularly for Gaussian kernel (48.421 seconds for SVM), suggesting increased computational complexity.

Kernels	ML							Kernels	ML							
	Algo.	Acc.	Prec.	Recall	F1 weigh.	F1 Macro	ROC-AUC		Train. run-time (sec.)	Algo.	Acc.	Prec.	Recall	F1 weigh.	F1 Macro	ROC-AUC
Additive-chi2	SVM	0.792	0.804	0.792	0.793	0.617	0.800	6.584	SVM	0.782	0.798	0.782	0.784	0.669	0.838	7.323
	NB	0.651	0.696	0.651	0.649	0.550	0.783	0.119	NB	0.603	0.659	0.603	0.591	0.582	0.812	0.148
	MLP	0.769	0.776	0.789	0.763	0.516	0.755	17.339	MLP	0.766	0.765	0.766	0.761	0.533	0.761	14.881
	KNN	0.811	0.818	0.811	0.811	0.623	0.810	0.525	KNN	0.799	0.804	0.799	0.799	0.685	0.841	0.475
	RF	0.841	0.844	0.841	0.833	0.687	0.831	9.255	RF	0.838	0.841	0.838	0.830	0.787	0.881	8.281
LR	0.838	0.847	0.838	0.832	0.707	0.842	30.790	LR	0.828	0.844	0.828	0.806	0.817	0.908	3.718	
DT	0.793	0.797	0.793	0.789	0.612	0.831	1.606	DT	0.794	0.795	0.794	0.791	0.651	0.845	1.782	
Chi-squared	SVM	0.547	0.654	0.547	0.548	0.373	0.650	6.912	SVM	0.796	0.810	0.796	0.797	0.599	0.795	7.362
	NB	0.242	0.650	0.242	0.314	0.190	0.659	0.110	NB	0.649	0.698	0.649	0.645	0.535	0.771	0.126
	MLP	0.613	0.693	0.613	0.603	0.362	0.647	15.225	MLP	0.763	0.760	0.763	0.757	0.483	0.786	11.369
	KNN	0.606	0.617	0.606	0.601	0.342	0.649	0.389	KNN	0.763	0.776	0.763	0.764	0.593	0.796	0.465
	RF	0.648	0.654	0.648	0.642	0.437	0.683	5.678	RF	0.850	0.849	0.850	0.843	0.687	0.831	7.497
LR	0.535	0.721	0.535	0.481	0.190	0.565	4.452	LR	0.845	0.846	0.845	0.839	0.704	0.848	26.772	
DT	0.640	0.673	0.640	0.638	0.422	0.682	1.226	DT	0.799	0.799	0.799	0.796	0.624	0.823	2.007	
Cosine	SVM	0.795	0.804	0.795	0.795	0.616	0.798	10.433	SVM	0.791	0.812	0.791	0.792	0.648	0.814	6.077
	NB	0.600	0.709	0.600	0.579	0.526	0.788	0.171	NB	0.615	0.671	0.615	0.604	0.557	0.791	0.112
	MLP	0.763	0.768	0.763	0.759	0.554	0.766	13.698	MLP	0.761	0.763	0.761	0.757	0.534	0.760	11.356
	KNN	0.792	0.787	0.792	0.788	0.665	0.832	0.372	KNN	0.792	0.798	0.792	0.792	0.629	0.810	0.358
	RF	0.838	0.839	0.838	0.830	0.695	0.836	7.258	RF	0.842	0.845	0.842	0.834	0.715	0.842	6.802
LR	0.751	0.771	0.751	0.738	0.541	0.750	7.210	LR	0.568	0.471	0.568	0.475	0.223	0.602	5.735	
DT	0.796	0.793	0.796	0.791	0.616	0.821	2.442	DT	0.796	0.798	0.796	0.792	0.654	0.836	2.048	
Isolation	SVM	0.393	0.465	0.393	0.273	0.078	0.519	4.374	SVM	0.788	0.799	0.788	0.789	0.600	0.792	5.511
	NB	0.377	0.472	0.377	0.252	0.068	0.518	0.068	NB	0.576	0.653	0.576	0.552	0.535	0.769	0.090
	MLP	0.399	0.442	0.399	0.281	0.077	0.518	3.610	MLP	0.763	0.763	0.763	0.757	0.469	0.726	7.849
	KNN	0.193	0.158	0.193	0.162	0.066	0.511	0.267	KNN	0.797	0.801	0.797	0.795	0.592	0.795	0.342
	RF	0.403	0.486	0.403	0.285	0.075	0.518	0.773	RF	0.844	0.843	0.844	0.836	0.672	0.826	3.472
LR	0.337	0.389	0.337	0.182	0.036	0.502	0.492	LR	0.377	0.240	0.377	0.256	0.053	0.510	3.475	
DT	0.400	0.450	0.400	0.282	0.081	0.520	0.087	DT	0.798	0.795	0.798	0.793	0.597	0.821	1.597	
Gaussian	SVM	0.615	0.620	0.615	0.612	0.315	0.648	48.421								
	NB	0.138	0.653	0.138	0.170	0.122	0.622	0.199								
	MLP	0.633	0.619	0.633	0.620	0.289	0.631	20.938								
	KNN	0.484	0.506	0.484	0.483	0.257	0.599	0.377								
	RF	0.658	0.696	0.658	0.630	0.371	0.646	6.835								
LR	0.536	0.714	0.536	0.483	0.184	0.563	5.401									
DT	0.604	0.603	0.604	0.600	0.293	0.653	1.756									

Table 23: Classification comparison for different kernel methods and classifiers on spaced kmer for Host data.

10.3 Results for ShortRead Data

Table 24 demonstrates exceptional classification performance on ShortRead data using OHE encoding, with linear and additive-chi2 kernels paired with logistic regression achieving perfect accuracy (1.000) and ROC-AUC scores. SVM and KNN classifiers also deliver outstanding results across multiple kernels, with accuracies exceeding 0.998 for additive-chi2, cosine, laplacian, polynomial, and sigmoid kernels. The isolation and Gaussian kernels exhibit significantly degraded performance, with accuracy values near or below chance level (0.602 and 0.547, respectively), indicating complete failure to capture meaningful patterns in the data. Notably, laplacian kernel with logistic regression shows anomalous behavior with accuracy dropping to 0.897, while maintaining strong performance with other classifiers. The high performance across different kernel-classifier combinations suggests that OHE encoding is highly effective for ShortRead sequence classification.

Kernels	ML Algo.	Acc.	Prec.	Recall	F1 weigh.	F1 Macro	ROC-AUC	Train. run-time (sec.)	Kernels	ML Algo.	Acc.	Prec.	Recall	F1 weigh.	F1 Macro	ROC-AUC	Train. run-time (sec.)
Additive-chi2	SVM	0.998	0.998	0.998	0.998	0.992	0.994	4.316	SVM	0.998	0.998	0.998	0.998	0.993	0.997	0.997	5.858
	NB	0.959	0.961	0.959	0.959	0.904	0.953	0.068	NB	0.964	0.967	0.964	0.965	0.912	0.960	0.960	0.094
	MLP	0.980	0.979	0.980	0.979	0.823	0.919	4.969	MLP	0.977	0.977	0.977	0.977	0.841	0.922	0.922	3.990
	KNN	0.999	0.999	0.999	0.999	0.995	0.995	0.559	KNN	0.999	0.999	0.999	0.999	0.993	0.994	0.994	0.471
	RF	0.998	0.998	0.998	0.998	0.985	0.986	9.400	RF	0.998	0.998	0.998	0.998	0.986	0.987	0.987	8.571
	LR	1.000	1.000	1.000	1.000	0.999	1.000	0.946	LR	0.897	0.811	0.807	0.850	0.213	0.598	0.598	2.798
DT	0.997	0.998	0.997	0.998	0.937	0.974	1.044	DT	0.998	0.998	0.998	0.998	0.968	0.987	0.987	1.543	
Chi-squared	SVM	0.772	0.786	0.772	0.756	0.425	0.658	10.724	SVM	0.999	0.999	0.999	0.999	0.999	0.997	0.997	6.964
	NB	0.616	0.879	0.616	0.705	0.306	0.740	0.068	NB	0.962	0.964	0.962	0.962	0.959	0.975	0.975	0.076
	MLP	0.913	0.906	0.913	0.905	0.476	0.707	10.868	MLP	0.979	0.980	0.979	0.979	0.851	0.933	0.933	6.609
	KNN	0.952	0.952	0.952	0.951	0.622	0.801	0.628	KNN	0.999	0.999	0.999	0.999	0.999	0.993	0.994	0.576
	RF	0.975	0.972	0.975	0.973	0.696	0.829	11.993	RF	0.999	0.999	0.999	0.999	0.992	0.993	0.993	8.171
	LR	0.620	0.735	0.620	0.608	0.117	0.514	2.749	LR	1.000	1.000	1.000	1.000	1.000	1.000	1.000	6.454
DT	0.969	0.967	0.969	0.967	0.694	0.839	2.280	DT	0.998	0.999	0.998	0.998	0.973	0.990	0.990	1.391	
Cosine	SVM	0.998	0.998	0.998	0.998	0.988	0.992	5.224	SVM	0.998	0.998	0.998	0.998	0.991	0.994	0.994	4.886
	NB	0.961	0.963	0.961	0.962	0.906	0.947	0.084	NB	0.963	0.965	0.963	0.963	0.938	0.964	0.964	0.088
	MLP	0.981	0.980	0.981	0.980	0.819	0.903	6.338	MLP	0.978	0.978	0.978	0.978	0.815	0.908	0.908	5.466
	KNN	0.999	0.999	0.999	0.999	0.987	0.990	0.507	KNN	0.998	0.998	0.998	0.998	0.991	0.992	0.992	0.493
	RF	0.998	0.998	0.998	0.998	0.973	0.977	9.371	RF	0.998	0.998	0.998	0.998	0.990	0.991	0.991	7.848
	LR	0.892	0.892	0.892	0.843	0.218	0.599	2.412	LR	0.890	0.798	0.890	0.840	0.212	0.597	0.597	2.379
DT	0.996	0.997	0.996	0.997	0.894	0.968	1.203	DT	0.998	0.998	0.998	0.998	0.961	0.982	0.982	1.332	
Isolation	SVM	0.602	0.754	0.602	0.475	0.155	0.523	9.788	SVM	0.998	0.998	0.998	0.998	0.989	0.992	0.992	4.649
	NB	0.059	0.989	0.059	0.109	0.091	0.528	0.083	NB	0.964	0.966	0.964	0.965	0.932	0.962	0.962	0.077
	MLP	0.599	0.710	0.599	0.472	0.145	0.520	4.306	MLP	0.981	0.981	0.981	0.981	0.871	0.937	0.937	5.048
	KNN	0.528	0.528	0.528	0.501	0.172	0.524	0.459	KNN	0.999	0.999	0.999	0.999	0.992	0.993	0.993	0.457
	RF	0.602	0.753	0.602	0.477	0.152	0.522	1.151	RF	0.998	0.998	0.998	0.998	0.988	0.989	0.989	6.060
	LR	0.577	0.459	0.577	0.423	0.081	0.500	0.339	LR	0.580	0.337	0.580	0.426	0.082	0.500	0.500	1.538
DT	0.603	0.755	0.603	0.477	0.159	0.524	0.060	DT	0.997	0.997	0.997	0.997	0.942	0.974	0.974	0.879	
Gaussian	SVM	0.547	0.515	0.547	0.447	0.107	0.507	580.124									
	NB	0.029	0.661	0.029	0.043	0.023	0.512	0.067									
	MLP	0.461	0.456	0.461	0.458	0.119	0.507	5.684									
	KNN	0.520	0.449	0.520	0.468	0.108	0.503	0.445									
	RF	0.579	0.584	0.579	0.448	0.106	0.507	14.050									
	LR	0.575	0.653	0.575	0.421	0.083	0.501	1.815									
DT	0.441	0.446	0.441	0.444	0.121	0.506	5.336										

Table 24: Classification comparison for different kernel methods and classifiers on OHE for ShortRead Data.

For k-mer embeddings on ShortRead data (Table 25), linear and cosine kernels with SVM achieve near-perfect classification (accuracies: 0.988 and 0.987, respectively), accompanied by excellent ROC-AUC scores above 0.93. Polynomial kernel with logistic regression also demonstrates strong performance (accuracy: 0.975), though with substantially longer training time (290.504 seconds). Additive-chi2 kernel paired with logistic regression yields competitive results (accuracy: 0.975, ROC-AUC: 0.862). However, laplacian, chi-squared, isolation, Gaussian, and sigmoid kernels show severe performance degradation, with accuracies clustered around 0.50 or below, suggesting these kernels are fundamentally incompatible with k-mer representations for this dataset. The sigmoid kernel exhibits complete classification failure with fixed accuracy of 0.581 across all classifiers, indicating numerical instability or kernel inappropriateness.

Kernels	ML Algo.	Acc.	Prec.	Recall	F1 weigh.	F1 Macro	ROC-AUC	Train. run-time (sec.)	Kernels	ML Algo.	Acc.	Prec.	Recall	F1 weigh.	F1 Macro	ROC-AUC	Train. run-time (sec.)
Additive-chi2	SVM	0.979	0.979	0.979	0.978	0.877	0.930	4.957	Laplacian	SVM	0.501	0.446	0.501	0.436	0.098	0.501	282.036
	NB	0.332	0.572	0.332	0.354	0.160	0.543	0.084		NB	0.128	0.450	0.128	0.192	0.060	0.516	0.084
	MLP	0.929	0.930	0.929	0.929	0.592	0.760	5.721		MLP	0.453	0.442	0.453	0.447	0.115	0.501	6.366
	KNN	0.835	0.836	0.835	0.826	0.496	0.692	0.475		KNN	0.496	0.447	0.496	0.466	0.110	0.502	0.491
	RF	0.866	0.876	0.866	0.850	0.378	0.647	10.544		RF	0.570	0.431	0.570	0.438	0.089	0.500	14.257
Chi-squared	LR	0.975	0.974	0.975	0.974	0.731	0.862	170.000	LR	0.579	0.335	0.579	0.425	0.084	0.500	1.731	
	DT	0.845	0.851	0.845	0.848	0.414	0.696	7.863	DT	0.433	0.443	0.433	0.438	0.112	0.501	4.649	
	SVM	0.513	0.446	0.513	0.446	0.103	0.505	309.276	Linear	SVM	0.988	0.988	0.988	0.988	0.875	0.939	2.709
	NB	0.071	0.455	0.071	0.110	0.044	0.510	0.085		NB	0.569	0.714	0.569	0.583	0.466	0.744	0.120
	MLP	0.446	0.439	0.446	0.442	0.114	0.501	7.147		MLP	0.975	0.975	0.975	0.975	0.716	0.862	4.765
KNN	0.496	0.445	0.496	0.461	0.108	0.500	0.509	KNN		0.922	0.923	0.922	0.918	0.681	0.792	0.527	
RF	0.571	0.449	0.571	0.441	0.091	0.501	13.760	RF		0.902	0.907	0.902	0.889	0.403	0.467	3.605	
Cosine	LR	0.577	0.333	0.577	0.423	0.083	0.500	1.731	LR	0.970	0.867	0.970	0.866	0.536	0.767	89.808	
	DT	0.434	0.443	0.434	0.438	0.113	0.502	4.686	DT	0.891	0.892	0.891	0.892	0.510	0.752	1.687	
	SVM	0.987	0.988	0.987	0.987	0.884	0.937	2.821	Polynomial	SVM	0.581	0.338	0.581	0.338	0.082	0.500	12.838
	NB	0.566	0.720	0.566	0.580	0.489	0.735	0.109		NB	0.439	0.657	0.439	0.412	0.298	0.611	0.074
	MLP	0.971	0.971	0.971	0.971	0.678	0.838	6.816		MLP	0.952	0.952	0.952	0.951	0.700	0.853	4.406
KNN	0.918	0.919	0.918	0.913	0.659	0.782	0.524	KNN		0.922	0.924	0.922	0.917	0.673	0.787	0.471	
RF	0.903	0.909	0.903	0.891	0.416	0.671	3.721	RF		0.912	0.912	0.912	0.898	0.402	0.468	12.492	
Isolation	LR	0.577	0.333	0.577	0.422	0.081	0.500	0.369	LR	0.975	0.971	0.975	0.972	0.564	0.789	290.504	
	DT	0.889	0.891	0.889	0.889	0.457	0.724	1.014	DT	0.892	0.897	0.892	0.894	0.488	0.750	4.562	
	SVM	0.586	0.622	0.586	0.454	0.120	0.511	7.759	Sigmoid	SVM	0.581	0.338	0.581	0.427	0.082	0.500	12.838
	NB	0.052	0.834	0.052	0.095	0.049	0.510	0.070		NB	0.316	0.100	0.316	0.152	0.053	0.500	0.089
	MLP	0.585	0.602	0.585	0.651	0.114	0.510	4.607		MLP	0.581	0.338	0.581	0.427	0.082	0.500	2.093
KNN	0.507	0.489	0.507	0.476	0.124	0.507	0.416	KNN		0.418	0.191	0.418	0.258	0.064	0.500	0.388	
RF	0.584	0.713	0.584	0.461	0.115	0.511	1.240	RF		0.581	0.338	0.581	0.427	0.082	0.500	1.541	
Gaussian	LR	0.576	0.463	0.576	0.421	0.081	0.500	0.416	LR	0.581	0.338	0.581	0.427	0.082	0.500	0.056	
	DT	0.592	0.669	0.592	0.461	0.119	0.512	0.119	DT	0.581	0.338	0.581	0.427	0.082	0.500	0.052	
	SVM	0.490	0.433	0.490	0.429	0.096	0.497	278.828	Laplacian	SVM	0.501	0.442	0.501	0.433	0.096	0.500	276.660
	NB	0.121	0.439	0.121	0.161	0.061	0.518	0.076		NB	0.124	0.451	0.124	0.187	0.059	0.502	0.074
	MLP	0.441	0.433	0.441	0.437	0.109	0.499	7.060		MLP	0.443	0.432	0.443	0.437	0.112	0.500	6.526
KNN	0.497	0.435	0.497	0.463	0.105	0.501	0.531	KNN		0.484	0.428	0.484	0.453	0.103	0.498	0.517	
RF	0.565	0.426	0.565	0.432	0.086	0.500	13.854	RF		0.570	0.442	0.570	0.439	0.088	0.500	13.744	

Table 25: Classification comparison for different kernel methods and classifiers on **kmer** for **ShortRead** data.

Table 26 reveals that cosine and linear kernels with SVM deliver outstanding performance on minimizer-encoded ShortRead data (accuracies: 0.982 and 0.980, respectively), with ROC-AUC scores exceeding 0.93. Additive-chi2 and polynomial kernels also demonstrate strong results when paired with SVM (accuracies: 0.969 and 0.971). Naive Bayes shows improved performance with cosine kernel (accuracy: 0.860) compared to other embeddings. However, laplacian, chi-squared, isolation, Gaussian, and sigmoid kernels exhibit catastrophic failure, with accuracies hovering around chance level (0.43-0.58). The sigmoid kernel maintains complete classification collapse with fixed accuracy of 0.581 across all classifiers, mirroring the pattern observed with k-mer embeddings. Overall, minimizer encoding achieves comparable performance to k-mer representations when using appropriate kernels.

Kernels	ML Algo.	Acc.	Prec.	Recall	F1 weigh.	F1 Macro	ROC-AUC	Train. run-time (sec.)	Kernels	ML Algo.	Acc.	Prec.	Recall	F1 weigh.	F1 Macro	ROC-AUC	Train. run-time (sec.)
Additive-chi2	SVM	0.969	0.969	0.969	0.968	0.847	0.899	3.786	Laplacian	SVM	0.501	0.442	0.501	0.433	0.096	0.500	276.660
	NB	0.502	0.678	0.502	0.532	0.211	0.578	0.093		NB	0.124	0.451	0.124	0.187	0.059	0.502	0.074
	MLP	0.912	0.915	0.912	0.913	0.536	0.768	4.798		MLP	0.443	0.432	0.443	0.437	0.112	0.500	6.526
	KNN	0.853	0.851	0.853	0.845	0.521	0.706	0.521		KNN	0.484	0.428	0.484	0.453	0.103	0.498	0.517
	RF	0.906	0.909	0.906	0.894	0.462	0.682	10.083		RF	0.570	0.442	0.570	0.439	0.088	0.500	13.744
Chi-squared	LR	0.966	0.969	0.966	0.965	0.683	0.820	177.371	LR	0.577	0.333	0.577	0.422	0.081	0.500	1.541	
	DT	0.891	0.897	0.891	0.894	0.438	0.717	8.654	DT	0.435	0.440	0.435	0.438	0.108	0.499	5.570	
	SVM	0.510	0.455	0.510	0.446	0.097	0.499	348.830	Linear	SVM	0.980	0.981	0.980	0.980	0.845	0.934	1.548
	NB	0.120	0.438	0.120	0.179	0.058	0.491	0.077		NB	0.876	0.930	0.876	0.899	0.606	0.823	0.106
	MLP	0.440	0.439	0.440	0.439	0.113	0.501	6.398		MLP	0.971	0.971	0.971	0.971	0.695	0.855	8.042
KNN	0.481	0.434	0.481	0.453	0.103	0.498	0.487	KNN		0.945	0.941	0.945	0.939	0.693	0.804	0.570	
RF	0.572	0.440	0.572	0.437	0.087	0.500	13.499	RF		0.928	0.929	0.928	0.915	0.441	0.684	2.511	
Cosine	LR	0.580	0.336	0.580	0.426	0.082	0.500	1.632	LR	0.960	0.957	0.960	0.953	0.466	0.732	37.225	
	DT	0.431	0.444	0.431	0.439	0.110	0.499	4.587	DT	0.929	0.931	0.929	0.930	0.503	0.755	0.645	
	SVM	0.982	0.983	0.982	0.982	0.869	0.943	1.790	Polynomial	SVM	0.971	0.971	0.971	0.970	0.842	0.899	3.080
	NB	0.860	0.936	0.860	0.894	0.623	0.805	0.084		NB	0.663	0.847	0.663	0.711	0.456	0.709	0.078
	MLP	0.972	0.972	0.972	0.972	0.732	0.879	5.307		MLP	0.938	0.940	0.938	0.938	0.642	0.822	4.636
KNN	0.948	0.945	0.948	0.944	0.717	0.812	0.616	KNN		0.943	0.939	0.943	0.937	0.654	0.781	0.449	
RF	0.929	0.929	0.929	0.917	0.694	0.814	2.394	RF		0.926	0.927	0.926	0.913	0.429	0.678	11.632	
Isolation	LR	0.574	0.329	0.574	0.418	0.081	0.500	0.282	LR	0.969	0.967	0.969	0.967	0.590	0.792	356.439	
	DT	0.927	0.927	0.927	0.927	0.514	0.750	0.249	DT	0.921	0.925	0.921	0.922	0.488	0.509	4.192	
	SVM	0.594	0.644	0.594	0.466	0.138	0.517	7.439	Sigmoid	SVM	0.581	0.338	0.581	0.427	0.082	0.500	10.661
	NB	0.055	0.878	0.055	0.099	0.057	0.518	0.068		NB	0.311	0.097	0.311	0.148	0.053	0.500	0.091
	MLP	0.593	0.620	0.593	0.462	0.121	0.512	3.484		MLP	0.581	0.338	0.581	0.427	0.082	0.500	1.704
KNN	0.521	0.488	0.521	0.487	0.124	0.508	0.452	KNN		0.532	0.294	0.532	0.376	0.076	0.500	0.381	
RF	0.601	0.734	0.601	0.471	0.141	0.519	1.165	RF		0.581	0.338	0.581	0.427	0.082	0.500	1.497	
Gaussian	LR	0.581	0.337	0.581	0.427	0.082	0.500	0.403	LR	0.581	0.338	0.581	0.427	0.082	0.500	0.058	
	DT	0.600	0.692	0.600	0.472	0.135	0.517	0.126	DT	0.581	0.338	0.581	0.427	0.082	0.500	0.037	
	SVM	0.485	0.432	0.485	0.422	0.095	0.497	288.422	Laplacian	SVM	0.501	0.442	0.501	0.433	0.096	0.500	276.660
	NB	0.118	0.435	0.118	0.179	0.055	0.505	0.077		NB	0.124	0.451	0.124	0.187	0.059	0.502	0.074
	MLP	0.450	0.442	0.450	0.446	0.113	0.502	7.179		MLP	0.443	0.432	0.443	0.437	0.112	0.500	6.526
KNN	0.482	0.437	0.482	0.455	0.105	0.500	0.500	KNN		0.484	0.428	0.484	0.453	0.103	0.498	0.51	

Classification results for spaced k-mer embeddings on ShortRead data (Table 27) show that cosine and linear kernels with SVM achieve near-perfect accuracy (0.995 and 0.996, respectively) with exceptional ROC-AUC scores approaching 0.98. Additive-chi2 kernel paired with logistic regression also delivers outstanding performance (accuracy: 0.994, ROC-AUC: 0.982). Polynomial kernel demonstrates robust results across multiple classifiers, with SVM achieving 0.996 accuracy. Random forest with cosine kernel yields competitive performance (accuracy: 0.961), while decision tree classifiers also show strong results across appropriate kernels. The isolation, Gaussian, laplacian, chi-squared, and sigmoid kernels continue their pattern of severe under-performance, with accuracies near chance level. Training times for logistic regression with polynomial and linear kernels are substantially elevated (468.754 and 100.837 seconds), suggesting computational challenges with spaced k-mer dimensionality.

Kernels	ML Algo.							Kernels	ML Algo.							
	Algo.	Acc.	Prec.	Recall	F1 weighh.	F1 Macro	ROC-AUC		Train. run-time (sec.)	Algo.	Acc.	Prec.	Recall	F1 weighh.	F1 Macro	ROC-AUC
Additive-chi2	SVM	0.994	0.994	0.994	0.994	0.969	0.973	3.749	SVM	0.487	0.427	0.487	0.421	0.094	0.496	275.879
	NB	0.384	0.612	0.384	0.368	0.316	0.608	0.080	NB	0.119	0.430	0.119	0.179	0.056	0.496	0.088
	MLP	0.951	0.951	0.951	0.951	0.734	0.876	3.700	MLP	0.443	0.430	0.443	0.436	0.111	0.500	7.825
	KNN	0.886	0.888	0.886	0.880	0.643	0.766	0.458	KNN	0.488	0.449	0.488	0.457	0.106	0.500	0.514
	RF	0.870	0.888	0.870	0.860	0.519	0.701	9.926	RF	0.563	0.425	0.563	0.430	0.087	0.500	17.216
DT	0.868	0.876	0.868	0.872	0.427	0.716	5.942	DT	0.438	0.441	0.438	0.440	0.117	0.504	5.267	
Chi-squared	SVM	0.497	0.432	0.497	0.431	0.092	0.496	294.065	SVM	0.996	0.996	0.996	0.995	0.965	0.970	4.529
	NB	0.129	0.456	0.129	0.193	0.061	0.508	0.076	NB	0.838	0.913	0.838	0.870	0.595	0.772	0.095
	MLP	0.443	0.439	0.443	0.440	0.106	0.498	6.653	MLP	0.944	0.944	0.944	0.944	0.711	0.851	5.265
	KNN	0.494	0.441	0.494	0.464	0.105	0.500	0.478	KNN	0.943	0.944	0.943	0.939	0.736	0.815	0.483
	RF	0.567	0.420	0.567	0.437	0.086	0.499	13.467	RF	0.955	0.951	0.955	0.947	0.516	0.726	10.909
DT	0.581	0.337	0.581	0.427	0.082	0.500	1.548	DT	0.986	0.986	0.986	0.985	0.721	0.858	468.754	
Cosine	SVM	0.995	0.995	0.995	0.995	0.976	0.978	7.967	SVM	0.996	0.996	0.996	0.996	0.964	0.969	4.323
	NB	0.835	0.913	0.835	0.867	0.628	0.786	0.126	NB	0.828	0.928	0.828	0.868	0.562	0.746	0.083
	MLP	0.952	0.952	0.952	0.952	0.739	0.866	6.891	MLP	0.951	0.951	0.951	0.950	0.768	0.876	4.426
	KNN	0.952	0.953	0.952	0.949	0.783	0.844	0.670	KNN	0.945	0.947	0.945	0.942	0.773	0.833	0.499
	RF	0.961	0.958	0.961	0.955	0.540	0.736	13.395	RF	0.956	0.952	0.956	0.949	0.517	0.726	14.046
DT	0.963	0.964	0.963	0.963	0.631	0.822	3.830	DT	0.986	0.985	0.986	0.985	0.708	0.851	100.837	
Isolation	SVM	0.588	0.605	0.588	0.458	0.138	0.517	7.247	SVM	0.582	0.339	0.582	0.429	0.082	0.500	10.724
	NB	0.055	0.850	0.055	0.099	0.051	0.516	0.067	NB	0.312	0.097	0.312	0.148	0.053	0.500	0.095
	MLP	0.590	0.614	0.590	0.460	0.128	0.514	4.466	MLP	0.582	0.339	0.582	0.429	0.082	0.500	1.978
	KNN	0.523	0.492	0.523	0.492	0.129	0.511	0.449	KNN	0.465	0.235	0.465	0.308	0.069	0.500	0.434
	RF	0.597	0.714	0.597	0.465	0.129	0.515	1.156	RF	0.582	0.339	0.582	0.429	0.082	0.500	1.358
DT	0.578	0.587	0.578	0.424	0.082	0.500	0.375	DT	0.582	0.339	0.582	0.429	0.082	0.500	0.053	
Gaussian	SVM	0.493	0.433	0.493	0.423	0.095	0.499	394.075	SVM	0.582	0.339	0.582	0.429	0.082	0.500	0.053
	NB	0.123	0.435	0.123	0.185	0.059	0.519	0.092	NB	0.312	0.097	0.312	0.148	0.053	0.500	0.095
	MLP	0.459	0.441	0.459	0.450	0.111	0.502	6.578	MLP	0.582	0.339	0.582	0.429	0.082	0.500	1.978
	KNN	0.489	0.425	0.489	0.453	0.103	0.498	0.516	KNN	0.465	0.235	0.465	0.308	0.069	0.500	0.434
	RF	0.561	0.424	0.561	0.428	0.086	0.500	13.978	RF	0.582	0.339	0.582	0.429	0.082	0.500	1.358
DT	0.423	0.429	0.423	0.426	0.107	0.497	5.004	DT	0.582	0.339	0.582	0.429	0.082	0.500	0.053	

Table 27: Classification comparison for different kernel methods and classifiers on spaced kmer for ShortRead data.

10.4 Results for Rabies Data

Table 28 presents classification results for Rabies data using OHE encoding. Linear and cosine kernels with random forest achieve the highest accuracies (0.831 and 0.831, respectively), accompanied by strong ROC-AUC scores (0.848 and 0.850). Laplacian kernel also demonstrates competitive performance across multiple classifiers, with random forest yielding 0.827 accuracy. SVM classifiers paired with additive-chi2, laplacian, linear, cosine, and sigmoid kernels achieve accuracies above 0.80, indicating robust kernel adaptability for Rabies sequence classification. The isolation and Gaussian kernels show severe underperformance, with accuracies near chance level (0.452-0.567), suggesting fundamental incompatibility with OHE-encoded Rabies data. Training times vary considerably, with logistic regression requiring up to 864 seconds for additive-chi2 kernel, while KNN maintains efficient computation across all kernels. Chi-squared kernel exhibits moderate performance (best accuracy: 0.642 with random forest), considerably lower than top-performing kernels.

Kernels	ML Algo.	Acc.	Prec.	Recall	F1 weigh.	F1 Macro	ROC-AUC	Train. run-time (sec.)	Kernels	ML Algo.	Acc.	Prec.	Recall	F1 weigh.	F1 Macro	ROC-AUC	Train. run-time (sec.)	
Additive-chi2	SVM	0.802	0.788	0.802	0.790	0.704	0.835	164.270	Laplacian	SVM	0.799	0.786	0.799	0.787	0.700	0.832	392.048	
	NB	0.238	0.470	0.238	0.202	0.264	0.670	2.122		NB	0.246	0.493	0.246	0.213	0.269	0.673	2.052	
	MLP	0.799	0.785	0.799	0.787	0.686	0.832	291.650		MLP	0.802	0.785	0.802	0.791	0.686	0.831	338.192	
	KNN	0.808	0.794	0.808	0.797	0.705	0.835	8.592		KNN	0.807	0.794	0.807	0.796	0.703	0.833	9.491	
	RF	0.824	0.814	0.824	0.812	0.730	0.845	139.136		RF	0.827	0.817	0.827	0.817	0.733	0.847	154.094	
	LR	0.806	0.790	0.806	0.791	0.697	0.834	864.016		LR	0.804	0.770	0.804	0.774	0.262	0.583	37.003	
DT	0.761	0.758	0.761	0.759	0.673	0.823	30.155	DT	0.762	0.761	0.762	0.761	0.672	0.821	68.036			
Chi-squared	SVM	0.601	0.711	0.601	0.534	0.380	0.624	385.677	Linear	SVM	0.801	0.790	0.801	0.790	0.703	0.834	221.750	
	NB	0.210	0.682	0.210	0.265	0.258	0.617	0.492		NB	0.226	0.478	0.226	0.189	0.247	0.660	0.579	
	MLP	0.623	0.712	0.623	0.563	0.411	0.643	319.315		MLP	0.805	0.792	0.805	0.795	0.692	0.831	243.603	
	KNN	0.584	0.559	0.584	0.553	0.414	0.658	6.874		KNN	0.814	0.803	0.814	0.804	0.712	0.838	5.072	
	RF	0.642	0.647	0.642	0.608	0.479	0.683	156.857		RF	0.831	0.823	0.831	0.820	0.736	0.848	129.530	
	LR	0.558	0.725	0.558	0.474	0.290	0.582	15.217		LR	0.813	0.800	0.813	0.799	0.704	0.836	555.609	
DT	0.621	0.611	0.621	0.592	0.466	0.682	36.300	DT	0.765	0.762	0.765	0.763	0.672	0.822	35.170			
Cosine	SVM	0.818	0.807	0.818	0.808	0.722	0.844	231.021	Polynomial	SVM	0.799	0.786	0.799	0.788	0.700	0.831	367.065	
	NB	0.307	0.560	0.307	0.300	0.338	0.706	0.503		NB	0.227	0.523	0.227	0.198	0.256	0.662	2.511	
	MLP	0.802	0.789	0.802	0.794	0.689	0.833	225.703		MLP	0.800	0.786	0.800	0.790	0.686	0.832	305.637	
	KNN	0.811	0.798	0.811	0.801	0.708	0.837	4.911		KNN	0.809	0.797	0.809	0.799	0.710	0.836	7.549	
	RF	0.831	0.823	0.831	0.822	0.740	0.850	80.703		RF	0.827	0.818	0.827	0.817	0.737	0.849	181.812	
	LR	0.785	0.781	0.785	0.760	0.631	0.782	37.155		LR	0.817	0.803	0.817	0.811	0.383	0.636	43.400	
DT	0.766	0.767	0.766	0.769	0.679	0.827	32.122	DT	0.763	0.761	0.763	0.762	0.676	0.825	35.149			
Isolation	SVM	0.452	0.332	0.452	0.290	0.061	0.502	106.114	Sigmoid	SVM	0.805	0.793	0.805	0.794	0.704	0.834	237.152	
	NB	0.076	0.586	0.076	0.046	0.025	0.505	0.254		NB	0.235	0.475	0.235	0.200	0.255	0.667	1.940	
	MLP	0.455	0.385	0.455	0.292	0.062	0.503	6.026		MLP	0.803	0.789	0.803	0.793	0.688	0.832	255.452	
	KNN	0.355	0.247	0.355	0.283	0.073	0.501	2.900		KNN	0.809	0.795	0.809	0.797	0.702	0.833	3.769	
	RF	0.456	0.416	0.456	0.292	0.062	0.503	4.248		RF	0.828	0.819	0.828	0.818	0.736	0.848	80.747	
	LR	0.452	0.204	0.452	0.281	0.052	0.500	2.220		LR	0.486	0.318	0.486	0.338	0.118	0.528	19.354	
DT	0.455	0.381	0.455	0.291	0.062	0.503	0.413	DT	0.764	0.762	0.764	0.763	0.674	0.823	44.113			
Gaussian	SVM	0.564	0.716	0.564	0.487	0.312	0.590	219.587										
	NB	0.103	0.654	0.103	0.116	0.138	0.559	1.176										
	MLP	0.561	0.687	0.561	0.483	0.305	0.589	266.812										
	KNN	0.487	0.464	0.487	0.436	0.274	0.583	9.324										
	RF	0.567	0.714	0.567	0.492	0.321	0.594	204.050										
	LR	0.549	0.725	0.549	0.462	0.276	0.575	38.109										
DT	0.566	0.712	0.566	0.491	0.319	0.594	26.276											

Table 28: Classification comparison for different kernel methods and classifiers on OHE for Rabies Data.

For k-mer embeddings on Rabies data (Table 29), cosine and laplacian kernels with random forest achieve the highest accuracies (0.825 and 0.829, respectively), with excellent ROC-AUC scores approaching 0.85. KNN demonstrates strong performance across multiple kernels, particularly with cosine and laplacian (accuracies: 0.821 and 0.820). Chi-squared kernel with SVM yields competitive results (accuracy: 0.782), though substantially lower than optimal configurations. Isolation and Gaussian kernels maintain their pattern of poor performance, with accuracies around 0.45-0.57, indicating these kernels remain unsuitable for k-mer representations. Sigmoid kernel shows varied performance, with SVM achieving reasonable accuracy (0.781) but requiring exceptionally long training time (789.653 seconds). The polynomial and linear kernels demonstrate moderate effectiveness, with random forest achieving accuracies of 0.828

and 0.814, respectively. Overall computational costs are elevated compared to OHE, with several configurations exceeding 500 seconds.

Kernel	ML Algo.	Acc.	Prec.	Recall	F1 weigh.	F1 Macro	ROC-AUC	Train. run-time (sec.)	Kernel	ML Algo.	Acc.	Prec.	Recall	F1 weigh.	F1 Macro	ROC-AUC	Train. run-time (sec.)
Additive-chi2	SVM	0.794	0.781	0.794	0.782	0.692	0.824	659.962	Laplacian	SVM	0.802	0.792	0.802	0.792	0.707	0.832	538.657
	NB	0.124	0.470	0.124	0.107	0.143	0.367	1.000		NB	0.267	0.645	0.267	0.227	0.331	0.678	1.667
	MLP	0.768	0.753	0.768	0.759	0.645	0.810	373.167		MLP	0.763	0.756	0.763	0.758	0.647	0.812	229.206
	KNN	0.817	0.805	0.817	0.806	0.709	0.837	5.972		KNN	0.820	0.809	0.820	0.810	0.718	0.843	5.070
	RF	0.822	0.814	0.822	0.809	0.729	0.839	111.861		RF	0.829	0.821	0.829	0.817	0.734	0.844	92.672
	LR	0.797	0.781	0.797	0.779	0.680	0.822	243.465		LR	0.566	0.522	0.566	0.471	0.244	0.579	21.589
DT	0.743	0.743	0.743	0.743	0.650	0.811	49.992	DT	0.758	0.756	0.758	0.756	0.666	0.818	38.626		
Chi-squared	SVM	0.782	0.782	0.782	0.762	0.666	0.795	710.571	Linear	SVM	0.760	0.750	0.760	0.728	0.623	0.788	215.395
	NB	0.462	0.691	0.462	0.492	0.447	0.776	1.434		NB	0.100	0.378	0.100	0.061	0.101	0.361	1.227
	MLP	0.791	0.780	0.791	0.776	0.680	0.811	230.237		MLP	0.767	0.745	0.767	0.744	0.622	0.795	255.829
	KNN	0.784	0.771	0.784	0.772	0.677	0.817	6.364		KNN	0.815	0.801	0.815	0.804	0.710	0.839	7.647
	RF	0.796	0.784	0.796	0.785	0.692	0.822	197.843		RF	0.814	0.808	0.814	0.802	0.721	0.832	65.506
	LR	0.760	0.779	0.760	0.737	0.631	0.765	35.220		LR	0.672	0.706	0.672	0.647	0.539	0.746	330.867
DT	0.751	0.746	0.751	0.748	0.653	0.812	59.370	DT	0.733	0.734	0.733	0.733	0.641	0.807	35.263		
Cosine	SVM	0.753	0.746	0.753	0.716	0.611	0.781	424.287	Polynomial	SVM	0.772	0.760	0.772	0.755	0.649	0.807	180.462
	NB	0.072	0.348	0.072	0.037	0.063	0.538	2.241		NB	0.072	0.293	0.072	0.041	0.066	0.528	1.666
	MLP	0.770	0.746	0.770	0.748	0.621	0.796	285.515		MLP	0.772	0.754	0.772	0.754	0.636	0.802	192.313
	KNN	0.821	0.807	0.821	0.810	0.712	0.841	14.192		KNN	0.818	0.807	0.818	0.808	0.713	0.840	5.579
	RF	0.825	0.818	0.825	0.813	0.728	0.838	103.609		RF	0.828	0.821	0.828	0.816	0.730	0.842	81.917
	LR	0.601	0.579	0.601	0.526	0.339	0.618	33.187		LR	0.464	0.516	0.464	0.410	0.183	0.572	465.349
DT	0.736	0.737	0.736	0.737	0.642	0.808	24.903	DT	0.736	0.737	0.736	0.736	0.638	0.806	27.801		
Isolation	SVM	0.450	0.346	0.450	0.287	0.061	0.502	106.662	Sigmoid	SVM	0.781	0.769	0.781	0.769	0.681	0.821	789.653
	NB	0.061	0.601	0.061	0.042	0.023	0.505	0.369		NB	0.196	0.499	0.196	0.194	0.188	0.600	1.573
	MLP	0.453	0.387	0.453	0.289	0.062	0.503	12.559		MLP	0.737	0.723	0.737	0.728	0.606	0.787	139.062
	KNN	0.358	0.249	0.358	0.283	0.074	0.501	2.344		KNN	0.816	0.803	0.816	0.805	0.708	0.837	9.892
	RF	0.453	0.413	0.453	0.289	0.061	0.503	5.328		RF	0.814	0.809	0.814	0.799	0.712	0.825	76.203
	LR	0.449	0.202	0.449	0.278	0.052	0.500	2.175		LR	0.480	0.348	0.480	0.334	0.085	0.513	14.373
DT	0.453	0.391	0.453	0.289	0.063	0.503	0.330	DT	0.725	0.725	0.725	0.725	0.624	0.796	20.921		
Gaussian	SVM	0.572	0.710	0.572	0.497	0.323	0.594	259.289		SVM	0.572	0.710	0.572	0.497	0.323	0.594	259.289
	NB	0.106	0.630	0.106	0.129	0.137	0.558	2.046		NB	0.106	0.630	0.106	0.129	0.137	0.558	2.046
	MLP	0.566	0.679	0.566	0.488	0.303	0.589	222.969		MLP	0.566	0.679	0.566	0.488	0.303	0.589	222.969
	KNN	0.490	0.471	0.490	0.441	0.280	0.584	10.377		KNN	0.490	0.471	0.490	0.441	0.280	0.584	10.377
	RF	0.575	0.712	0.575	0.502	0.330	0.597	109.450		RF	0.575	0.712	0.575	0.502	0.330	0.597	109.450
	LR	0.557	0.716	0.557	0.473	0.285	0.579	23.231		LR	0.557	0.716	0.557	0.473	0.285	0.579	23.231
DT	0.574	0.709	0.574	0.501	0.329	0.597	21.935	DT	0.574	0.709	0.574	0.501	0.329	0.597	21.935		

Table 29: Classification comparison for different kernel methods and classifiers on kmer for Rabies data.

Table 30 reveals that cosine and polynomial kernels with random forest deliver the highest classification performance on minimizer-encoded Rabies data (accuracies: 0.820 and 0.822, respectively), with strong ROC-AUC scores above 0.83. Laplacian and additive-chi2 kernels also demonstrate competitive results when paired with random forest (accuracies: 0.824 and 0.808). KNN shows good performance across appropriate kernels, with cosine achieving 0.812 accuracy and exceptional efficiency (2.330 seconds). Linear kernel exhibits reduced effectiveness compared to other embeddings, with peak accuracy of 0.815 using random forest. The isolation, Gaussian, and sigmoid kernels continue to show poor performance, with accuracies clustered around chance level or below 0.60, except for sigmoid-KNN which achieves moderate success (0.599 accuracy). Chi-squared kernel demonstrates mixed results, with random forest reaching 0.771 accuracy but requiring substantial training time (313.655 seconds). Minimizer encoding generally yields slightly lower peak performance compared to OHE and k-mer approaches.

Classification results for spaced k-mer embeddings on Rabies data (Table 31) demonstrate that laplacian and linear kernels with random forest achieve peak accuracies (0.831 and 0.828, respectively), with ROC-AUC scores exceeding 0.84. Additive-chi2 and cosine kernels also deliver strong performance when combined with random forest (accuracies: 0.830 and 0.826). KNN maintains robust classification across multiple kernels, with cosine achieving 0.825 accuracy. Laplacian kernel with logistic regression shows competitive results (accuracy: 0.802), with moderate training time (30.393 seconds). The isolation and Gaussian kernels exhibit their characteristic poor performance, with accuracies near 0.45-0.57 for most classifiers. Notably, sigmoid kernel demonstrates improved effectiveness compared to other embeddings, with KNN achieving 0.793 accuracy and MLP reaching 0.662, suggesting better compatibility

Kernels	ML Algo.	Acc.	Prec.	Recall	F1 weigh.	F1 Macro	ROC-AUC	Train. run-time (sec.)	Kernels	ML Algo.	Acc.	Prec.	Recall	F1 weigh.	F1 Macro	ROC-AUC	Train. run-time (sec.)
Additive-chi2	SVM	0.784	0.771	0.784	0.770	0.677	0.815	693.775	Laplacian	SVM	0.808	0.802	0.808	0.787	0.693	0.821	86.831
	NB	0.135	0.438	0.135	0.123	0.173	0.572	1.021		NB	0.424	0.603	0.424	0.432	0.406	0.744	0.265
	MLP	0.756	0.758	0.756	0.744	0.626	0.788	250.236		MLP	0.797	0.779	0.797	0.783	0.674	0.821	342.256
	KNN	0.811	0.798	0.811	0.799	0.700	0.834	5.544		KNN	0.814	0.799	0.814	0.802	0.705	0.836	4.214
	RF	0.808	0.804	0.808	0.794	0.708	0.822	124.885		RF	0.824	0.814	0.824	0.813	0.730	0.843	44.289
	LR	0.767	0.750	0.767	0.744	0.641	0.801	448.436		LR	0.778	0.774	0.778	0.753	0.641	0.785	9.343
DT	0.731	0.728	0.731	0.729	0.629	0.800	31.926	DT	0.762	0.759	0.762	0.760	0.670	0.821	8.087		
Chi-squared	SVM	0.743	0.744	0.743	0.721	0.623	0.765	751.147	Linear	SVM	0.661	0.655	0.661	0.603	0.502	0.717	286.512
	NB	0.434	0.718	0.434	0.498	0.429	0.742	1.086		NB	0.120	0.443	0.120	0.098	0.150	0.568	0.762
	MLP	0.766	0.758	0.766	0.747	0.649	0.788	250.236		MLP	0.739	0.712	0.739	0.709	0.575	0.772	385.189
	KNN	0.757	0.741	0.757	0.743	0.644	0.793	5.245		KNN	0.810	0.798	0.810	0.799	0.702	0.834	4.067
	RF	0.771	0.760	0.771	0.759	0.668	0.805	313.655		RF	0.815	0.808	0.815	0.803	0.720	0.833	12.188
	LR	0.706	0.756	0.706	0.673	0.546	0.712	58.762		LR	0.683	0.626	0.683	0.563	0.332	0.634	54.695
DT	0.730	0.723	0.730	0.726	0.627	0.796	143.665	DT	0.736	0.734	0.736	0.734	0.636	0.803	3.030		
Cosine	SVM	0.669	0.654	0.669	0.610	0.504	0.721	43.279	Polynomial	SVM	0.635	0.646	0.635	0.582	0.471	0.691	63.930
	NB	0.084	0.406	0.084	0.063	0.113	0.545	0.084		NB	0.073	0.507	0.073	0.043	0.067	0.529	0.196
	MLP	0.740	0.712	0.740	0.710	0.572	0.769	32.879		MLP	0.737	0.703	0.737	0.709	0.575	0.769	318.687
	KNN	0.812	0.800	0.812	0.801	0.708	0.837	2.330		KNN	0.810	0.798	0.810	0.798	0.703	0.834	3.006
	RF	0.820	0.812	0.820	0.807	0.722	0.836	10.028		RF	0.822	0.813	0.822	0.810	0.723	0.857	26.565
	LR	0.362	0.440	0.362	0.384	0.154	0.537	1.760		LR	0.340	0.538	0.340	0.356	0.218	0.584	240.148
DT	0.738	0.737	0.738	0.737	0.638	0.805	1.492	DT	0.723	0.729	0.723	0.726	0.629	0.801	6.610		
Isolation	SVM	0.449	0.335	0.449	0.287	0.061	0.502	102.421	Sigmoid	SVM	0.454	0.260	0.454	0.285	0.053	0.500	19.658
	NB	0.103	0.585	0.103	0.053	0.029	0.505	0.355		NB	0.047	0.280	0.047	0.007	0.010	0.501	0.015
	MLP	0.452	0.366	0.452	0.288	0.061	0.503	10.511		MLP	0.480	0.389	0.480	0.334	0.084	0.511	11.617
	KNN	0.351	0.252	0.351	0.281	0.075	0.502	2.647		KNN	0.599	0.579	0.599	0.578	0.454	0.685	0.374
	RF	0.453	0.462	0.453	0.288	0.061	0.503	6.502		RF	0.459	0.426	0.459	0.285	0.060	0.502	1.061
	LR	0.449	0.201	0.449	0.278	0.052	0.500	2.217		LR	0.455	0.207	0.455	0.284	0.052	0.500	0.230
DT	0.452	0.384	0.452	0.289	0.062	0.503	0.446	DT	0.461	0.399	0.461	0.298	0.061	0.503	0.032		
Gaussian	SVM	0.584	0.711	0.584	0.517	0.350	0.606	835.225	Gaussian	SVM	0.584	0.711	0.584	0.517	0.350	0.606	835.225
	NB	0.118	0.659	0.118	0.141	0.153	0.568	0.555		NB	0.118	0.659	0.118	0.141	0.153	0.568	0.555
	MLP	0.582	0.707	0.582	0.513	0.335	0.602	163.950		MLP	0.582	0.707	0.582	0.513	0.335	0.602	163.950
	KNN	0.511	0.496	0.511	0.464	0.306	0.597	5.282		KNN	0.511	0.496	0.511	0.464	0.306	0.597	5.282
	RF	0.590	0.717	0.590	0.525	0.360	0.611	149.602		RF	0.590	0.717	0.590	0.525	0.360	0.611	149.602
	LR	0.567	0.728	0.567	0.488	0.311	0.589	44.386		LR	0.567	0.728	0.567	0.488	0.311	0.589	44.386
DT	0.590	0.718	0.590	0.524	0.358	0.610	42.641	DT	0.590	0.718	0.590	0.524	0.358	0.610	42.641		

Table 30: Classification comparison for different kernel methods and classifiers on minimizer for Rabies.

with spaced k-mer representations. Chi-squared kernel shows moderate performance (best accuracy: 0.710 with random forest), while polynomial kernel yields mixed results with substantial training time requirements.

Kernels	ML Algo.	Acc.	Prec.	Recall	F1 weigh.	F1 Macro	ROC-AUC	Train. run-time (sec.)	Kernels	ML Algo.	Acc.	Prec.	Recall	F1 weigh.	F1 Macro	ROC-AUC	Train. run-time (sec.)
Additive-chi2	SVM	0.802	0.792	0.802	0.793	0.706	0.834	426.061	Laplacian	SVM	0.820	0.808	0.820	0.809	0.722	0.842	180.689
	NB	0.349	0.594	0.349	0.359	0.408	0.712	0.708		NB	0.282	0.640	0.282	0.281	0.382	0.714	0.469
	MLP	0.763	0.757	0.763	0.759	0.650	0.812	197.302		MLP	0.794	0.784	0.794	0.787	0.683	0.832	177.217
	KNN	0.820	0.807	0.820	0.809	0.711	0.839	4.457		KNN	0.818	0.805	0.818	0.808	0.716	0.841	4.347
	RF	0.830	0.820	0.830	0.818	0.733	0.845	120.819		RF	0.831	0.821	0.831	0.821	0.737	0.849	71.988
	LR	0.823	0.810	0.823	0.811	0.721	0.845	302.296		LR	0.802	0.795	0.802	0.779	0.670	0.808	30.393
DT	0.755	0.754	0.755	0.754	0.660	0.816	54.611	DT	0.772	0.767	0.772	0.769	0.681	0.827	35.270		
Chi-squared	SVM	0.672	0.705	0.672	0.637	0.513	0.695	449.020	Linear	SVM	0.802	0.790	0.802	0.789	0.692	0.824	374.927
	NB	0.305	0.709	0.305	0.380	0.343	0.671	0.711		NB	0.114	0.312	0.114	0.087	0.128	0.565	0.606
	MLP	0.712	0.735	0.712	0.683	0.564	0.728	169.579		MLP	0.775	0.760	0.775	0.765	0.650	0.812	185.657
	KNN	0.688	0.676	0.688	0.670	0.559	0.738	5.000		KNN	0.821	0.808	0.821	0.810	0.712	0.840	4.783
	RF	0.710	0.702	0.710	0.692	0.583	0.750	190.406		RF	0.828	0.821	0.828	0.815	0.730	0.840	96.590
	LR	0.620	0.735	0.620	0.567	0.404	0.632	29.577		LR	0.784	0.801	0.784	0.776	0.665	0.821	446.614
DT	0.677	0.666	0.677	0.668	0.551	0.748	108.810	DT	0.749	0.749	0.749	0.749	0.655	0.814	25.855		
Cosine	SVM	0.806	0.796	0.806	0.793	0.694	0.826	482.196	Polynomial	SVM	0.670	0.678	0.670	0.636	0.504	0.710	122.016
	NB	0.067	0.183	0.067	0.029	0.059	0.533	0.866		NB	0.072	0.326	0.072	0.039	0.067	0.529	0.723
	MLP	0.777	0.763	0.777	0.768	0.655	0.814	198.749		MLP	0.763	0.742	0.763	0.741	0.612	0.788	201.405
	KNN	0.825	0.813	0.825	0.814	0.715	0.842	6.989		KNN	0.819	0.806	0.819	0.808	0.714	0.841	3.408
	RF	0.826	0.819	0.826	0.813	0.723	0.836	74.431		RF	0.828	0.819	0.828	0.815	0.725	0.841	58.476
	LR	0.734	0.743	0.734	0.688	0.557	0.746	38.065		LR	0.422	0.572	0.422	0.401	0.220	0.582	379.210
DT	0.745	0.743	0.745	0.744	0.645	0.808	29.849	DT	0.749	0.748	0.749	0.748	0.652	0.813	18.035		
Isolation	SVM	0.453	0.325	0.453	0.291	0.060	0.502	81.442	Sigmoid	SVM	0.524	0.436	0.524	0.403	0.209	0.562	18.261
	NB	0.075	0.613	0.075	0.045	0.025	0.505	0.267		NB	0.263	0.489	0.263	0.307	0.222	0.604	0.014
	MLP	0.457	0.380	0.457	0.293	0.061	0.503	7.016		MLP	0.662	0.631	0.662	0.606	0.447	0.690	33.259
	KNN	0.359	0.249	0.359	0.286	0.076	0.502	1.604		KNN	0.793	0.779	0.793	0.781	0.670	0.818	0.304
	RF	0.457	0.401	0.457	0.293	0.062	0.503	3.541		RF	0.773	0.780	0.773	0.758	0.664	0.798	4.252
	LR	0.453	0.265	0.453	0.283	0.052	0.500	1.382		LR	0.484	0.338	0.484	0.337	0.084	0.512	0.314
DT	0.457	0.380	0.457	0.293	0.062	0.503	0.277	DT	0.711	0.705	0.711	0.700	0.602	0.770	0.187		
Gaussian	SVM	0.570	0.708	0.570	0.495	0.323	0.595	321.822	Gaussian	SVM	0.570	0.708	0.570	0.495	0.323	0.595	321.822
	NB	0.099	0.645	0.099	0.111	0.140	0.561	1.139		NB	0.099	0.645	0.099	0.111	0.140	0.561	1.139
	MLP	0.565	0.690	0.565	0.490	0.316	0.592	162.739		MLP							

10.5 Results for Genome Data

Table 32 presents classification results for Genome data using OHE encoding, revealing moderate overall performance compared to other datasets. Cosine, sigmoid, and linear kernels with random forest achieve the highest accuracies (0.673, 0.666, and 0.668, respectively), though these values remain substantially lower than performance on Spike7k or Host datasets. SVM classifiers paired with cosine, sigmoid, and linear kernels demonstrate reasonable performance around 0.63-0.64 accuracy. The isolation, chi-squared, and Gaussian kernels exhibit severe classification failure, with accuracies near or below chance level (0.28-0.32), indicating fundamental incompatibility with OHE-encoded genome sequences. Laplacian kernel with logistic regression shows anomalous behavior with accuracy dropping to 0.277, while maintaining reasonable performance with other classifiers. Training times vary considerably, with logistic regression requiring exceptionally long computation for additive-chi2 (2091.413 seconds) and linear (1134.426 seconds) kernels. Naive Bayes underperforms across different kernels, suggesting this classifier is unsuitable for genome-scale OHE data.

Kernel	ML Algo.	Acc.	Prec.	Recall	F1 weigh.	F1 Macro	ROC-AUC	Train. run-time (sec.)	Kernel	ML Algo.	Acc.	Prec.	Recall	F1 weigh.	F1 Macro	ROC-AUC	Train. run-time (sec.)
Additive-chi2	SVM	0.630	0.651	0.630	0.632	0.347	0.673	23.473	Laplacian	SVM	0.631	0.642	0.631	0.630	0.340	0.668	23.992
	NB	0.024	0.219	0.024	0.017	0.043	0.550	0.603		NB	0.023	0.257	0.023	0.017	0.049	0.551	0.488
	MLP	0.595	0.568	0.595	0.575	0.440	0.613	77.501		MLP	0.591	0.556	0.591	0.566	0.421	0.601	79.025
	KNN	0.627	0.621	0.627	0.608	0.318	0.642	0.761		KNN	0.631	0.626	0.631	0.611	0.318	0.639	0.679
	RF	0.668	0.678	0.668	0.652	0.428	0.679	21.451		RF	0.676	0.686	0.676	0.659	0.441	0.683	23.256
	LR	0.559	0.576	0.559	0.574	0.283	0.625	2091.413		LR	0.277	0.088	0.277	0.138	0.011	0.500	19.540
DT	0.562	0.569	0.562	0.564	0.308	0.649	14.166	DT	0.566	0.574	0.566	0.568	0.311	0.653	13.414		
Chi-squared	SVM	0.283	0.373	0.283	0.136	0.035	0.508	2.272	Linear	SVM	0.632	0.647	0.632	0.632	0.348	0.672	19.174
	NB	0.017	0.461	0.017	0.019	0.021	0.511	0.017		NB	0.025	0.210	0.025	0.019	0.045	0.542	0.402
	MLP	0.285	0.376	0.285	0.141	0.043	0.511	7.569		MLP	0.592	0.556	0.592	0.568	0.429	0.605	69.392
	KNN	0.253	0.219	0.253	0.218	0.072	0.524	0.097		KNN	0.626	0.621	0.626	0.606	0.315	0.636	0.759
	RF	0.324	0.403	0.324	0.233	0.087	0.524	1.380		RF	0.668	0.680	0.668	0.651	0.437	0.678	30.919
	LR	0.281	0.362	0.281	0.131	0.019	0.502	0.379		LR	0.578	0.555	0.578	0.547	0.264	0.612	1134.426
DT	0.319	0.388	0.319	0.230	0.084	0.523	0.057	DT	0.566	0.573	0.566	0.567	0.305	0.647	16.228		
Cosine	SVM	0.635	0.651	0.635	0.636	0.347	0.676	16.333	Polynomial	SVM	0.624	0.634	0.624	0.621	0.329	0.662	16.698
	NB	0.025	0.253	0.025	0.020	0.045	0.546	0.281		NB	0.021	0.214	0.021	0.016	0.042	0.545	0.360
	MLP	0.600	0.566	0.600	0.576	0.231	0.609	53.049		MLP	0.594	0.554	0.594	0.567	0.225	0.604	52.971
	KNN	0.635	0.631	0.635	0.616	0.325	0.643	0.758		KNN	0.627	0.618	0.627	0.607	0.306	0.638	0.709
	RF	0.673	0.685	0.673	0.657	0.441	0.683	21.308		RF	0.666	0.674	0.666	0.648	0.424	0.676	22.384
	LR	0.280	0.120	0.280	0.143	0.027	0.506	20.823		LR	0.277	0.093	0.277	0.124	0.014	0.501	16.481
DT	0.563	0.571	0.563	0.565	0.308	0.656	8.756	DT	0.558	0.564	0.558	0.559	0.290	0.642	9.404		
Isolation	SVM	0.281	0.292	0.281	0.145	0.023	0.503	11.139	Sigmoid	SVM	0.642	0.658	0.642	0.644	0.365	0.684	21.319
	NB	0.030	0.329	0.030	0.038	0.018	0.506	0.192		NB	0.027	0.214	0.027	0.019	0.056	0.552	0.483
	MLP	0.279	0.276	0.279	0.144	0.025	0.504	11.601		MLP	0.591	0.557	0.591	0.568	0.232	0.608	70.397
	KNN	0.208	0.155	0.208	0.165	0.033	0.505	0.470		KNN	0.630	0.621	0.630	0.611	0.320	0.641	0.714
	RF	0.288	0.388	0.288	0.148	0.029	0.505	1.464		RF	0.666	0.674	0.666	0.648	0.422	0.674	19.287
	LR	0.278	0.250	0.278	0.123	0.011	0.500	1.821		LR	0.282	0.079	0.282	0.124	0.011	0.500	16.922
DT	0.278	0.239	0.278	0.140	0.020	0.502	0.251	DT	0.555	0.561	0.555	0.556	0.299	0.643	8.041		
Gaussian	SVM	0.324	0.573	0.324	0.231	0.132	0.543	929.006		SVM	0.324	0.573	0.324	0.231	0.132	0.543	929.006
	NB	0.021	0.314	0.021	0.023	0.062	0.528	0.303		NB	0.021	0.314	0.021	0.023	0.062	0.528	0.303
	MLP	0.272	0.247	0.272	0.214	0.081	0.524	77.877		MLP	0.272	0.247	0.272	0.214	0.081	0.524	77.877
	KNN	0.204	0.184	0.204	0.172	0.069	0.519	0.721		KNN	0.204	0.184	0.204	0.172	0.069	0.519	0.721
	RF	0.325	0.385	0.325	0.236	0.149	0.543	96.319		RF	0.325	0.385	0.325	0.236	0.149	0.543	96.319
	LR	0.302	0.561	0.302	0.168	0.025	0.504	17.754		LR	0.302	0.561	0.302	0.168	0.025	0.504	17.754
DT	0.199	0.203	0.199	0.200	0.102	0.543	21.241	DT	0.199	0.203	0.199	0.200	0.102	0.543	21.241		

Table 32: Classification comparison for different kernel methods and classifiers on OHE for Genome Data.

For k-mer embeddings on Genome data (Table 33), linear and cosine kernels with SVM achieve the highest accuracies (0.858 and 0.852, respectively), representing substantial improvement over OHE encoding. Additive-chi2 and laplacian kernels also demonstrate strong performance with SVM (accuracies: 0.846 and 0.848). Polynomial kernel paired with logistic regression yields competitive results (accuracy: 0.774), though with extremely long training time (5079.515 seconds), indicating severe computational challenges. Random forest performance varies across kernels, with modest accuracies ranging from 0.68-0.73. The isolation, chi-squared, Gaussian, and sigmoid kernels show catastrophic failure, with accuracies near or below 0.30, maintaining the pattern observed with OHE encoding. Notably, sigmoid kernel exhibits complete classification collapse with fixed accuracy of 0.276 across all classifiers, indicating numerical

instability. The k-mer representation substantially enhances classification capability for appropriate kernel-classifier combinations.

Kernel	ML Algo.	Acc.	Prec.	Recall	F1 weigh.	F1 Macro	ROC-AUC	Train. run-time (sec.)	Kernel	ML Algo.	Acc.	Prec.	Recall	F1 weigh.	F1 Macro	ROC-AUC	Train. run-time (sec.)
Additive-chi2	SVM	0.846	0.847	0.846	0.843	0.740	0.861	23.699	Laplacian	SVM	0.848	0.851	0.848	0.845	0.718	0.832	18.319
	NB	0.076	0.423	0.076	0.092	0.132	0.585	0.429		NB	0.649	0.731	0.649	0.671	0.543	0.741	0.408
	MLP	0.708	0.704	0.708	0.702	0.361	0.683	75.695		MLP	0.670	0.671	0.670	0.668	0.315	0.657	41.940
	KNN	0.670	0.678	0.670	0.652	0.444	0.692	1.018		KNN	0.770	0.774	0.770	0.757	0.554	0.742	0.748
	RF	0.684	0.739	0.684	0.648	0.395	0.649	32.336		RF	0.729	0.787	0.729	0.700	0.460	0.679	32.163
	LR	0.773	0.731	0.773	0.729	0.292	0.633	107.704		LR	0.726	0.729	0.726	0.676	0.260	0.619	23.627
DT	0.552	0.561	0.552	0.554	0.289	0.649	10.967	DT	0.606	0.615	0.606	0.608	0.336	0.666	12.955		
Chi-squared	SVM	0.286	0.115	0.286	0.137	0.015	0.502	2.883	Linear	SVM	0.858	0.860	0.858	0.856	0.744	0.873	12.923
	NB	0.091	0.117	0.091	0.083	0.017	0.524	0.014		NB	0.257	0.663	0.257	0.302	0.328	0.692	0.498
	MLP	0.294	0.184	0.294	0.181	0.028	0.507	25.091		MLP	0.733	0.741	0.733	0.744	0.387	0.693	221.908
	KNN	0.269	0.234	0.269	0.235	0.098	0.534	0.090		KNN	0.728	0.733	0.728	0.712	0.496	0.715	1.271
	RF	0.312	0.283	0.312	0.292	0.176	0.569	2.281		RF	0.689	0.774	0.689	0.653	0.419	0.660	8.764
	LR	0.286	0.115	0.286	0.137	0.015	0.501	0.436		LR	0.856	0.851	0.856	0.847	0.664	0.810	41.262
DT	0.263	0.261	0.263	0.260	0.149	0.563	0.079	DT	0.583	0.587	0.583	0.583	0.315	0.656	3.059		
Cosine	SVM	0.852	0.854	0.852	0.851	0.711	0.860	19.627	Polynomial	SVM	0.851	0.855	0.851	0.850	0.763	0.864	19.152
	NB	0.245	0.656	0.245	0.291	0.318	0.680	0.999		NB	0.175	0.482	0.175	0.221	0.282	0.640	0.569
	MLP	0.756	0.742	0.756	0.745	0.393	0.696	219.173		MLP	0.695	0.701	0.695	0.695	0.351	0.675	34.380
	KNN	0.733	0.744	0.733	0.719	0.503	0.718	1.131		KNN	0.710	0.718	0.710	0.693	0.475	0.703	0.815
	RF	0.690	0.772	0.690	0.655	0.406	0.656	11.545		RF	0.676	0.768	0.676	0.640	0.392	0.646	29.225
	LR	0.276	0.076	0.276	0.119	0.011	0.500	5.893		LR	0.774	0.747	0.774	0.736	0.337	0.659	5079.515
DT	0.560	0.567	0.560	0.562	0.297	0.646	3.463	DT	0.569	0.576	0.569	0.570	0.320	0.655	12.245		
Isolation	SVM	0.291	0.390	0.291	0.158	0.034	0.506	11.197	Sigmoid	SVM	0.276	0.076	0.276	0.119	0.011	0.500	26.593
	NB	0.035	0.449	0.035	0.047	0.017	0.505	0.187		NB	0.086	0.007	0.086	0.014	0.004	0.500	1.070
	MLP	0.287	0.323	0.287	0.153	0.028	0.505	9.804		MLP	0.276	0.076	0.276	0.119	0.011	0.500	14.011
	KNN	0.209	0.159	0.209	0.165	0.028	0.503	0.440		KNN	0.199	0.048	0.199	0.076	0.008	0.500	1.104
	RF	0.295	0.445	0.295	0.161	0.031	0.506	1.487		RF	0.276	0.076	0.276	0.119	0.011	0.500	5.003
	LR	0.281	0.243	0.281	0.127	0.012	0.500	1.902		LR	0.276	0.076	0.276	0.119	0.011	0.500	0.924
DT	0.288	0.352	0.288	0.155	0.028	0.505	0.212	DT	0.276	0.076	0.276	0.119	0.011	0.500	0.110		
Gaussian	SVM	0.326	0.568	0.326	0.233	0.140	0.547	1410.142	Gaussian	SVM	0.326	0.568	0.326	0.233	0.140	0.547	1410.142
	NB	0.023	0.379	0.023	0.028	0.006	0.532	1.229		NB	0.023	0.379	0.023	0.028	0.006	0.532	1.229
	MLP	0.263	0.257	0.263	0.209	0.076	0.521	304.053		MLP	0.263	0.257	0.263	0.209	0.076	0.521	304.053
	KNN	0.224	0.203	0.224	0.188	0.081	0.524	2.195		KNN	0.224	0.203	0.224	0.188	0.081	0.524	2.195
	RF	0.326	0.598	0.326	0.338	0.158	0.546	120.125		RF	0.326	0.598	0.326	0.338	0.158	0.546	120.125
	LR	0.298	0.527	0.298	0.162	0.022	0.503	59.320		LR	0.298	0.527	0.298	0.162	0.022	0.503	59.320
DT	0.204	0.208	0.204	0.204	0.111	0.546	66.299	DT	0.204	0.208	0.204	0.204	0.111	0.546	66.299		

Table 33: Classification comparison for different kernel methods and classifiers on kmer for Genome data.

Table 34 reveals that laplacian kernel with SVM achieves the highest accuracy (0.704) on minimizer-encoded Genome data, though performance remains substantially below k-mer encoding results. Chi-squared kernel with KNN demonstrates unexpected strong performance (accuracy: 0.793), representing an anomaly given poor chi-squared performance across other configurations. Polynomial and additive-chi2 kernels with SVM yield moderate accuracies (0.619 and 0.609, respectively). The isolation, Gaussian, and sigmoid kernels maintain their pattern of severe underperformance, with accuracies clustered around 0.28 or below, indicating fundamental unsuitability for minimizer representations. Cosine and linear kernels show mixed results across classifiers, with peak accuracies around 0.60 for appropriate configurations. Training times are generally moderate, though polynomial kernel with logistic regression requires exceptionally long computation (4727.354 seconds). Overall, minimizer encoding demonstrates reduced classification effectiveness compared to k-mer representations for genome sequences, with most configurations achieving modest performance.

Classification results for spaced k-mer embeddings on Genome data (Table 35) demonstrate exceptional performance improvement, with linear kernel paired with logistic regression achieving peak accuracy (0.961) and outstanding ROC-AUC (0.948). Polynomial kernel with logistic regression also delivers excellent results (accuracy: 0.963, ROC-AUC: 0.943), though requiring substantial training time (123.578 seconds). Additive-chi2, cosine, and laplacian kernels with SVM achieve accuracies exceeding 0.94, indicating robust kernel adaptability for spaced k-mer representations. Laplacian kernel with naive Bayes shows remarkably strong performance (accuracy: 0.850), contrasting sharply with naive Bayes underperformance on other encodings. The isolation, chi-squared, Gaussian, and sigmoid kernels continue their pattern of

Kernels	ML Algo.	Acc.	Prec.	Recall	F1 weigh.	F1 Macro	ROC-AUC	Train. run-time (sec.)	Kernels	ML Algo.	Acc.	Prec.	Recall	F1 weigh.	F1 Macro	ROC-AUC	Train. run-time (sec.)
Additive- χ^2	SVM	0.609	0.603	0.609	0.596	0.510	0.773	15.843	SVM	0.704	0.706	0.704	0.700	0.626	0.791	55.339	
	NB	0.094	0.323	0.094	0.108	0.155	0.603	0.289	NB	0.482	0.584	0.482	0.496	0.499	0.717	0.943	
	MLP	0.538	0.500	0.538	0.568	0.257	0.627	362.872	MLP	0.554	0.554	0.554	0.552	0.283	0.632	67.028	
	KNN	0.521	0.538	0.521	0.497	0.369	0.651	0.626	KNN	0.635	0.638	0.635	0.618	0.479	0.704	1.255	
	RF	0.599	0.698	0.599	0.570	0.427	0.659	12.784	RF	0.602	0.717	0.602	0.574	0.408	0.651	60.583	
LR	0.566	0.521	0.566	0.513	0.227	0.596	24.497	LR	0.619	0.608	0.606	0.549	0.203	0.586	59.755		
DT	0.436	0.443	0.436	0.437	0.279	0.637	2.562	DT	0.429	0.435	0.429	0.430	0.283	0.628	20.696		
Chi-squared	SVM	0.524	0.436	0.524	0.403	0.209	0.562	18.261	SVM	0.606	0.589	0.606	0.571	0.491	0.745	35.667	
	NB	0.263	0.489	0.263	0.307	0.222	0.604	0.014	NB	0.199	0.466	0.199	0.224	0.292	0.677	1.236	
	MLP	0.662	0.631	0.662	0.666	0.447	0.690	33.259	MLP	0.567	0.518	0.567	0.524	0.283	0.632	243.401	
	KNN	0.793	0.779	0.793	0.781	0.670	0.818	0.304	KNN	0.552	0.557	0.552	0.530	0.386	0.664	0.948	
	RF	0.773	0.780	0.773	0.758	0.664	0.798	4.252	RF	0.616	0.726	0.616	0.590	0.451	0.672	7.789	
LR	0.484	0.538	0.484	0.337	0.084	0.512	0.314	LR	0.585	0.552	0.585	0.542	0.371	0.662	36.660		
DT	0.711	0.705	0.711	0.700	0.602	0.770	0.197	DT	0.451	0.456	0.451	0.451	0.296	0.647	1.882		
Cosine	SVM	0.602	0.592	0.602	0.567	0.493	0.739	36.318	SVM	0.619	0.645	0.619	0.625	0.544	0.791	27.262	
	NB	0.194	0.466	0.194	0.217	0.285	0.674	0.669	NB	0.131	0.365	0.131	0.156	0.233	0.618	0.495	
	MLP	0.551	0.492	0.551	0.566	0.472	0.631	191.742	MLP	0.492	0.487	0.492	0.492	0.233	0.613	49.752	
	KNN	0.568	0.568	0.568	0.546	0.397	0.669	0.972	KNN	0.539	0.538	0.539	0.515	0.336	0.643	0.585	
	RF	0.608	0.732	0.608	0.581	0.433	0.663	5.336	RF	0.581	0.714	0.581	0.548	0.375	0.638	25.444	
LR	0.478	0.478	0.478	0.121	0.011	0.500	2.852	LR	0.560	0.538	0.560	0.521	0.259	0.616	477.354		
DT	0.453	0.461	0.453	0.455	0.300	0.649	1.270	DT	0.423	0.430	0.423	0.425	0.256	0.627	7.355		
Isolation	SVM	0.282	0.311	0.282	0.147	0.028	0.505	11.243	SVM	0.277	0.077	0.277	0.120	0.011	0.500	28.613	
	NB	0.029	0.353	0.029	0.038	0.011	0.503	0.195	NB	0.087	0.008	0.087	0.014	0.004	0.500	0.880	
	MLP	0.290	0.282	0.290	0.144	0.023	0.503	9.475	MLP	0.277	0.077	0.277	0.120	0.011	0.500	11.214	
	KNN	0.200	0.144	0.200	0.157	0.025	0.502	0.466	KNN	0.220	0.054	0.220	0.086	0.009	0.500	0.829	
	RF	0.286	0.369	0.286	0.146	0.021	0.503	1.566	RF	0.277	0.077	0.277	0.120	0.011	0.500	3.414	
LR	0.277	0.252	0.277	0.122	0.011	0.500	1.913	LR	0.277	0.077	0.277	0.120	0.011	0.500	0.737		
DT	0.279	0.271	0.279	0.141	0.021	0.503	0.261	DT	0.277	0.077	0.277	0.120	0.011	0.500	0.080		
Gaussian	SVM	0.337	0.658	0.337	0.241	0.125	0.536	328.055	SVM	0.337	0.658	0.337	0.241	0.125	0.536	328.055	
	NB	0.017	0.392	0.017	0.018	0.044	0.516	0.776	NB	0.017	0.392	0.017	0.018	0.044	0.516	0.776	
	MLP	0.286	0.284	0.286	0.228	0.085	0.524	144.268	MLP	0.286	0.284	0.286	0.228	0.085	0.524	144.268	
	KNN	0.223	0.170	0.223	0.170	0.044	0.509	1.198	KNN	0.223	0.170	0.223	0.170	0.044	0.509	1.198	
	RF	0.331	0.591	0.331	0.247	0.126	0.538	58.119	RF	0.331	0.591	0.331	0.247	0.126	0.538	58.119	
LR	0.304	0.553	0.304	0.172	0.025	0.504	28.159	LR	0.304	0.553	0.304	0.172	0.025	0.504	28.159		
DT	0.209	0.211	0.209	0.209	0.098	0.538	19.748	DT	0.209	0.211	0.209	0.209	0.098	0.538	19.748		

Table 34: Classification comparison for different kernel methods and classifiers on minimizer for Genome.

severe failure, with accuracies near or below 0.47, maintaining incompatibility across all genome encoding methods. Sigmoid kernel exhibits complete classification collapse with fixed accuracy of 0.276 across all classifiers. Spaced k-mer encoding emerges as the most effective representation for genome classification, substantially outperforming OHE, k-mer, and minimizer approaches when paired with appropriate kernels.

Kernels	ML Algo.	Acc.	Prec.	Recall	F1 weigh.	F1 Macro	ROC-AUC	Train. run-time (sec.)	Kernels	ML Algo.	Acc.	Prec.	Recall	F1 weigh.	F1 Macro	ROC-AUC	Train. run-time (sec.)
Additive- χ^2	SVM	0.944	0.942	0.944	0.941	0.892	0.932	29.804	SVM	0.951	0.951	0.951	0.950	0.895	0.941	18.776	
	NB	0.245	0.591	0.245	0.290	0.080	0.780	0.780	NB	0.850	0.887	0.850	0.860	0.763	0.854	0.386	
	MLP	0.788	0.794	0.788	0.789	0.486	0.744	73.071	MLP	0.813	0.821	0.813	0.814	0.524	0.774	49.666	
	KNN	0.718	0.738	0.718	0.701	0.496	0.715	0.983	KNN	0.862	0.866	0.862	0.856	0.704	0.827	0.810	
	RF	0.732	0.798	0.732	0.709	0.689	0.785	37.285	RF	0.825	0.851	0.825	0.804	0.588	0.744	36.846	
LR	0.920	0.912	0.920	0.909	0.676	0.819	120.697	LR	0.806	0.708	0.806	0.756	0.294	0.634	27.203		
DT	0.617	0.628	0.617	0.620	0.333	0.672	13.004	DT	0.736	0.743	0.736	0.737	0.425	0.717	12.642		
Chi-squared	SVM	0.441	0.397	0.441	0.361	0.065	0.523	6.297	SVM	0.945	0.945	0.945	0.943	0.902	0.938	16.846	
	NB	0.111	0.410	0.111	0.129	0.034	0.543	0.020	NB	0.270	0.651	0.270	0.311	0.403	0.692	0.630	
	MLP	0.488	0.400	0.488	0.414	0.100	0.541	12.814	MLP	0.784	0.792	0.784	0.785	0.482	0.745	52.468	
	KNN	0.468	0.444	0.468	0.436	0.195	0.583	0.108	KNN	0.796	0.802	0.796	0.785	0.600	0.766	0.931	
	RF	0.539	0.523	0.539	0.514	0.301	0.627	3.028	RF	0.779	0.817	0.779	0.744	0.477	0.694	29.177	
LR	0.396	0.291	0.396	0.281	0.035	0.511	0.577	LR	0.961	0.961	0.961	0.959	0.912	0.948	117.378		
DT	0.472	0.468	0.472	0.465	0.259	0.618	0.142	DT	0.698	0.704	0.698	0.699	0.402	0.705	10.394		
Cosine	SVM	0.948	0.948	0.948	0.947	0.909	0.941	28.529	SVM	0.945	0.945	0.945	0.943	0.891	0.927	15.734	
	NB	0.300	0.669	0.300	0.330	0.418	0.697	0.744	NB	0.267	0.655	0.267	0.299	0.395	0.684	0.668	
	MLP	0.793	0.799	0.793	0.793	0.494	0.749	55.129	MLP	0.790	0.796	0.790	0.791	0.473	0.739	55.134	
	KNN	0.867	0.815	0.867	0.798	0.669	0.774	0.983	KNN	0.805	0.813	0.805	0.794	0.611	0.770	0.965	
	RF	0.786	0.827	0.786	0.753	0.480	0.695	42.687	RF	0.791	0.825	0.791	0.758	0.484	0.696	34.621	
LR	0.276	0.077	0.276	0.120	0.011	0.500	25.902	LR	0.963	0.964	0.963	0.962	0.909	0.943	123.578		
DT	0.705	0.712	0.705	0.706	0.389	0.699	12.238	DT	0.700	0.704	0.700	0.700	0.387	0.697	15.392		
Isolation	SVM	0.296	0.423	0.296	0.161	0.033	0.506	10.898	SVM	0.276	0.076	0.276	0.120	0.011	0.500	40.752	
	NB	0.041	0.569	0.041	0.062	0.022	0.506	0.191	NB	0.088	0.008	0.088	0.014	0.004	0.500	1.434	
	MLP	0.292	0.374	0.292	0.158	0.029	0.505	9.863	MLP	0.276	0.076	0.276	0.120	0.011	0.500	18.267	
	KNN	0.215	0.170	0.215	0.173	0.034	0.505	0.456	KNN	0.218	0.054	0.218	0.065	0.009	0.500	1.014	
	RF	0.302	0.477	0.302	0.168	0.031	0.506	1.391	RF	0.276	0.076	0.276	0.120	0.011	0.500	3.556	
LR	0.285	0.250	0.285	0.130	0.012	0.500	1.723	LR	0.276	0.076	0.276	0.120	0.011	0.500	0.816		
DT	0.295	0.288	0.295	0.161	0.027	0.504	0.235	DT	0.276	0.076	0.276	0.120	0.011	0.500	0.098		
Gaussian	SVM	0.325	0.575	0.325	0.229	0.126	0.539	1620.742	SVM	0.325	0.575	0.325	0.229	0.126	0.539	1620.742	
	NB	0.018	0.383	0.018	0.022	0.045	0.520	0.942	NB	0.018	0.383	0.018	0.022	0.045	0.520	0.	

10.6 Results For Breast Cancer Data

The OHE embedding results in Table 36 demonstrate strong performance across multiple kernel-classifier combinations, with the Chi-squared kernel achieving the highest accuracy of 89.8% when paired with Random Forest. Notably, the Isolation kernel shows robust results across different classifiers, with Naive Bayes and Random Forest both exceeding 88% accuracy and ROC-AUC scores above 0.75. The Gaussian kernel exhibits relatively poor performance, particularly with KNN, achieving only 9.9% accuracy, suggesting that this kernel struggles with the high-dimensional sparse representations inherent in OHE. Training times remain relatively low across all combinations, with most models completing in under 2 seconds, though MLP requires more time for convergence.

Kernel	ML Algo.	Acc.	Prec.	Recall	F1 weigh.	F1 Macro	ROC-AUC	Train. run-time (sec.)	Kernel	ML Algo.	Acc.	Prec.	Recall	F1 weigh.	F1 Macro	ROC-AUC	Train. run-time (sec.)		
Additive-chi2	SVM	0.848	0.832	0.848	0.839	0.495	0.698	0.152	Laplacian	SVM	0.883	0.878	0.883	0.878	0.566	0.747	0.154		
	NB	0.780	0.804	0.780	0.786	0.443	0.676	0.007		NB	0.793	0.833	0.793	0.806	0.436	0.491	0.008		
	MLP	0.659	0.757	0.659	0.695	0.365	0.625	1.183		MLP	0.632	0.783	0.632	0.684	0.351	0.627	1.322		
	KNN	0.531	0.814	0.531	0.614	0.334	0.640	0.014		KNN	0.635	0.863	0.635	0.702	0.384	0.672	0.015		
	RF	0.836	0.788	0.836	0.795	0.405	0.608	0.755		RF	0.852	0.812	0.852	0.814	0.414	0.609	0.730		
	DT	0.878	0.879	0.878	0.872	0.553	0.742	0.166		LR	0.807	0.652	0.807	0.721	0.223	0.500	0.052		
Chi-squared	SVM	0.820	0.823	0.820	0.817	0.523	0.700	0.212	Linear	SVM	0.863	0.848	0.863	0.854	0.527	0.715	0.154		
	NB	0.879	0.882	0.879	0.872	0.547	0.763	0.007		NB	0.765	0.798	0.765	0.778	0.422	0.673	0.007		
	MLP	0.676	0.866	0.676	0.720	0.454	0.708	1.901		MLP	0.655	0.743	0.655	0.688	0.352	0.612	1.589		
	KNN	0.213	0.821	0.213	0.231	0.163	0.538	0.014		KNN	0.620	0.850	0.620	0.681	0.400	0.671	0.014		
	RF	0.898	0.885	0.898	0.880	0.642	0.786	0.893		RF	0.828	0.780	0.828	0.784	0.398	0.604	0.799		
	DT	0.787	0.620	0.787	0.694	0.220	0.500	0.063		LR	0.880	0.872	0.880	0.872	0.577	0.747	0.145		
Cosine	SVM	0.863	0.868	0.863	0.864	0.550	0.757	0.283	Polynomial	DT	0.839	0.838	0.839	0.837	0.503	0.719	0.416		
	SVM	0.861	0.853	0.861	0.856	0.527	0.722	0.165		SVM	0.846	0.833	0.846	0.838	0.511	0.711	0.145		
	NB	0.838	0.880	0.838	0.831	0.497	0.703	0.007		NB	0.768	0.793	0.768	0.777	0.418	0.674	0.008		
	MLP	0.628	0.773	0.628	0.682	0.358	0.625	1.601		MLP	0.726	0.766	0.726	0.743	0.406	0.642	1.365		
	KNN	0.813	0.852	0.813	0.827	0.451	0.717	0.015		KNN	0.616	0.849	0.616	0.677	0.377	0.669	0.013		
	RF	0.835	0.780	0.835	0.788	0.369	0.584	0.736		RF	0.825	0.776	0.825	0.779	0.394	0.599	0.741		
Isolation	LR	0.860	0.820	0.860	0.832	0.435	0.651	0.078	Sigmoid	LR	0.778	0.606	0.778	0.681	0.219	0.500	0.053		
	DT	0.834	0.837	0.834	0.835	0.447	0.686	0.421		DT	0.822	0.828	0.822	0.823	0.460	0.696	0.439		
	SVM	0.854	0.849	0.854	0.850	0.547	0.732	0.057		SVM	0.853	0.870	0.853	0.858	0.536	0.750	0.045		
	NB	0.857	0.879	0.857	0.865	0.576	0.782	0.008		NB	0.857	0.850	0.857	0.851	0.523	0.735	0.004		
	MLP	0.851	0.852	0.851	0.850	0.569	0.747	1.867		MLP	0.784	0.815	0.784	0.796	0.448	0.685	1.225		
	KNN	0.825	0.785	0.825	0.777	0.372	0.587	0.012		KNN	0.663	0.861	0.663	0.727	0.406	0.680	0.015		
Gaussian	RF	0.889	0.885	0.889	0.882	0.583	0.755	0.224		RF	0.865	0.828	0.865	0.840	0.462	0.662	0.560		
	LR	0.793	0.629	0.793	0.701	0.221	0.500	0.021		LR	0.798	0.637	0.798	0.708	0.222	0.500	0.027		
	DT	0.871	0.878	0.871	0.874	0.566	0.770	0.055		DT	0.839	0.852	0.839	0.844	0.499	0.716	0.160		
	SVM	0.578	0.685	0.578	0.622	0.295	0.536	0.188											
	NB	0.847	0.868	0.847	0.856	0.519	0.750	0.007											
	MLP	0.579	0.686	0.579	0.621	0.273	0.538	1.393											
	KNN	0.099	0.648	0.099	0.050	0.083	0.497	0.012											
	RF	0.796	0.707	0.796	0.719	0.280	0.531	0.868											
	LR	0.784	0.615	0.784	0.689	0.220	0.500	0.055											
	DT	0.762	0.767	0.762	0.764	0.361	0.623	0.308											

Table 36: Classification comparison for different kernel methods and classifiers on OHE for Breast Cancer.

The Spike2Vec embedding results in Table 37 yield competitive results, with several kernel-classifier pairs achieving accuracies above 88%. The Chi-squared and Isolation kernels demonstrate particular effectiveness, both reaching 89.1% accuracy with Random Forest. Interestingly, the Cosine kernel with Naive Bayes achieves 89.1% accuracy—the highest for this encoding—while maintaining exceptional training efficiency at 0.008 seconds. The Linear kernel shows strong performance with Logistic Regression (88.3% accuracy), suggesting that kmer features exhibit good linear separability. Similar to OHE, the Gaussian kernel underperforms significantly, indicating that kmer’s characteristic feature distributions are not well-suited to Gaussian kernel transformations.

The minimizer embedding results in Table 38 reveal more variable performance patterns compared to OHE and kmer representations. The Isolation kernel emerges as the strongest performer, achieving 87.3% accuracy with Random Forest and demonstrating reasonable results across multiple classifiers. Chi-squared and Cosine kernels also show robust performance, with Random Forest achieving approximately 85%

Kernel	ML Algo.	Acc.	Prec.	Recall	F1 weigh.	F1 Macro	ROC-AUC	Train. run-time (sec.)	Kernel	ML Algo.	Acc.	Prec.	Recall	F1 weigh.	F1 Macro	ROC-AUC	Train. run-time (sec.)		
Additive-chi2	SVM	0.801	0.836	0.801	0.813	0.499	0.718	0.150	Laplacian	SVM	0.840	0.858	0.840	0.848	0.555	0.746	0.180		
	NB	0.853	0.854	0.853	0.849	0.494	0.728	0.008		NE	0.850	0.865	0.850	0.853	0.508	0.736	0.008		
	MLP	0.619	0.775	0.619	0.672	0.381	0.655	1.446		MLP	0.617	0.774	0.617	0.670	0.371	0.655	1.486		
	KNN	0.868	0.840	0.868	0.851	0.483	0.701	0.013		KNN	0.881	0.854	0.881	0.866	0.494	0.705	0.013		
	RF	0.874	0.852	0.874	0.856	0.560	0.715	0.667		RF	0.872	0.845	0.872	0.851	0.516	0.685	0.731		
Chi-squared	LR	0.886	0.879	0.886	0.880	0.560	0.755	0.352	Linear	LR	0.796	0.635	0.796	0.706	0.222	0.500	0.044		
	DT	0.833	0.846	0.833	0.838	0.499	0.727	0.365		DT	0.834	0.851	0.834	0.841	0.496	0.723	0.355		
	SVM	0.811	0.820	0.811	0.813	0.475	0.683	0.160		SVM	0.788	0.825	0.788	0.801	0.473	0.697	0.176		
	NB	0.862	0.875	0.862	0.860	0.508	0.738	0.008		NE	0.869	0.861	0.869	0.863	0.531	0.742	0.008		
	MLP	0.669	0.812	0.669	0.737	0.450	0.699	1.761		MLP	0.618	0.786	0.618	0.671	0.373	0.655	1.538		
Cosine	KNN	0.618	0.811	0.618	0.637	0.341	0.614	0.015	Polynomial	KNN	0.867	0.836	0.867	0.848	0.482	0.693	0.014		
	RF	0.891	0.880	0.891	0.883	0.570	0.753	0.899		RF	0.862	0.838	0.862	0.842	0.476	0.685	0.698		
	LR	0.785	0.651	0.785	0.705	0.225	0.501	0.061		LR	0.883	0.870	0.883	0.871	0.548	0.732	0.152		
	DT	0.847	0.854	0.847	0.849	0.518	0.740	0.314		DT	0.831	0.839	0.831	0.834	0.504	0.716	0.337		
	SVM	0.855	0.874	0.855	0.861	0.526	0.741	0.199		SVM	0.800	0.835	0.800	0.813	0.490	0.709	0.192		
Isolation	NB	0.891	0.882	0.891	0.882	0.507	0.732	0.008	Sigmoid	NE	0.864	0.853	0.864	0.855	0.498	0.725	0.007		
	MLP	0.565	0.802	0.565	0.636	0.338	0.643	1.642		MLP	0.613	0.768	0.613	0.669	0.353	0.628	1.607		
	KNN	0.877	0.875	0.877	0.874	0.504	0.737	0.017		KNN	0.865	0.835	0.865	0.848	0.481	0.694	0.014		
	RF	0.879	0.855	0.879	0.861	0.494	0.692	0.661		RF	0.854	0.822	0.854	0.831	0.455	0.674	0.701		
	LR	0.858	0.852	0.858	0.827	0.431	0.642	0.079		LR	0.777	0.604	0.777	0.679	0.219	0.500	0.047		
Gaussian	DT	0.845	0.859	0.845	0.851	0.491	0.719	0.352	DT	0.840	0.842	0.840	0.838	0.475	0.727	0.298			
	SVM	0.857	0.845	0.857	0.847	0.516	0.712	0.054	SVM	0.799	0.844	0.799	0.817	0.470	0.709	0.187			
	NB	0.882	0.897	0.882	0.882	0.572	0.784	0.008	NE	0.865	0.866	0.865	0.861	0.516	0.736	0.007			
	MLP	0.856	0.851	0.856	0.852	0.547	0.734	1.881	MLP	0.662	0.794	0.662	0.710	0.364	0.645	1.384			
	KNN	0.834	0.791	0.834	0.794	0.420	0.621	0.013	KNN	0.878	0.849	0.878	0.862	0.476	0.696	0.013			
Additive-chi2	RF	0.891	0.887	0.891	0.885	0.573	0.765	0.206	Laplacian	RF	0.873	0.847	0.873	0.855	0.462	0.689	0.647		
	LR	0.778	0.606	0.778	0.681	0.219	0.500	0.018		LR	0.800	0.640	0.800	0.711	0.222	0.500	0.039		
	DT	0.874	0.878	0.874	0.874	0.526	0.747	0.025		DT	0.856	0.862	0.856	0.858	0.486	0.720	0.339		
	SVM	0.570	0.711	0.570	0.623	0.278	0.564	0.183		Gaussian	SVM	0.681	0.786	0.681	0.722	0.372	0.642	0.170	
	NB	0.845	0.864	0.845	0.853	0.503	0.749	0.007			NE	0.659	0.810	0.659	0.707	0.439	0.697	0.007	
MLP	0.558	0.679	0.558	0.604	0.255	0.524	1.374	MLP	0.687		0.784	0.687	0.724	0.364	0.637	1.623			
KNN	0.126	0.491	0.126	0.094	0.104	0.518	0.013	KNN	0.556		0.785	0.456	0.542	0.285	0.582	0.014			
RF	0.865	0.723	0.865	0.786	0.326	0.528	0.866	RF	0.851		0.813	0.851	0.822	0.439	0.649	0.739			
Chi-squared	LR	0.849	0.825	0.849	0.832	0.449	0.676	0.147	LR	0.800	0.640	0.800	0.711	0.222	0.500	0.040			
	DT	0.790	0.815	0.790	0.801	0.450	0.685	0.369	DT	0.804	0.812	0.804	0.806	0.416	0.672	0.328			
	SVM	0.772	0.787	0.772	0.775	0.431	0.654	0.078	SVM	0.745	0.808	0.745	0.767	0.429	0.678	0.133			
	NB	0.728	0.811	0.728	0.756	0.446	0.700	0.008	NE	0.679	0.794	0.679	0.720	0.409	0.684	0.008			
	MLP	0.752	0.805	0.752	0.774	0.447	0.676	1.927	MLP	0.718	0.782	0.718	0.743	0.402	0.651	1.932			
Cosine	KNN	0.590	0.778	0.590	0.647	0.329	0.609	0.013	Linear	KNN	0.629	0.816	0.629	0.676	0.347	0.615	0.015		
	RF	0.853	0.827	0.853	0.834	0.467	0.666	1.038		RF	0.853	0.822	0.853	0.830	0.462	0.664	0.741		
	LR	0.820	0.758	0.820	0.763	0.352	0.569	0.069		LR	0.851	0.835	0.851	0.841	0.508	0.703	0.200		
	DT	0.827	0.841	0.827	0.832	0.468	0.716	0.615		DT	0.797	0.814	0.797	0.804	0.431	0.677	0.291		
	SVM	0.709	0.816	0.709	0.742	0.458	0.689	0.123		SVM	0.717	0.778	0.717	0.739	0.404	0.653	0.119		
Isolation	NB	0.688	0.787	0.688	0.726	0.381	0.659	0.007	Polynomial	NE	0.693	0.786	0.693	0.725	0.413	0.673	0.008		
	MLP	0.681	0.791	0.681	0.723	0.406	0.664	2.118		MLP	0.673	0.771	0.673	0.710	0.376	0.641	1.761		
	KNN	0.590	0.778	0.590	0.647	0.329	0.609	0.013		KNN	0.625	0.790	0.625	0.668	0.355	0.629	0.013		
	RF	0.848	0.813	0.848	0.826	0.441	0.658	0.742		RF	0.842	0.806	0.842	0.817	0.447	0.652	0.738		
	LR	0.839	0.800	0.839	0.803	0.414	0.624	0.081		LR	0.778	0.606	0.778	0.681	0.219	0.500	0.049		
Additive-chi2	DT	0.865	0.813	0.865	0.867	0.439	0.678	0.358	DT	0.805	0.814	0.805	0.808	0.469	0.697	0.358			
	SVM	0.818	0.822	0.818	0.818	0.465	0.696	0.052	SVM	0.700	0.808	0.700	0.738	0.404	0.655	0.160			
	NB	0.832	0.846	0.832	0.837	0.459	0.705	0.008	NE	0.671	0.800	0.671	0.720	0.374	0.656	0.008			
	MLP	0.822	0.834	0.822	0.826	0.461	0.694	1.918	MLP	0.681	0.789	0.681	0.721	0.383	0.655	1.795			
	KNN	0.833	0.783	0.833	0.787	0.380	0.591	0.013	KNN	0.623	0.797	0.623	0.674	0.341	0.620	0.014			
Chi-squared	RF	0.873	0.857	0.873	0.862	0.493	0.703	0.223	Sigmoid	RF	0.865	0.836	0.865	0.842	0.464	0.669	0.714		
	LR	0.799	0.638	0.799	0.709	0.222	0.500	0.021		LR	0.799	0.638	0.799	0.709	0.222	0.500	0.044		
	DT	0.847	0.849	0.847	0.847	0.470	0.699	0.046		DT	0.815	0.835	0.815	0.823	0.478	0.725	0.446		
	SVM	0.476	0.639	0.476	0.535	0.272	0.521	0.185		Gaussian	SVM	0.476	0.639	0.476	0.535	0.272	0.521	0.185	
	NB	0.754	0.863	0.754	0.790	0.427	0.725	0.008			NE	0.593	0.721	0.593	0.640	0.336	0.598	1.923	
MLP	0.593	0.721	0.593	0.640	0.336	0.598	1.923	MLP	0.798		0.734	0.798	0.728	0.308	0.544	0.016			
KNN	0.798	0.734	0.798	0.728	0.308	0.544	0.016	KNN	0.845		0.815	0.845	0.823	0.441	0.661	0.728			
RF	0.845	0.815	0.845	0.823	0.441	0.661	0.728	RF	0.784		0.625	0.784	0.690	0.223	0.502	0.071			
Cosine	LR	0.784	0.625	0.784	0.690	0.223	0.502	0.071	Laplacian	LR	0.845	0.841	0.845	0.842	0.469	0.703	0.172		
	DT	0.845	0.841	0.845	0.842	0.469	0.703	0.172		DT	0.845	0.841	0.845	0.842	0.469	0.703	0.172		

Table 37: Classification comparison for different kernel methods and classifiers on kmer for Breast Cancer.

accuracy in both cases. Notably, the performance gap between best and worst kernels is more pronounced in this encoding, with the Gaussian kernel’s SVM achieving only 47.6% accuracy. The overall stable training times across encodings suggest that minimizer representations maintain computational efficiency while potentially capturing different sequence characteristics than standard kmer approaches.

Kernel	ML Algo.	Acc.	Prec.	Recall	F1 weigh.	F1 Macro	ROC-AUC	Train. run-time (sec.)	Kernel	ML Algo.	Acc.	Prec.	Recall	F1 weigh.	F1 Macro	ROC-AUC	Train. run-time (sec.)
Additive-chi2	SVM	0.714	0.794	0.714	0.745	0.427	0.663	0.140	Laplacian	SVM	0.681	0.786	0.681	0.722	0.372	0	

Regression shows notably strong performance with several kernels, particularly achieving 86.9% accuracy with Additive-chi2 and 86.7% with Linear kernels. The Gaussian kernel again exhibits poor performance, reinforcing the pattern observed across all encodings that Gaussian transformations are ill-suited to these genomic feature representations. The spaced kmer approach appears to offer a balanced trade-off between discriminative power and computational efficiency, with training times comparable to other encodings.

Kernels	ML Algo.	Acc.	Prec.	Recall	F1 weigh.	F1 Macro	ROC-AUC	Train. run-time (sec.)	Kernels	ML Algo.	Acc.	Prec.	Recall	F1 weigh.	F1 Macro	ROC-AUC	Train. run-time (sec.)	
Additive-chi2	SVM	0.822	0.826	0.822	0.820	0.434	0.671	0.158	SVM	0.845	0.843	0.845	0.842	0.492	0.699	0.187		
	NB	0.561	0.842	0.561	0.646	0.353	0.663	0.007	NB	0.569	0.834	0.569	0.652	0.365	0.659	0.008		
	MLP	0.650	0.779	0.650	0.701	0.341	0.617	1.776	MLP	0.612	0.783	0.612	0.667	0.376	0.646	2.460		
	KNN	0.688	0.832	0.688	0.731	0.391	0.662	0.013	Laplacian	KNN	0.765	0.828	0.765	0.776	0.415	0.654	0.016	
	RF	0.871	0.860	0.871	0.862	0.503	0.719	0.609	RF	0.881	0.871	0.881	0.875	0.563	0.741	0.635		
LR	0.869	0.848	0.869	0.854	0.497	0.696	0.132	LR	0.792	0.629	0.792	0.701	0.221	0.590	0.039			
DT	0.835	0.844	0.835	0.837	0.452	0.695	0.216	DT	0.839	0.848	0.839	0.842	0.498	0.715	0.213			
Chi-squared	SVM	0.837	0.833	0.837	0.833	0.504	0.712	0.144	SVM	0.838	0.837	0.838	0.833	0.488	0.692	0.140		
	NB	0.603	0.831	0.603	0.678	0.376	0.684	0.007	NB	0.547	0.823	0.547	0.634	0.331	0.645	0.008		
	MLP	0.718	0.813	0.718	0.755	0.443	0.699	1.716	MLP	0.603	0.785	0.603	0.663	0.357	0.637	2.109		
	KNN	0.825	0.771	0.825	0.778	0.380	0.592	0.013	Linear	KNN	0.669	0.826	0.669	0.714	0.367	0.642	0.013	
	RF	0.883	0.877	0.883	0.877	0.564	0.747	0.662	RF	0.877	0.872	0.877	0.869	0.527	0.726	0.631		
LR	0.799	0.692	0.799	0.720	0.257	0.520	0.070	LR	0.867	0.839	0.867	0.845	0.488	0.679	0.113			
DT	0.841	0.856	0.841	0.847	0.498	0.723	0.225	DT	0.833	0.848	0.833	0.839	0.483	0.722	0.271			
Cosine	SVM	0.758	0.820	0.758	0.782	0.443	0.685	0.175	SVM	0.810	0.808	0.810	0.806	0.447	0.672	0.154		
	NB	0.624	0.842	0.624	0.693	0.277	0.639	0.008	NB	0.534	0.822	0.534	0.626	0.366	0.658	0.007		
	MLP	0.610	0.804	0.610	0.674	0.387	0.665	1.818	MLP	0.619	0.780	0.619	0.675	0.394	0.649	1.748		
	KNN	0.581	0.813	0.581	0.634	0.353	0.623	0.013	Polynomial	KNN	0.608	0.816	0.608	0.650	0.375	0.642	0.013	
	RF	0.888	0.880	0.888	0.881	0.574	0.753	0.626	RF	0.866	0.857	0.866	0.856	0.524	0.725	0.609		
LR	0.827	0.777	0.827	0.781	0.374	0.597	0.072	LR	0.774	0.599	0.774	0.676	0.218	0.560	0.037			
DT	0.853	0.864	0.853	0.856	0.537	0.746	0.224	DT	0.829	0.833	0.829	0.830	0.488	0.708	0.219			
Isolation	SVM	0.849	0.849	0.849	0.845	0.507	0.716	0.061	SVM	0.815	0.816	0.815	0.809	0.430	0.671	0.154		
	NB	0.869	0.879	0.869	0.871	0.520	0.751	0.008	NB	0.545	0.830	0.545	0.636	0.367	0.666	0.008		
	MLP	0.836	0.842	0.836	0.834	0.494	0.713	2.171	MLP	0.604	0.785	0.604	0.661	0.365	0.640	1.843		
	KNN	0.844	0.803	0.844	0.813	0.429	0.639	0.013	Sigmoid	KNN	0.524	0.796	0.524	0.600	0.327	0.606	0.012	
	RF	0.872	0.868	0.872	0.865	0.478	0.725	0.203	RF	0.874	0.865	0.874	0.868	0.517	0.730	0.633		
LR	0.790	0.625	0.790	0.698	0.221	0.500	0.017	LR	0.787	0.620	0.787	0.694	0.220	0.500	0.037			
DT	0.867	0.865	0.867	0.864	0.481	0.724	0.021	DT	0.843	0.853	0.843	0.846	0.498	0.721	0.218			
Gaussian	SVM	0.581	0.700	0.581	0.627	0.289	0.562	0.185	SVM	0.581	0.700	0.581	0.627	0.289	0.562	0.185		
	NB	0.819	0.847	0.819	0.830	0.455	0.702	0.008	NB	0.819	0.847	0.819	0.830	0.455	0.702	0.008		
	MLP	0.580	0.728	0.580	0.632	0.299	0.579	1.748	MLP	0.580	0.728	0.580	0.632	0.299	0.579	1.748		
	KNN	0.796	0.721	0.796	0.724	0.297	0.537	0.015	KNN	0.796	0.721	0.796	0.724	0.297	0.537	0.015		
	RF	0.862	0.853	0.862	0.844	0.458	0.689	0.888	RF	0.862	0.853	0.862	0.844	0.458	0.689	0.888		
LR	0.785	0.664	0.785	0.692	0.232	0.504	0.062	LR	0.785	0.664	0.785	0.692	0.232	0.504	0.062			
DT	0.820	0.818	0.820	0.818	0.426	0.673	0.289	DT	0.820	0.818	0.820	0.818	0.426	0.673	0.289			

Table 39: Classification comparison for different kernel methods and classifiers on Spaced kmer for Breast Cancer.

11 Runtime Analysis

Figure 9a illustrates the computational time required for calculating various kernel matrices as the number of sequences increases, with a magnified view presented in Figure 9b. The results demonstrate that the Cosine similarity kernel achieves the fastest computation time compared to all other kernel approaches. In contrast, the Gaussian kernel exhibits the highest computational cost. Additionally, the runtime scaling behavior for most kernels follows a linear pattern with respect to the number of input sequences.

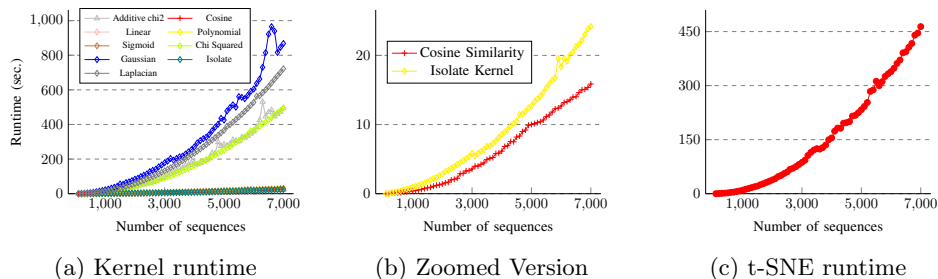


Fig. 9: (a) and (b) shows the kernel computation Runtime for an increasing number of sequences (using Spike2Vec-based embedding) for the **Spike7k dataset**. (c) shows the t-SNE computation runtime with an increasing number of sequences (using Spike2Vec-based embedding). This figure is best seen in color.

Given that the Cosine similarity kernel demonstrates superior performance in general in both objective evaluation metrics and computational efficiency relative to alternative kernel methods for t-SNE, we present the t-SNE computation time using the Cosine similarity kernel across varying sequence counts in Figure 9c. The results reveal a linear scaling relationship between runtime and the number of input sequences.

12 Conclusion

This comprehensive investigation across six diverse biological datasets demonstrates that, in general, cosine similarity outperforms traditional Gaussian and recently proposed isolation kernels for t-SNE-based dimensionality reduction of biological sequences. Through rigorous evaluation combining subjective visualization assessment, objective neighborhood preservation metrics ($AU C_{RNX}$), and extensive downstream analysis via classification and clustering experiments, we establish that kernel selection fundamentally impacts both visualization quality and analytical task performance. The cosine similarity kernel achieves superior computational efficiency with linear scaling behavior while maintaining robust performance across multiple embedding strategies (OHE, Spike2Vec, minimizers, and spaced k-mers), making it particularly suitable for large-scale genomic analysis. Our classification experiments across seven machine learning algorithms reveal that appropriate kernel-embedding combinations

can achieve higher accuracies on certain datasets, while clustering analyses expose substantial performance variations based on kernel choice. Notably, the Gaussian kernel’s underperformance across different datasets reinforces that Euclidean distance-based approaches inadequately capture categorical sequence dissimilarity. These findings provide practitioners with evidence-based guidance for method selection in biological sequence analysis pipelines, emphasizing that the angular similarity captured by cosine kernel better represents relationships in high-dimensional genomic feature spaces than distance-based alternatives.

References

- [1] GISAID Website <https://www.gisaid.org/>. [Online; accessed 29-December-2021] (2021)
- [2] Elbe, S., Buckland-Merrett, G.: Data, disease and diplomacy: GISAID’s innovative contribution to global health. *Global challenges* **1**(1), 33–46 (2017)
- [3] Stephens, Z.D., Lee, S.Y., Faghri, F., Campbell, R.H., Zhai, C., Efron, M.J., Iyer, R., Schatz, M.C., Sinha, S., Robinson, G.E.: Big data: astronomical or genomics? *PLoS biology* **13**(7), 1002195 (2015)
- [4] Harvey, W.T., Carabelli, A.M., Jackson, *et al.*: Sars-cov-2 variants, spike mutations and immune escape. *Nature Reviews Microbiology* **19**(7), 409–424 (2021)
- [5] Walls, A.C., Park, Y.-J., Tortorici, M.A., *et al.*: Structure, function, and antigenicity of the sars-cov-2 spike glycoprotein. *Cell* **181**(2), 281–292 (2020)
- [6] Libbrecht, M.W., Noble, W.S.: Machine learning applications in genetics and genomics. *Nature Reviews Genetics* **16**(6), 321–332 (2015)
- [7] Zou, J., Huss, M., Abid, A., Mohammadi, P., Torkamani, A., Telenti, A.: A primer on deep learning in genomics. *Nature genetics* **51**(1), 12–18 (2019)
- [8] Ali, S., Sahoo, B., Ullah, N., Zelikovskiy, A., Patterson, M., Khan, I.: A k-mer based approach for sars-cov-2 variant identification. In: *International Symposium on Bioinformatics Research and Applications*, pp. 153–164 (2021). Springer
- [9] Asgari, E., Mofrad, M.R.: Continuous distributed representation of biological sequences for deep proteomics and genomics. *PloS one* **10**(11), 0141287 (2015)
- [10] Ali, S., Patterson, M.: Spike2vec: An efficient and scalable embedding approach for covid-19 spike sequences. In: *International Conference on Big Data (Big Data)*, pp. 1533–1540 (2021)
- [11] Corso, G., Ying, Z., *et al.*: Neural distance embeddings for biological sequences. In: *Advances in Neural Information Processing Systems*, vol. 34, pp. 18539–18551 (2021)

- [12] Van der Maaten, L., Hinton, G.: Visualizing data using t-sne. *Journal of machine learning research* **9**(11) (2008)
- [13] Zhu, Y., Ting, K.M.: Improving the effectiveness and efficiency of stochastic neighbour embedding with isolation kernel. *Journal of Artificial Intelligence Research* **71**, 667–695 (2021)
- [14] Wolpert, D.H., Macready, W.G.: No free lunch theorems for optimization. *IEEE transactions on evolutionary computation* **1**(1), 67–82 (1997)
- [15] Tayebi, Z., Ali, S., Patterson, M.: Robust representation and efficient feature selection allows for effective clustering of sars-cov-2 variants. *Algorithms* **14**(12), 348 (2021)
- [16] Melnyk, A., et al.: From alpha to zeta: Identifying variants and subtypes of sars-cov-2 via clustering **28**(11), 1113–1129 (2021)
- [17] Chourasia, P., Murad, T., Ali, S., Patterson, M.: Enhancing t-sne performance for biological sequencing data through kernel selection. In: *International Symposium on Bioinformatics Research and Applications*, pp. 442–452 (2023). Springer
- [18] Wold, S., Esbensen, K., Geladi, P.: Principal component analysis. *Chemometrics and intelligent laboratory systems* **2**(1-3), 37–52 (1987)
- [19] Van Der Maaten, L., Postma, E., *et al.*: Dimensionality reduction: a comparative. *J Mach Learn Res* **10**(66-71), 13 (2009)
- [20] Tenenbaum, J.B., Silva, V.d., Langford, J.C.: A global geometric framework for nonlinear dimensionality reduction. *science* **290**(5500), 2319–2323 (2000)
- [21] Roweis, S.T., Saul, L.K.: Nonlinear dimensionality reduction by locally linear embedding. *science* **290**(5500), 2323–2326 (2000)
- [22] Belkin, M., Niyogi, P.: Laplacian eigenmaps for dimensionality reduction and data representation. *Neural computation* **15**(6), 1373–1396 (2003)
- [23] Hinton, G.E., Roweis, S.: Stochastic neighbor embedding. *Advances in neural information processing systems* **15** (2002)
- [24] Kobak, D., Berens, P.: The art of using t-sne for single-cell transcriptomics. *Nature communications* **10**(1), 5416 (2019)
- [25] Amir, E.-a.D., Davis, K.L., Tadmor, M.D., *et al.*: visne enables visualization of high dimensional single-cell data and reveals phenotypic heterogeneity of leukemia. *Nature biotechnology* **31**(6), 545–552 (2013)
- [26] Platzter, A.: Visualization of snps with t-sne. *PloS one* **8**(2), 56883 (2013)

- [27] Van Der Maaten, L.: Accelerating t-sne using tree-based algorithms. *The journal of machine learning research* **15**(1) (2014)
- [28] Van Der Maaten, L.: Learning a parametric embedding by preserving local structure. In: *Artificial Intelligence and Statistics*, pp. 384–391 (2009). PMLR
- [29] Yang, Z., King, I., Xu, Z., Oja, E.: Heavy-tailed symmetric stochastic neighbor embedding. *Advances in neural information processing systems* **22** (2009)
- [30] McInnes, L., Healy, J., Melville, J.: Umap: Uniform manifold approximation and projection for dimension reduction. *arXiv preprint arXiv:1802.03426* (2018)
- [31] Schölkopf, B., Smola, A.J.: *Learning with kernels: support vector machines, regularization, optimization, and beyond*. MIT press (2002)
- [32] Shawe-Taylor, J., Cristianini, N.: *Kernel methods for pattern analysis*. Cambridge university press (2004)
- [33] Cortes, C., Vapnik, V.: Support-vector networks. *Machine learning* **20**(3), 273–297 (1995)
- [34] Lodhi, H., Saunders, C., Shawe-Taylor, J., Cristianini, N., Watkins, C.: Text classification using string kernels. *Journal of machine learning research* **2**(Feb), 419–444 (2002)
- [35] Chapelle, O., Vapnik, V., Bousquet, O., Mukherjee, S.: Choosing multiple parameters for support vector machines. *Machine learning* **46**(1), 131–159 (2002)
- [36] Williams, C.K., Rasmussen, C.E.: *Gaussian processes for machine learning*. MIT press Cambridge, MA **2**(3) (2006)
- [37] Gönen, M., Alpaydm, E.: Multiple kernel learning algorithms. *The Journal of Machine Learning Research* **12**, 2211–2268 (2011)
- [38] Ting, K.M., Wells, J.R., Washio, T.: Isolation kernel: the x factor in efficient and effective large scale online kernel learning. *Data Mining and Knowledge Discovery* **35**(6), 2282–2312 (2021)
- [39] Leslie, C., Eskin, E., Noble, W.: The spectrum kernel: A string kernel for svm protein classification. In: *Symposium on Biocomputing*, pp. 566–575 (2002)
- [40] Kuang, R., Ie, E., Wang, K., Wang, K., Siddiqi, M., Freund, Y., Leslie, C.: Profile-based string kernels for remote homology detection and motif extraction. In: *Proceedings. 2004 IEEE Computational Systems Bioinformatics Conference, 2004. CSB 2004.*, pp. 152–160 (2004). IEEE
- [41] Khare, S., Gurry, C., Freitas, L., Schultz, M.B., Bach, G., Diallo, A., Akite, N., Ho, J., Lee, R.T., Yeo, W., *et al.*: Gisaid’s role in pandemic response. *China CDC*

weekly **3**(49), 1049 (2021)

- [42] Hadfield, J., Megill, C., Bell, S.M., *et al.*: Nextstrain: real-time tracking of pathogen evolution. *Bioinformatics* **34**, 4121–4123 (2018)
- [43] Kuzmin, K., Adeniyi, A.E., *et al.*: Machine learning methods accurately predict host specificity of coronaviruses based on spike sequences alone. *Biochemical and Biophysical Research Communications* **533**(3), 553–558 (2020)
- [44] Ali, S., Tamkanat-E-Ali, *et al.*: Effective and scalable clustering of sars-cov-2 sequences. In: *International Conference on Big Data Research (ICBDR)*, pp. 1–8 (2021)
- [45] Rambaut, A., Holmes, E.C., O’Toole, Á., Hill, V., McCrone, J.T., Ruis, C., Du Plessis, L., Pybus, O.G.: A dynamic nomenclature proposal for sars-cov-2 lineages to assist genomic epidemiology. *Nature microbiology* **5**(11), 1403–1407 (2020)
- [46] Huang, Y., Yang, C., Xu, X.-f., Xu, W., Liu, S.-w.: Structural and functional properties of sars-cov-2 spike protein: potential antiviral drug development for covid-19. *Acta Pharmacologica Sinica* **41**(9), 1141–1149 (2020)
- [47] Starr, T.N., Greaney, A.J., Hilton, S.K., Ellis, D., Crawford, K.H., Dingens, A.S., Navarro, M.J., Bowen, J.E., Tortorici, M.A., Walls, A.C., *et al.*: Deep mutational scanning of sars-cov-2 receptor binding domain reveals constraints on folding and ace2 binding. *cell* **182**(5), 1295–1310 (2020)
- [48] Meiler, J., Müller, M., Zeidler, A., Schmäschke, F.: Generation and evaluation of dimension-reduced amino acid parameter representations by artificial neural networks. *Molecular modeling annual* **7**(9), 360–369 (2001)
- [49] Zieleszinski, A., Vinga, S., Almeida, J., Karlowski, W.M.: Alignment-free sequence comparison: benefits, applications, and tools. *Genome biology* **18**(1), 186 (2017)
- [50] Roberts, M., Haynes, W., Hunt, B.R., Mount, S.M., Yorke, J.A.: Reducing storage requirements for biological sequence comparison. *Bioinformatics* **20**, 3363–9 (2004)
- [51] Schleimer, S., Wilkerson, D.S., Aiken, A.: Winnowing: local algorithms for document fingerprinting. In: *Proceedings of the 2003 ACM SIGMOD International Conference on Management of Data*, pp. 76–85 (2003)
- [52] Marçais, G., DeBlasio, D., Pandey, P., Kingsford, C.: Locality-sensitive hashing for the edit distance. *Bioinformatics* **35**(14), 127–135 (2019)
- [53] Rives, A., Meier, J., Sercu, T., Goyal, S., Lin, Z., Liu, J., Guo, D., Ott, M.,

- Zitnick, C.L., Ma, J., *et al.*: Biological structure and function emerge from scaling unsupervised learning to 250 million protein sequences. *Proceedings of the National Academy of Sciences* **118**(15), 2016239118 (2021)
- [54] Elnaggar, A., *et al.*: ProtTrans: Towards cracking the language of life’s code through self-supervised deep learning and high performance computing **44**(10), 7112–7127 (2022)
- [55] Lin, Z., Akin, H., Rao, R., Hie, B., Zhu, Z., Lu, W., Smetanin, N., Verkuil, R., Kabeli, O., Shmueli, Y., *et al.*: Evolutionary-scale prediction of atomic-level protein structure with a language model. *Science* **379**(6637), 1123–1130 (2023)
- [56] Lee, J.A., Peluffo-Ordóñez, D.H., Verleysen, M.: Multi-scale similarities in stochastic neighbour embedding: Reducing dimensionality while preserving both local and global structure. *Neurocomputing* **169**, 246–261 (2015)
- [57] Venna, J., Kaski, S.: Local multidimensional scaling. *Neural Networks* **19**(6-7), 889–899 (2006)
- [58] Lee, J.A., Verleysen, M.: Quality assessment of dimensionality reduction: Rank-based criteria. *Neurocomputing* **72**(7-9), 1431–1443 (2009)
- [59] Chen, L., Buja, A.: Local multidimensional scaling for nonlinear dimension reduction, graph drawing, and proximity analysis. *Journal of the American Statistical Association* **104**(485), 209–219 (2009)
- [60] Kruskal, J.B.: Nonmetric multidimensional scaling: a numerical method. *Psychometrika* **29**(2), 115–129 (1964)
- [61] Lee, J.A., Renard, *et al.*: Type 1 and 2 mixtures of kullback–leibler divergences as cost functions in dimensionality reduction based on similarity preservation. *Neurocomputing* **112**, 92–108 (2013)
- [62] Xue, J., Chen, Y., *et al.*: Classification and identification of unknown network protocols based on cnn and t-sne. In: *Journal of Physics: Conference Series*, vol. 1617, p. 012071 (2020)
- [63] Saha, D.K., *et al.*: Privacy-preserving quality control of neuroimaging datasets in federated environment. *Hum Brain Mapp* (2022)
- [64] Singh, R., Sekhon, A., *et al.*: Gakco: a fast gapped k-mer string kernel using counting. In: *Joint ECML and Knowledge Discovery in Databases*, pp. 356–373 (2017)
- [65] Pickett, B.E., Sadat, E.L., Zhang, Y., Noronha, J.M., Squires, R.B., Hunt, V., Liu, M., Kumar, S., Zaremba, S., Gu, Z., *et al.*: Vipr: an open bioinformatics database

- and analysis resource for virology research. *Nucleic acids research* **40**(D1), 593–598 (2012)
- [66] RABV GLUE Website <http://rabv-glue.cvr.gla.ac.uk/#/home>. [Online; accessed 10-October-2022] (2021)
- [67] Grisoni, *et al.*: 'de novo design of anticancer peptides by ensemble artificial neural networks'. *Journal of Molecular Modeling* '**25**'('5'), 112 ('2019')
- [68] Satopaa, V., Albrecht, J., Irwin, D., Raghavan, B.: Finding a "knee" in a haystack: Detecting knee points in system behavior. In: *International Conference on Distributed Computing Systems Workshops*, pp. 166–171 (2011). IEEE
- [69] Rousseeuw, P.J.: Silhouettes: a graphical aid to the interpretation and validation of cluster analysis. *Journal of computational and applied mathematics* **20**, 53–65 (1987)
- [70] Caliński, T., Harabasz, J.: A dendrite method for cluster analysis. *Comm. in Statistics-theory and Methods* **3**(1), 1–27 (1974)
- [71] Davies, D.L., Bouldin, D.W.: A cluster separation measure. *IEEE transactions on pattern analysis and machine intelligence* (2), 224–227 (1979)
- [72] Devijver, P., Kittler, J.: *Pattern recognition: A statistical approach*. In: London, GB: Prentice-Hall, pp. 1–448 (1982)